UNIVERSITY OF CAPE TOWN
IYUNIVESITHI YASEKAPA • UNIVERSITEIT VAN KAAPSTAD

Medical Biotechnology & Immunotherapy Research Unit
Institute for Infectious Disease & Molecular Medicine
South African Research Chair in Cancer Biotechnology
Department of Integrative Biomedical Sciences
Faculty of Health Sciences
University of Cape Town

University of Cape Town

Masters Thesis

Siyabulela Freddy-Junior Magugu

Development of potential immunodiagnostic & therapeutic techniques using SNAP-fusion proteins as tools for the validation of Triple-negative Breast Cancer

Supervisor: Prof. Dr. Dr. Stefan Barth

Co-supervisor: Dr. Krupa Naran

Start of the Masters (08/02/2018)

Date of completion (01/09/2020)

University of Cape Town, 2 September 2020

The copyright of this thesis vests in the author. No quotation from it or information derived from it is to be published without full acknowledgement of the source. The thesis is to be used for private study or non-commercial research purposes only.

Published by the University of Cape Town (UCT) in terms of the non-exclusive license granted to UCT by the author.

University of Cape Town

Declaration

1. I know that plagiarism is wrong. Plagiarism is to use another's work and claim it as one's own.

2. I have used the multiple databases including ***PubMed, Science Direct, Google Scholar and other internet platforms*** to obtain the information used to write up my research project proposal.

3. This ***research project/report/dissertation*** is my own work.

4. I have not allowed, and will not allow, anyone to copy my work with the intention of passing it off as his or her own work.

5. I know & acknowledge that copying someone's work or parts of it is wrong and declare that this is a product of my own work.

Signature: **Siyabulela Magugu**

Signature Removed

Date: **09/2020**

Acknowledgements

I would like to thank God almighty for giving me the opportunity to get this far in life, where others were not fortunate enough but more so that this work is a way I give back to the greater part of the future therapies in the world and I thank God that I may be part and parcel of it.

I would like to thank my supervisor Prof. Stefan Barth for allowing me another opportunity to further myself as a scientist under your supervision. It has been an honour and a privilege fulfilling the objectives of this project under your tutelage. From my honour's degree through my masters, you've been extremely supportive, and I could never discount that.

I would like to thank my friends and family in their multitudes for their constant support. Through the highs and the lows, you have always had my back and this piece of work reflects your love, admiration and support to the cause I support, which is a medical reprieve for this country and the continent at large.

I would like to thank my colleagues, Dr. Naran, Dr. Ramamurthy, Dr. Nsole, Dr. Padayachee, Ms. Malindi and Ms. Masuku for key contributions to this project and thank my MB&I family for always being supportive and contributing to my personal growth. I cannot thank you all enough for the lessons and guidance that built this work.

If I may, I'd like to give myself a pat on the back as well for successfully completing this piece of work, I could have never done it without the individuals I have praised above but I am proud to have gotten this far.

List of Abbreviations

TNBC	Triple Negative Breast Cancer
CSPG4	Chondroitin sulfate proteoglycan 4
CSAGAG	Chondroitin sulfate glycosaminoglycan
EGFR	Epidermal Growth Factor Receptor
MSLN	Mesothelin
mAb	Monoclonal antibody
scFv	Short chain variable fragment
SdAb	Single domain antibody
VHH	Variable heavy-heavy chain
BsAb	Bispecific antibody
DART	Dual affinity re-targeting antibody
ER	Estrogen receptor
PR	Progesterone receptor
HER-2	Human Epidermal growth factor receptor 2
BCS	Breast-conserving surgery
LRR	Locoregional recurrence
IHC	Immunohistochemical/ Immunohistochemistry
NGS	Next generation sequencing
ADC	Antibody-drug conjugate
hCFP	Human cytolytic fusion protein
IT	Immunotoxin
RIT	Radioimmunotherapy
CDR	Complementarity determining regions
AGT	06-alkylguanine-DNA-alkyltransferase
BG	Benzylguanine
ERK	Extracellular signal regulated kinase
PKCα	Protein kinase C-alpha
MAPK	Mitogen-activated protein kinase
PI3k	Phosphoinositol 3-kinase

AKT	Protein kinase B
NFKβ	Nuclear factor kappa beta
MITF	Melanocyte lineage specific transcription factor
RTK	Receptor tyrosine kinase
EMT	Epidermal-mesenchymal transition
MPF	Megakaryote potentiating factor
TNF-α	Tumour necrosis factor alpha
CDK2	Cyclin E/cyclin-dependent kinase
TGF-α	Transforming growth factor alpha
ORF	Open reading frame
RE	Restriction enzyme
NEB	New England Biolabs
SOC	Super Optimal broth with Catabolite expression
DH5-α	Calcium competent *E. coli*
HEK	Human Embryonic Kidney
RPMI	Roswell Park Memorial Institute
DMEM	Dulbecco's Modified Eagles Media
EGFP	Enhanced green fluorescent protein
PBS	Phosphate buffered saline
PFA	Paraformaldehyde
CCSN	Cell culture supernatant
IMAC	Immobilized ion metal affinity chromatography
SDS-PAGE	Sodium dodecyl sulfate-polyacrylamide gel electrophoresis
APS	Ammonium per sulfate
TBS	Tris-buffered saline
MW	Molecular weight
DTT	Dithiothreitol
PenStrep	Penicillin-streptomycin
FBS	Fetal Bovine Serum
LB	Luria Bertani broth

DMSO	Dimethyl Sulfoxide
PVDF	Polyvinylidene fluoride
AmpR	Ampicillin resistance
SEC	Size exclusion chromatography
7AAD	7-aminoactinomycin D
MMAE/F	Monomethyl Auristatin E/F
MB&I	Medical Biotechnology & Immunotherapy Research Unit

List of Tables & Figures

Tables

Figures

Title Page

Title of manuscript: Development of potential immunodiagnostic & therapeutic techniques using SNAP-fusion proteins as tools for the validation of Triple Negative Breast Cancer.

Authors: S. Magugu[1], K. Naran[1], S. Barth[1]

Affiliations: Medical Biotechnology & Immunology Research Unit, Division of Chemical & Systems Biology, Institute of Infectious Disease & Molecular Medicine; Faculty of Health Sciences, University of Cape Town.

Address correspondence to: Mr. Siyabulela Magugu

Division of Chemical & Systems Biology

Department of Integrative Biomedical Sciences

University of Cape Town

Cape Town

South Africa

7925

[mggsiy003@myuct.ac.za], +27 (073) 040 7954

Funding sources: This study was partially funded by the SarChI Chair in Cancer Biotechnology and the NRF Masters Innovation Bursary.

Financial disclosure: The authors have no financial relationships relevant to this article to disclose.

Conflicts of interest: The others have no conflict of interests to disclose.

Tables & Figures (Appendix included): Tables (14) and Figures (22) included in the text with appropriate captions.

Number of pages: 91 (including references & appendices)

77 (excluding references & appendices)

Word count: Abstract (416 words);

Main Text* (18061 words)

Acknowledgements: Prof. Dr. Dr. Stefan Barth, Family & Friends and Colleagues in the MB&I Research Unit.

Abstract

Globally, breast cancer is the leading cause of death in the female population aged 45 and below with a breast cancer incidence reaching 18.1 million in the year 2018. Triple negative breast cancer (TNBC) is part of a group of cancers that lack the expression of Progesterone receptor (PR), Estrogen receptor (ER) and Human epidermal growth factor receptor 2 (HER2). TNBC is commonly associated with early stage metastasis with low survival rates as well as a high frequency of recurrence and proves to be problematic in both the young and elderly female populations. Conventional diagnostic methods for TNBCs include mammography, magnetic resonance imaging (MRI) and ultrasound while therapeutic methods include mastectomy and breast conserving surgery (coupled with radiation therapy). The lack of effective therapeutic options, poor prognostic value and high rates of metastasis, has made treatment of TNBC difficult.

The major focus of this work was on the following tumour associated antigens (TAAs): CSPG4 (a transmembrane protein found in 50% of TNBC cases), EGFR (which is overexpressed in 13-76% of TNBCs), and MSLN (which is overexpressed in 67% of TNBCs) as potential targets for monospecific therapy. The evolution of antibody-based immunotherapy strategies has led to applications of single chain variable fragment (scFv) & single domain/nanobody (VHH) antibody formats for diagnostic and therapeutic purposes. In this work, these recombinant antibody fragments have been combined with SNAP-tag, a modified version of the human DNA repair enzyme O6-alkylguanine-DNA-alkyltransferase (AGT), which autocatalytically binds benzyl-guanine modified substrates such as fluorophores or small molecule toxins covalently in a 1:1 stoichiometry.

In this study, the primary aim was the comparison of different antibody formats fused to SNAP-tag and the potential of these biopharmaceuticals towards immunodiagnosis and therapy of TNBCs. First functionalities of two scFv SNAP fusion proteins and one VHH SNAP fusion protein previously not having been described are provided through binding analyses on receptor positive tumour cell lines.

This was achieved by *in-silico* design and molecular cloning of genetically fused anti-CSPG4(scFv), -MSLN(scFv), -MSLN(VHH), -EGFR(scFv) & -EGFR(VHH) to SNAP-tag. The final constructs were confirmed by Sanger sequencing and subsequently transfected into a mammalian vector system (HEK293T) for transient expression of the engineered fusion proteins. Full length protein purified from cell culture supernatant was analysed for diagnostic/therapeutic activities dependant on the substrate attached in the form of a

fluorophore or small molecule toxin resulting in recombinant antibody-drug conjugates (ADCs). The study shows promise in providing new immunodiagnostic and therapeutic agents that are specific and less harmful than the current state of the art procedures.

Key words: TNBC, CSPG4, MSLN, EGFR, scFv, VHH, SNAP-tag

Contents

Chapter 1: Introduction

1.1 Breast cancer and triple-negative breast cancer

Breast cancer is the leading cause of cancer-related deaths in women below the age of 45 worldwide, due to its heterogeneity and complexity [1]. Some biological risk factors of breast cancers include early menarche, late menopause, late aged pregnancies and short or no periods of breast feeding and some lifestyle risk factors include obesity, alcoholism and hormone replacement therapy or inactivity [2]. In 2004, South African women showed an increasing incidence of 5-10 per 100 000, with women living an urban lifestyle having a greater risk of getting disease [3]. In developing countries, about 55% of the population are dealing with the burden of breast cancer related deaths with an increasing incidence of breast cancer in developed countries [4]. As per the World Health Organization (WHO), 2018, the current global breast cancer burden is recorded at 18.1 million cases worldwide and the cancer mortality is 9.6 million. Breast cancer has also been identified as an increasing problem in developing countries e.g. African countries [5].

Invasive breast cancers are classified into 5 subtypes according to their expression of certain genes, including expression of estrogen receptor (ER), progesterone receptor (PR) and human epidermal growth factor receptor 2 (HER2). These subtypes are classified as normal breast-like, HER2 overexpressing, luminal A (ER and PR-positive, HER2-negative), luminal B (ER and PR-positive, HER2-positive or negative) and basal-like or triple negative breast cancers (TNBC, lack of ER, PR and HER2 expression) [6], [7]; as illustrated in Figure 1. For the purposes of this study, the focus will be on basal-like breast cancers. Basal-like breast cancer are a unique group of cancers due to their lack of immunohistochemical expression of HER2, ER and PR. Approximately 80% of TNBC are basal-like cancers which are clinically and immunohistochemically distinct [8], [9].

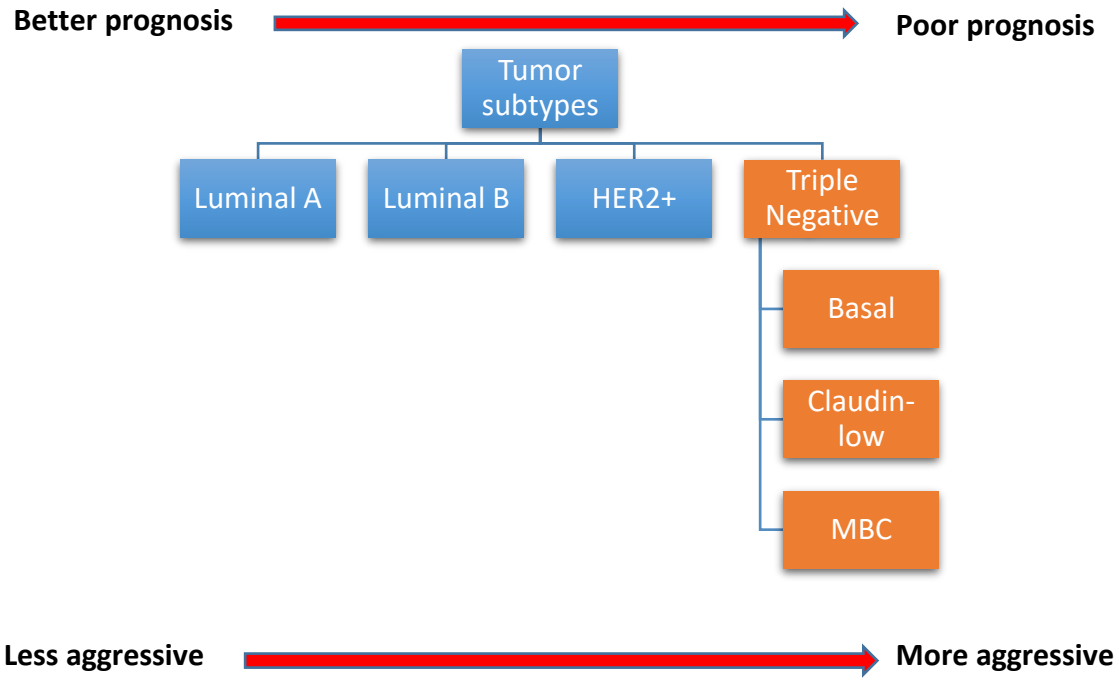

Figure 1. Classification of tumour subtypes, their prognosis and aggression profiles. *Triple negative breast cancers (orange) consists of three subtypes including basal-like, claudin-low and mucinous breast carcinoma (MBC). This subset of tumours show the worst prognosis and are highly aggressive tumours in comparison to the other subtypes i.e. Luminal A, B and HER2+. Adapted from Dai et al. 2017* [10].

Thus, it would be impractical to use hormone-based therapies and it would not be cost-effective to have routine genetic profiling in hospitals [11]. However, gene expression techniques can identify basal-like cancers, which have been suggested to be almost entirely made up of TNBCs [12]. This subtype of breast cancer accounts for only 12-17% of all breast cancer related cases, but is the leader in terms of early stage metastasis as well as cancer recurrence [13]. The prevalence of TNBC has been largely in young women of African descent, but has also been seen in American and Hispanic women and TNBC accounts for 12-15% of all breast cancers [14]. Furthermore, TNBCs are associated with poor prognosis and premenopausal women [15]. Scientists have yet to confirm whether the disease is molecularly different in African populations or if there is a genetic predisposition to the disease [16].

1.2 A brief overview of current treatments and their limitations.

1.2.1 Conventional and modern approaches for TNBC diagnosis & treatment.

Early diagnosis is pivotal in ensuring timely treatment of cancers. Conventional tools for breast cancer identification include imaging techniques such as mammography, magnetic resonance

imaging (MRI) and ultrasound. Boisserie-Lacroix *et al*. 2014, visualized round to oval lobular cells with undefined, micro-lobulated or rimmed margins using the above mentioned imaging techniques [17]. The limitations of this technology are that it is not readily available to low-income countries, also requiring skilled professionals to operate them [18] and moreover these techniques have been shown to give false-positives [19], leading to unnecessary and costly treatments. This is because TNBC usually shows benign or intermediate tumours on ultrasound and mammography as shown by Zhang *et al*., 2017. Surgery, such as mastectomy, and radiation are preferred methods of treatment but are accompanied by risks such as higher toxicity levels with increased dosages and long treatment schedules, resulting in the death of healthy tissues and complications during surgery [20]. The rise of new technologies such as molecular subtyping or precision medicine have revolutionized cancer classification [21]. Molecular subtyping has shown that surgery, in particular breast-conserving surgery (BCS), is more favourable in luminal A cancers as opposed to TNBCs [22]. However, a study has shown locoregional outcomes that mimic those of mastectomies through surgery and post-surgery radiation that gave a low risk of recurrence for over a 5-year study period in women with T1-2N0 TNBC [23]. Age is also thought to be a contributing factor to locoregional recurrence (LRR) and survival of breast cancer patients. A lower age has been associated with more positive results amongst the different subtypes, but a study by Kuijer & King, 2017, showed that surgical therapy results from both BCS or mastectomy and does not differ significantly amongst age groups, but that tumour biology is the main predictor of pathology [24].

The conventional administration of radiotherapy for TNBC is the same as in other breast cancers post BCS or mastectomy, but is still a controversial issue [9] as the effectiveness of early stage radiation after mastectomy or BCS in T1-2N0 may not be the same as in other cancer subtypes [25]. The effectiveness of adjuvant radiotherapy is still under scrutiny by the scientific community, but a study by Bhoo-Pathy *et al.,* 2015, compared adjuvant radiotherapy with BCS and mastectomies for TNBC in a cohort of Asian women. Radiotherapy was associated with higher survival rates in younger women, but overall BCS and mastectomies were associated with a decreased risk of disease [26]. Designating specific treatments for heterogenous breast cancer subtypes would improve the management of early breast cancer as stated in the 14th St Gallen International Breast Cancer Conference of 2015 [27], but recent work has suggested that breast cancer subtypes and their genetic assays can be useful in the thought process for radiation therapy, by serving as predictive biomarkers and prognostic information that is critical in future clinical research [28].

Although TNBC prognosis remains poor, this subset of cancers responds better to chemotherapies as compared to the other cancer subsets [29]. Common chemotherapy regimens to manage TNBC include damaging cell integrity using platinum compounds, taxanes and anthracycline containing regimens leading to loss of cell proliferation and apoptosis induction [30]. Some chemotherapy regimens are not defined for early and advanced stages of TNBC and makes using the appropriate dosages for chemotherapy very challenging [31]. However, third-generation chemotherapy regimens that utilize dose dense polychemotherapy as an effective regimen that is available and administration of chemotherapy preoperatively has become a standard in clinical practice [32]. Systemic treatments include cytotoxic, immunotherapeutic and hormonal agents, which can be used as adjuvant, neoadjuvant and metastatic treatment. Systemic adjuvant therapy is used post-surgery when an individual is expected to relapse and neoadjuvant is used for patients with locally advanced and inflamed breast cancer [33]. Cytotoxic treatments use a target based system e.g. targeting HER2 and using drugs such as trastuzumab and lapatinib, which then deliver antibody targeted cytotoxic effects to the tumours but these are still ineffective against TNBCs [34]. Due to the lack of a suitable conventional therapy against TNBCs, the discovery of novel biomarkers and therapeutic strategies is of high importance.

1.2.2 Cancer Immunodiagnosis & Immunotherapy

Immunodiagnosis is a broad field that focuses on the discovery, evaluation, validation and application of markers that provide critical information about a patient's disease states, both pre-and post-therapy, while also predicting the responses to immunodiagnostic agents and immunomodulatory or cytotoxic drugs. Immunodiagnostic markers may be either cell-specific, which may be classified as: i) histopathological (based on cell morphology assessments) or ii) immunophenotypic (based on immunohistochemical (IHC) assessments). The markers can be tumour-specific; classified as 1) Immune-response related gene expression profiles and 2) Tumour genotype characteristics, assessed by large scale genotypic methods such as next generation sequencing (NGS) [35].

Immunotherapy is an arm of targeted therapies that seeks to utilize an individual's adaptive and innate immune responses to combat disease. It encompasses a passive approach (in the introduction of ex-vivo agents such as antibodies and other immune cells) which does not stimulate a host immune response and an active approach stimulates an immune response and promotes the development of immune effector cells such as antibodies or T-cells [36]–[38].

Immunotherapy offers an alternative to chemotherapy and hormone therapy, such as the blocking of CTLA-4, which functions in the down-regulation of T-cell responses activated by tumour development, but this method of treatment is limited to intrinsic immunogenic tumours [39]. Hormonal therapy with tamoxifen or aromatase inhibitors have shown clinical efficacy, but issues are found when the patient takes the incorrect dosages or discontinues treatment, which suggests that the treatment is only effective when taken for extended periods of time [40]. Cancer immunotherapy has shifted the paradigm of cancer therapies which is necessary for cancers that cannot be treated by conventional means, such as TNBC [41], [42]. There are various types of immunotherapy which include T-cell based therapies, T-cell engineering & Antibody based therapies. An example of T-cell based therapies is the use of vaccines which is a host-directed immunotherapy [43]. Since their introduction by Edward Jenner and his smallpox vaccine in 1796 [44], there have been various types of vaccines that have been designed such as: Live attenuated vaccines (makes use of a weakened strain of a pathogenic inducing long-lived immunity to disease but is not suitable for the immunocompromised due to adverse immune effects [45]); Inactivated vaccine (comprised of a killed pathogen that cannot double in number but the immune response is relatively weak [46]); Subunit vaccine (A highly secure vaccine that focuses on inducing an immune response for the most dominant epitopes on a pathogen but normally requires more than one dose [47]); Toxoid vaccine (induces a strong and lasting immune response to the toxin of the pathogen but an additional dose may be required [48]); Conjugate vaccine (a vaccine that is safe for infants that consists of a protein fused to a weak antigen from a pathogen which induces a lasting immune response but it is relatively expensive to make [49]); DNA vaccine (a non-infectious vaccine that uses fragments of DNA that encode for certain antigens from pathogens but is limited to the production of protein antigens [50]) and Recombinant vaccines (introduces recombinant DNA using a viral or bacterial vector producing a strong immune response but vector immunity may result in adverse immune effects [51]).

T-cell engineering is an arm of medicine that makes use of genetic engineering and molecular biology techniques to produce synthetic probes to combat a variety of diseases by recruiting and activating T-cells [52], [53]. Examples of these synthetic probes include Bispecific antibodies (BsAbs) which have two binding sites that work synergistically and are able to bind different epitopes with different specificities [54]. Other BsAbs formats have been used such as bi-specific T-cell engagers (BiTEs), dual affinity re-targeting antibodies (DARTs) and Tandem diabodies but the antibody formats that are commonly used in present day are single

chained variable fragments (scFv) and single domain antibody (SdAb) formats [55]. Antibody or ligand based therapies have the goal of eliminating or neutralising diseased cells by inhibiting the functionality of certain substances, specific targeting of diseased cells or by adopting the role of signalling molecules [56].

Antibody conjugates are different formats of antibodies fused an effector molecule(s), examples of these include radionuclides to form radioimmunotherapy which uses mAbs combined with radioisotopes to treat diseases such as low-grade lymphoma [57], [58] but the downfall to this technology is that the radiation is not limited to the target organ but continues in circulation, decays and harm healthy tissues [59]. Immunotoxins are a combination of a targeting domain and a toxic protein and, in most cases a bacterial or plant derived toxin, in order to treat disease [60]. Historically, immunotoxins would induce a neutralizing immune response but immunogenicity can be greatly reduced by removing the B or T-cell epitopes from the protein toxins and humanization of bacteria/plant toxins [61], and prime candidates for immunotoxin research include granzyme B, angiogenin, DAP-K and Map-Tau [62]–[66]. Specific novel immunotherapeutic agents such as antibody drug conjugates (ADCs) including human cytolytic fusion proteins (hCFPs) and immunotoxins (IT) hold promise in being treatments for breast cancers and other diseases [67]. ADCs have the ability to transfer toxic agents to specific tumour cells. hCFPs are a class of humanized immunotoxins that contains a ligand which binds specifically to target cells, which have an apoptosis inducing enzyme genetically attached. hCFPs can bind to targeted cancer cells by any type of recombinant antibody or scFvs [68]**.** There are currently only two ADCs that are FDA approved, Ado-trastuzumab (which is a HER-2 targeting conjugate that exerts its cytotoxic effects by inhibiting microtubule assembly) and Brentuximab Vedotin (which targets CD30 on Hodgkin and anaplastic large cell lymphomas but has also been used for HIV treatment [69]–[71].

1.2.3 ScFv and Nanobody formats as a branch of Immuno-diagnostics & therapy

Monoclonal antibodies (mAbs) have been established as biotherapeutic proteins that are used as modes of treatment for a variety of diseases [72]. The use of animal serum containing polyclonal antibodies and toxins saw the dawning of antibody based therapies which sired hybridoma technology (1975) and the eventual rise in the use of mAbs which impacted the pharmaceutical industry [73]. mAbs are an example of immunotherapeutic agents that can induce cellular toxicity by antibody or complement dependent cytotoxicity [74]. As of 2017,

there are 61 mAbs in clinical use but only two mAb's, trastuzumab and cetuximab, are approved for therapy in breast cancer [75]. The utilization of mAbs for cancer therapy may have proven to be efficacious by activating inhibitory immune complexes, altering tumour-relating signalling pathways and inducing immune responses against tumours but only have intermediate activity in reducing tumours and therefore have to be administered in high doses [76].

Table 1. The advantages and disadvantages of monoclonal and single domain antibody formats*. Adapted from Runcie et al, 2018* [77] *and ProSci, 2018 (https://www.prosci-inc.com/resources/antibody-development-guide/antibody-structure-and-properties/).*

	Antibody format	
	Monoclonal antibody	Single domain antibodies
Advantages	• Highly specific • Constant and renewable supply • Can be used for imaging • Homogenic nature allows for reproducibility	• Highly specific • Constant and renewable supply • High stability • Large scale production at low cost. • Can be used for imaging. • Homogenic nature allows for reproducibility. • Small size allows for faster clearance and therefore low immunogenicity. • High thermostability and good solubility.
Disadvantages	• Limited penetrative ability • Long and costly development periods • Large molecules take longer to clear and increases potential of aggregation and immunogenicity	• Costly development periods. • Targeting single epitope may lead to acquired resistance. • Extent of genetic engineering is limited.

- Targeting single epitope may lead to acquired resistance

mAbs are generally Y-shaped molecule with two upper branches (V shape) each housing receptor binding regions which contribute towards specificity and affinity. The single stem of the molecule is called the Fc or constant region and is responsible for cell killing mechanisms and extended half-life in circulation through interactions with Fc receptors [78], [79]. Typically, mAbs consists of two light (LC) and two heavy variable chains (HC) that make up the fragment antigen binding region (Fab). These chains are held by highly conserved amino acid residues (C_{H1} for the heavy chain and C_L for the light chain) extending from the framework region of the antibody as seen in Figure 2 [80]. The light chains are categorized under lambda (λ) and kappa (κ) class, and the heavy chains are categorized into alpha (α), gamma (γ), delta (δ), epsilon (ε) and mu (μ) dependent on the class of immunoglobulins (Ig) [81]. The binding component of antibodies have been at the heart of antibody engineering research because of their targeting ability. They consist of six complementarity-determining regions (CDRs) i.e. three from the HC and LC respectively [82]. The Within the binding domain there is variability in the amino acid sequences on the heavy and light chains (V_H and V_L) of about 110 amino acids, which are the determinants of the antibody isotype, referred to as the V-domain (Fv) which confers the specificity of the paratope of the antibody [83], [84]. Antibody derivatives can be used as diagnostic or therapeutic tools and are more easily produced than monoclonal antibodies. They are usually engineered in the form of fusion proteins [85]. The use of engineered antibodies has proven advantageous in fields of research, diagnosis and therapy. Although full-length mAbs have provided advancements, their size limits their penetrative ability *in vivo* [86].

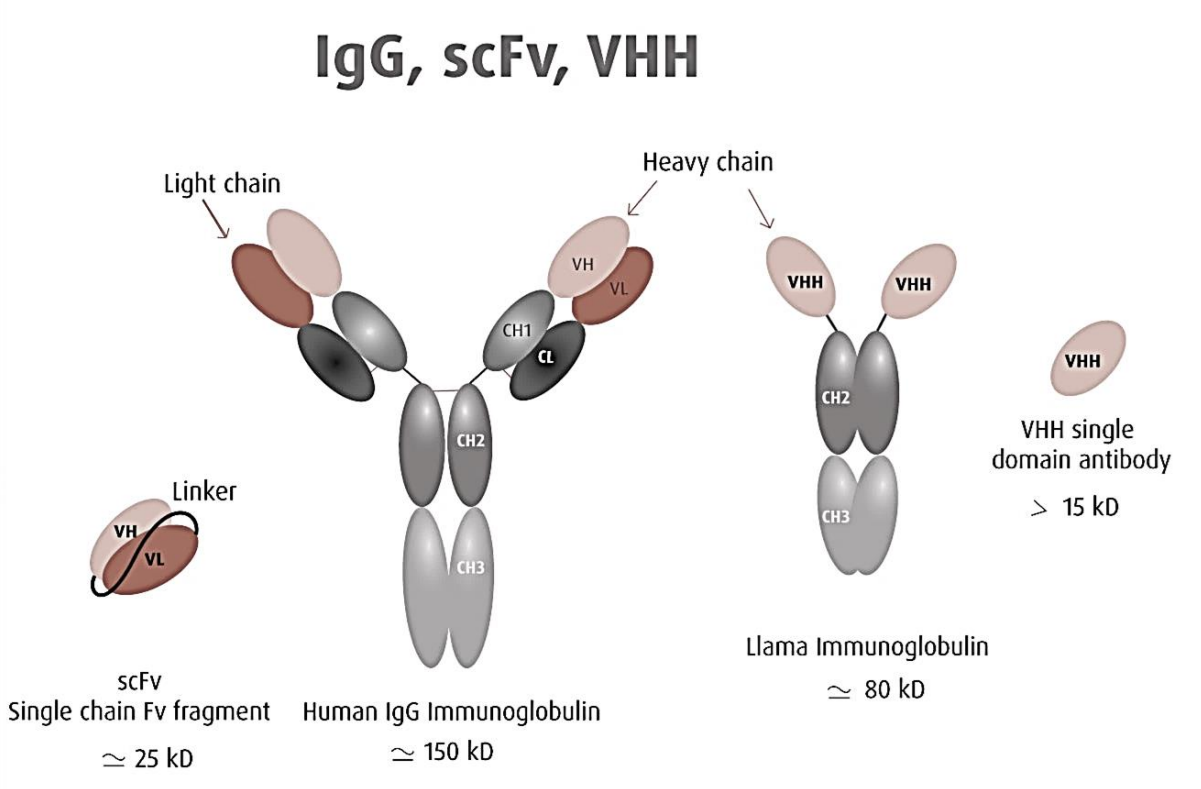

Figure 2. Schematic diagram of different antibody formats. *The illustration shows the development of antibodies in the immunotherapy field. Antibody development initially started with full sized monoclonal antibodies to single chain Fv fragments and thereafter further improving to single body formats.. Acquired from (https://www.hybribody.com/contenu/synthetic-vhh-library-menu/take-advantage-of-vhh-antibody-properties).*

The improvements in antibody engineering have allowed for the synthesis of smaller antibody formats without interfering with the paratope of the antibody. The smaller antibody formats such as scFv and antigen binding fragments have shown favourable characteristics towards diagnostic and therapeutic applications without the limitations seen in the larger antibodies as seen in Table 1 [87]. The structure of the scFv molecule consists of variable regions of the heavy chain (V_H) and light chain (V_L) chains bound together by e.g. a serine/threonine linker (~3.5 nm in length) [88]–[91]. Furthermore, the scFv antibody shows target specificity and affinity *in vivo* that propelled its development as delivery molecules towards cancer treatment [92], [93] It confers some favourable characteristics such as reduced immunogenicity, faster clearance from blood circulation and low retention in non-target tissue, and improved tumour penetration as compared to full sized antibodies [94]–[96]. This antibody format has been genetically modified to be used in conjunction with toxins, drugs and radioisotopes [96]–[98], they may be used as gene delivery tools and as anticancer agents [93]. Along with scFv, nanobody formats have shown promise in research, diagnosis and therapy.

Fully functional antibodies consisting of only heavy chain fragments were first found in the sera of camelids and described by Professor Hamers research group at the University of

Brussels in the early 90s. Nanobodies are single domain antibodies derived from camelid immunoglobulins that naturally consist of two variable heavy chains (VHH) and one antigen-binding domain and are approximately 13-15kDa in size as shown in Figure 2. These homodimeric antibodies contain providing advantageous properties such as size, high affinity, stability, specificity, low production costs and their generation is less laborious as compared to mAbs and scFvs [99]–[102]. The VHH show about 90% similarity to the heavy chain fragment of human antibodies thus minimizing their immunogenic response. Furthermore, humanization of this antibody by CDR grafting has shown to increased similarity up to 99% [103], [104]. CDR grafting is a process that is based on selecting the CDR sequences of the non-human antibody and combining this with the framework of a human antibody [105], [106]. As previously mentioned, nanobodies naturally show 90% similarity to the VH of human antibodies and the humanization of these antibodies could possibly hinder functionality based on possibly incorrect amino acid substitutions. A study by Vincke *et al*, 2009, proposed a single humanized nanobody, h-NbBcII10FGLA that was synthesized from nanobody NbBcII10 (belonging to subfamily-2 of nanobodies), that ensures full retention of antibody stability & functionality [107], [108]. The small size of the antibody makes it easier to express high yields of antibodies in expression systems and because it is made up of 1 domain, the posttranslational modifications are far less complex [101], [103]. The domain stability affinity of nanobodies (VHH) is contributed by an additional disulphide bond between CDR 1 and CDR3 regions. This link forms an interloping bond which allows for the recognition of different and unique epitopes that may be inaccessible to conventional antibodies [102], [109], [110]. Nanobodies have the potential to make significant contributions towards advanced microscopy and immuno-imaging. Immuno-imaging is an imaging tool with the aim of studying patient diseases using radiolabelled Ig probes in conjunction with positron emission tomography. Nanobodies are fast and highly specific delivery molecules *in vivo* and show potential in being the new state of the art in diagnostics [100], [111].

1.3 CSPG4, Mesothelin and Epidermal Growth Factor Receptor targeting SNAP fusion proteins as an approach to TNBC antibody-based diagnosis & therapy

1.3.1 SNAP-tag technology as a powerful tool for diagnosis

SNAP-tag is a 20kDa modified version of the human DNA repair enzyme O6-alkylguanine-DNA-alkyltransferase (AGT) which permits site-specific self-labelling of SNAP tag-based fusion proteins. This technology can also be used to generate a novel antibody format by its

fusion to a recombinant antibody fragment allowing directed conjugation to benzylguanine (BG)-modified substrates in a 1:1 stoichiometry [112]. SNAP-tag is unique compared to other self-labelling proteins in that it ensures rapid, specific and covalent binding to derivatives, is easily producible [113] and are of greater preference compared to conventional small peptide tags [114].

SNAP-tag is a versatile and novel technology that allows for the labelling of covalently linked proteins with a variety of fluorophores that contain a BG moiety [115]. SNAP-tag is also considered to be an efficient labelling tool due to its multi-purposed mode-of-action. SNAP-tag can be used to label surface molecules or intracellular organelles, such as cytosolic proteins, the nucleus and mitochondria, based on the permeability of the BG substrate [116]. SNAP-tag has numerous applications in protein labelling, because its auto-catalytic reaction to BG derivatives is independent to the nature of the attached synthetic probe, which allows for the labelling of SNAP fusion proteins to a variety of synthetic probes [117].

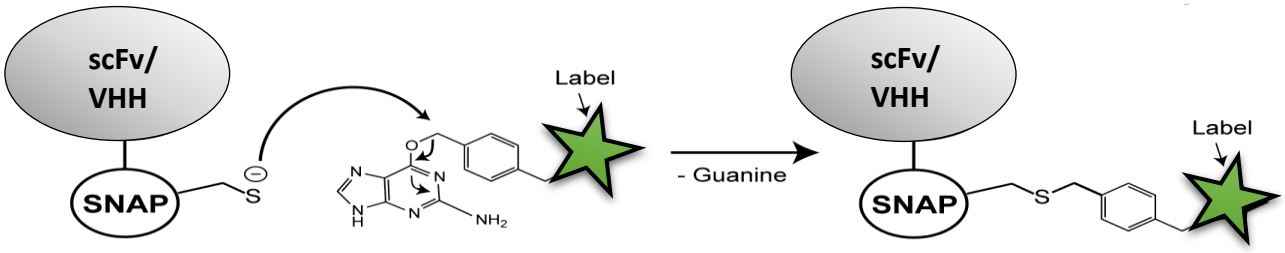

Figure 3. Schematic diagram of SNAP-fusion protein reacting with BG-substrates. *The scFv or VHH component of the fusion protein is recombinantly fused with SNAP-tag which allows for covalent binding with BG-modified substrates in a 1:1 stoichiometric ratio.*

SNAP-tag technology allows for numerous approaches to diagnosing disease such as using a targeting SNAP-tag fusion protein conjugated to a BG-fluorophore to identify markers on diseased tissues [118]. SNAP-tag can also be used for the treatment of cancer through site-directed delivery of effector molecules, such as synthetic small molecule toxins, photosensitizers or nanoparticles in the form of antibody drug conjugates (ADCs) to diseased tissues. SNAP-tag-based ADCs have a multitude of benefits over traditional ADCs. The 1:1 stoichiometry allows production of homogeneous conjugates, providing a defined drug to antibody ratio and facilitating the quantification of pharmacokinetic properties of the therapeutic moiety. Additionally, the self-labelling process eliminates the need for additional chemical conjugation steps, lends ease and simplicity to the development of such therapeutic tools and preserves the structure and function of the antibody, which is not subjected to the harsh conditions by chemical modifications. The intermediate size of the scFv-SNAP construct

still allows rapid accumulation and efficacious binding to tumour tissue soon after injection, together with rapid renal clearance, producing a high tumour-to-background ratio [119]–[121]. SNAP-tag fusion proteins have thus far been a great success in preclinical xenograft tumour models. Live cell imaging approaches to visualize tumour behaviour are more challenging to address, specifically since they require use of chemical probes that give off background fluorescence due to off-target effects [122], [123]. SNAP-tag technology has also allowed for the visualization of live cells by manipulation of SNAP-tag fusion proteins with fluorescent labels, but also getting a three-dimensional framework and surface patterns of the cell [124]. SNAP-tagged probes have minimal to no off-target effects due to its monovalency and high specificity to a single protein of interest when fused to a targeting antibody [125]. Improvements have been made to this technology with the design of a variant called SNAP-F. SNAP-F was generated by the addition of point mutations a C-terminal deletion that resulted in a 19 amino acid difference between SNAP-F and the hAGT sequence , and a 10 amino acid difference between SNAP-F the commercially available SNAP-tag [123], [126]. It has been shown to be more efficient in terms of versatility, speed, sensitivity and shows up to tenfold increased reactivity to BG-substrates in comparison to the conventional SNAP-tag [123], [127], [128]. This study will involve synthesizing SNAP fusion proteins that encompass an anti-CSPG4, anti-Mesothelin and anti-EGFR scFvs as well as VHH formats conjugated to SNAP-tag and the SNAP-F variant.

1.3.2 Chondroitin sulfate proteoglycan 4 (CSPG4) as a target on TNBCs

CSPG4 was originally described as a transmembrane proteoglycan that functions to facilitate the growth and survival of cancer cells. It serves as a highly immunogenic tumour antigen on the surfaces of melanoma cells, but has been shown to be expressed in various types of human carcinoma and sarcomas [85]. An orthologue of CSPG4, n/glial antigen 2 (NG2), has also been described in rats [129], [130]. The functionality of tumour cells associated with CSPG4 can be inhibited by the use of CSPG4-specific monoclonal antibodies *in vitro* and *in vivo*, and its inhibitory properties are thought to stem from the blocking of migratory, proliferative and survival pathways of the tumours [131]. CSPG4 has a large extracellular domain, a 25 amino acid transmembrane region and a 75 amino acid region intracellularly as shown in the illustration below (Fig. 4) [132]–[134]. CSPG4 is constituted by three extracellular domains (D1, D2 & D3) which are structurally and functionally distinct leading to the activation of factors that trigger cascades in the pathway and transcription [133]. The D1 domain, on the N-

terminal, is home to a plethora of signalling sites including Laminin G binding sites. Although the exact function of laminin domains is unclear, they have been shown to be involved in site-directed mutagenesis, tumour migration and proliferation through activation of specified pathways [135], [136]. The largest extracellular domain (D2) is rich in glycine and serine, and is also characterized by chondroitin sulfate glycosaminoglycan (CSGAG) modifications as well as N- and O- linked glycosylation sites [137], [138]. The C-terminal D3 is globular region involved in N-linked glycosylation and has pronounced carbohydrate modifications that allow binding of galectin 3 or other lectins such as p-selectin [12], [139], [140]. The threonine cluster consists of Extracellular-signal-regulated-kinase (ERK) 1,2 and Protein Kinase C-alpha (PKCα) phosphorylation sites and a PDZ-motif, which comprises of anchoring proteins such as syntenin, MUPP1 and GRIP1 [132], [133], [141], [142] to attach the CSPG4 to the actin cytoskeleton. Upon phosphorylation of the threonine cluster by ERK 1,2 & PKCα there is activation of cell survival and proliferation pathways leading to more cell motility and epidermal-mesenchymal transition (EMT) [137], [140].

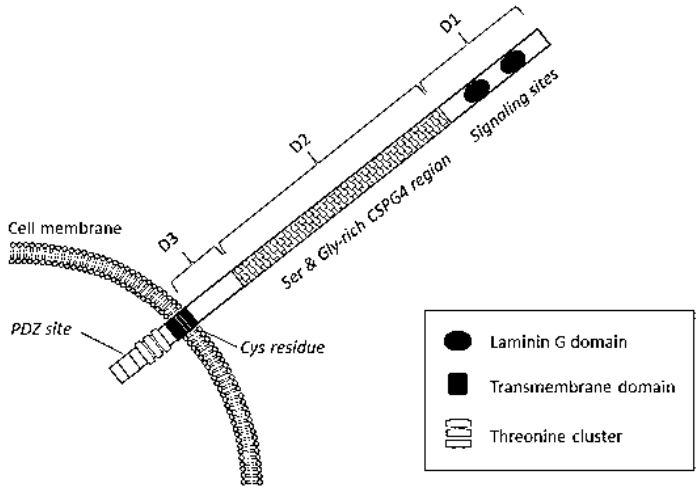

Figure 4. Schematic diagram of the structure of the transmembrane CSPG4 receptor. *The organization of CSPG4 consists of D1, D2 & D3 extracellular domains, a transmembrane domain a threonine cluster intracellularly. D1 houses Laminin G binding sites and D2 is rich with serine and glycine. Adapted from Amoury et al, 2016.*

Phosphorylation of the threonine cluster results in the activation of signalling proteins that result in cell proliferation which is commonly via the mitogen-activated protein kinase (MAPK) and Focal adhesion kinase (FAK) pathway [143], [144]. CSPG4 interacts with the anchoring protein, syntenin, promoting the activation of FAK resulting in signalling cascades inclusive of FAK-integrin-extracellular matrix (ECM) assembly and activation of phosphoinositol 3-Kinase (PI3K)/ protein kinase B (AKT)/ nuclear factor kappa beta

(NFKβ)/melanocyte lineage specific transcription factor (MITF) pathways as illustrated in Figure 5. The consequence of this activity is cytoskeleton remodelling, cell survival, chemoresistance and migration [145], [146]. The activation of CSPG4 also triggers cascades associated with receptor tyrosine kinases (RTK) i.e. RAS-RAF-MEK-ERK1,2 [145], [147]. The activation of ERK 1,2 by CPG4 results in changes in gene transcription as a result of MITF resulting in EMT [148].

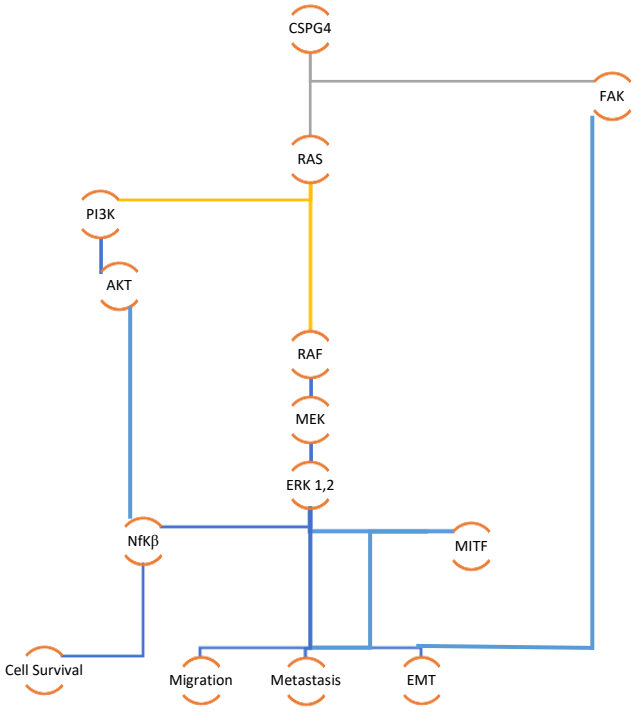

Figure 5. Schematic diagram of CSPG4 pathway leading to cancer survival and metastasis. Adapted from Price et al, 2011.

CSPG4 has evident potential as a target for immunotherapy in breast cancer. CSPG4 has been attributed to P-selectin binding in aggressive cancer cell lines, and contributes to metastasis of breast cancer [112]. According to Beard, *et al.*, 2014 and Amoury, *et al.*, 2016, CSPG4 is expressed in 50% of TNBC, and therefore is an effective model for monoclonal antibody-based treatment, which has been shown to block CSPG4-linked signalling pathways and inhibit tumour growth *in vitro*. In this study, a high affinity anti-CSPG4 (scFv) antibody conjugated to SNAP-tag to generate a CSPG4-specific SNAP-tag fusion protein will be used as a novel diagnostic tool for TNBC.

1.3.3 Mesothelin as a potential target on TNBCs

Organs in the abdominopelvic regions of the human body are normally covered by a single layer of mesothelium which comprises of flat squamous-like cells containing laminin,

fibronectin and collagen I & IV, all originating the mesoderm [149]–[152]. Mesothelin (MSLN) is a 40kDa glycosylphosphatidylinositol-linked cell surface antigen that is present in normal human tissues. Antigen expression is limited to the linings of pleura, the peritoneum and the pericardium of these tissues. The mesothelin antigen is overexpressed in several human malignancies, including mesothelioma, pancreatic, ovarian, lung adenocarcinomas and TNBC [153]. Mesothelin was initially described in 1992 as a cleavable 70kDa protein resulting in a 40kDa protein anchored to the membrane by GPI and a 30kDa megakaryote potentiating factor (MPF) as seen in figure 6 [154]–[156]. However, with the knowledge of the furin cleavage that the precursor undergoes, the three-dimensional structure and biological function of mesothelin is still poorly understood. Recent studies have shown that mesothelin is involved in driving cancer progression through the interactions with MUC16/CA-125, particularly in mesothelioma and ovarian cancer [156]–[160]. The binding motif of MSLN is separated into an MCAT and an SP-1-like region [161], [162]. Previous studies have also shown that the eight nucleotides of MCAT are important toward the function of the receptor and mutations in the SP-1-like domain are characteristic of cancer progression and metastasis, however, the transcription factor that promotes overexpression in human malignancies is yet to be identified [163].

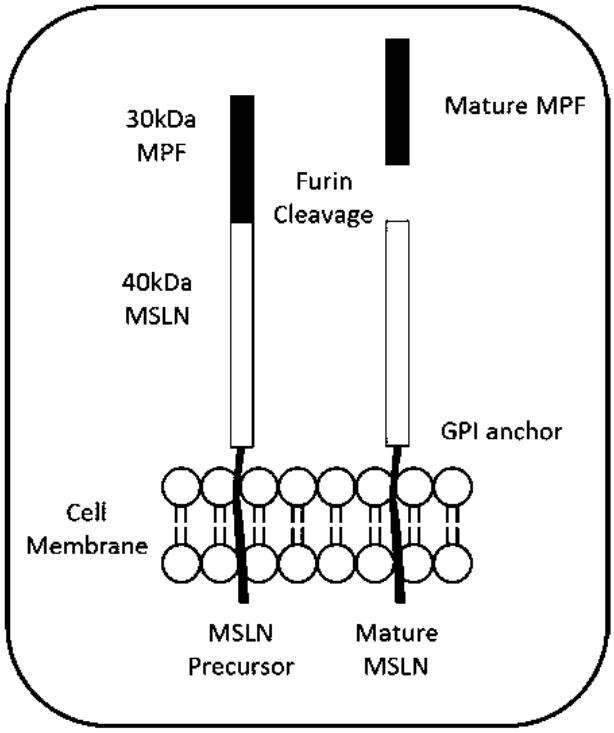

Figure 6. Schematic diagram of transmembrane mesothelin receptor. *The full mesothelin transmembrane protein is cleavable releasing the 30kDA MPF and leaving the 40kDa membrane bound protein (adapted from https://www.mdpi.com/2072-6694/10/9/277/htm#B42-cancers-10-00277).*

Stimulation of mesothelin triggers a cascade that ultimately results in cell proliferation, adhesion, survival, migration and invasion by cancerous tissues as seen in Figure 7 [158], [164]–[166]. Cancer progression, survival, invasion and resistance as a result of mesothelin has been linked to the induction of MMP-7 via the MAPK/ERK & PI3K/AKT pathways resulting in the inhibition of proapoptotic family of proteins, such as Bad & Bax, and activation of anti-apoptotic proteins, such as Bcl-2 & Mcl-1, leading to inhibition of apoptosis (Fig. 7) [167]–[169]. The MAPK/ERK pathway results in the down regulation of proapoptotic family. The phosphorylation of AKT via PI3K activation results in the inhibition of tumour necrosis factor (TNF-α) driven apoptosis due to the inhibition of pro-apoptotic family and increased expressions of anti-apoptotic proteins [167], [168], [170]. The overexpression of MSLN on the cell surface has shown to increase the levels of interleuken-6 (IL-6) which activates transcription factor protein 3 or Stat3. Stat3 results in the upregulation of cyclin E/cyclin-dependent kinase (CDK2) complex, activating the cell cycle and also accelerating the G1-S phase transition, contributing to proliferation of cancerous cells [164], [166].

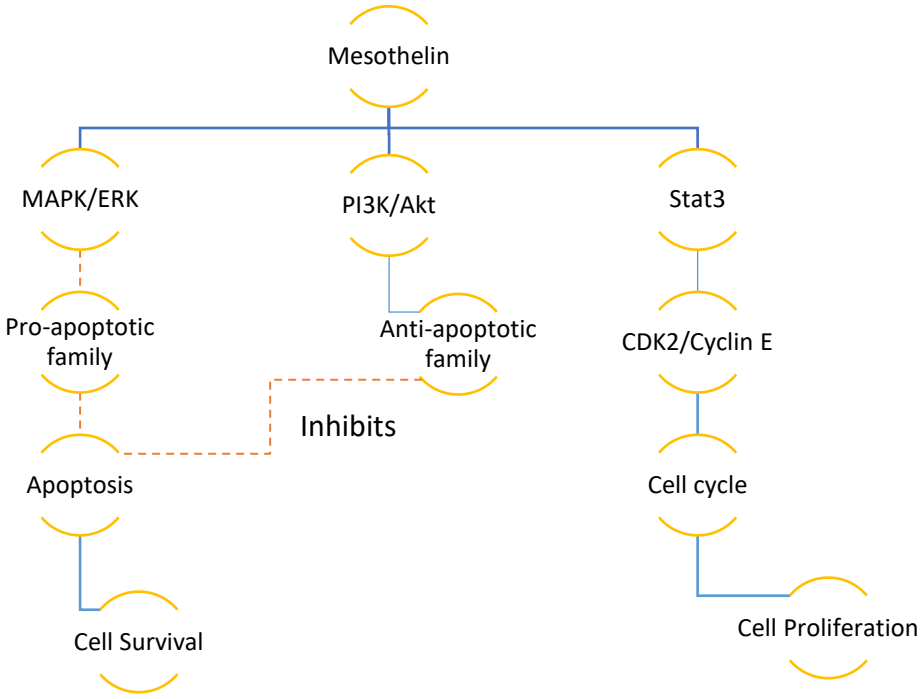

Figure 7. Schematic diagram of Mesothelin pathway leading to cancer survival and cell proliferation. Adapted from Tang et al, 2013.

MSLN is not characteristically expressed in breast cancer but a study by Tchou *et al*, 2012, found that the surface antigen is expressed in about 67% of TNBC tissues [171]. In normal tissues, mesothelin is expressed on mesothelial cells which are expendable, thus making it an attractive target for immunotherapy against TNBC, for which there is currently no therapy

[160], [172]. Attempts towards a long-lasting therapy for mesothelin related cancers have been made. These include antibody-based therapy such as immunotoxins, chimeric monoclonal antibody & antibody-drug conjugates, as well as mesothelin vaccines but no long-lasting therapies have been described [156], [173]. Different imaging platforms have shown successful imaging data on mesothelin related cancers which is are important steps to improving immunodiagnostics of these diseases. In a study by Weele *et al*, 2015, an αMSLN antibody was labelled with zirconium, a strong & malleable metal, to assess the biodistribution of MSLN in mice with pancreatic tumours using micro PET imaging [174]. A different study, made use of immunoPET imaging making use of a phase I αMSLN antibody conjugated to monomethyl auristatin E (MMAE) and MSLN expression, tumour uptake & whole body distribution in patients with pancreatic and ovarian cancers [175]. Another study by Prantner *et al*, 2015, produced αMSLN nanobodies that could recognize native and denatured mesothelin antigens using optical imaging, flow cytometry & immunofluorescence [86]. In this study, a high affinity anti-MSLN scFv and VHH recombinantly fused to SNAP-tag to generate a MSLN-specific SNAP-tag fusion protein will be used as a novel diagnostic tool for TNBC.

1.3.4 Epidermal Growth Factor Receptor (EGFR) as a potential target on TNBCs.

EGFR is a transmembrane protein that is a member of the ErbB family of receptor tyrosine kinases. It is activated when bound to peptides of the EGF-family. This group of RTKs protein consists of four members which are ErbB2/HER2, ErbB3/HER3 ErbB4/ HER4 and EGFR. EGFR is a 170 to 185kDa glycoprotein, also known as HER-1 or c-ErbB-1 and was the first member of this RTK to be described. There has been confirmation of EGFR involvement in progression of cancers of the lung, oesophagus and breast tissues when the protein is overexpressed, making it an attractive target [176]–[181]. The structure of each RTK is made up of an extracellular ligand binding domain, a single transmembrane domain (TM) and an intracellular domain with tyrosine function. Characteristically, members of ErbB family consist of an extracellular domain abundant in cysteine at the N-terminus, a hydrophobic transmembrane region and a highly conserved intracellular C-terminus with many phosphorylating sites as shown in Figure 8 [182]–[184]. The extracellular domain of EGFR is made up of 4 subunits (I, II, III & IV) that have open and closed conformations. The open conformation is considered as the active form as it allows binding to the corresponding ligands at regions I & II. Subunits II & IV interact with each other in the inactive form or closed

conformation thus prohibiting the binding of any ligands [184]–[187]. ErbB receptors are regulated by at least 12 different growth factors which include transforming growth factor-α (TGF-α) and EGF. Activation of RTK begins when ligand (growth factor) binds to the extracellular receptor domain, which triggers the homo and/or heterodimerization of the receptor, follow by internalization within the cell [188], [189].

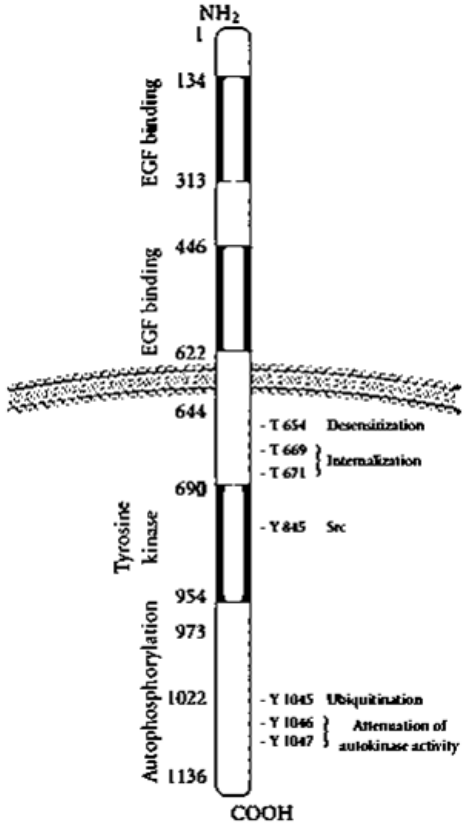

Figure 8. Schematic diagram of transmembrane EGF receptor*. Extracellularly EGFR has four subunits that may be in an open (active) or closed (inactive) conformations. This region has It has a hydrophobic transmembrane region and a highly conserved intracellular domain that houses the tyrosine kinase domain and has autophosphorylation sites (adapted from https://www.hindawi.com/journals/jo/2010/568938/fig1/).*

Mutations in this protein have also shown an increase in the activation of the downstream signalling pathways such as RAS-RAF-MEK-ERK-MAPK and AKT-PI3T-mTOR pathways, resulting in proliferation of the diseased tissues (Fig. 9) [190], [191]. Upon internalization, intracytoplasmic tyrosine kinase domain of the EGFR is autophosphorylated and assists in recruiting signal transducers and activators of intracellular substrate such as Rat sarcoma (Ras). Once activated, Ras will activate downstream signaling cascades such as RAF/MEK1/2/ERK1/2 and/ or PI3k/Akt which will culminate in translocation of their effector molecules (e.g.: ERK1/2) into the nucleus where they will control the transcriptional activity of genes regulating cell proliferation, survival, differentiation and migration [191].

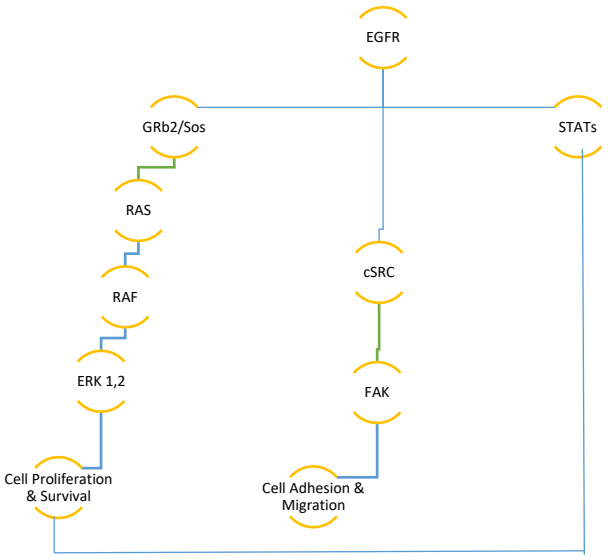

Figure 9. Schematic diagram of EGFR leading to cancer proliferation and migration. *Adapted from Krawczyk et al, 2009.*

Overexpression of EGFR has been shown to be a problem particularly in breast cancers. Approximately 50% of TNBC overexpress EGFR and there is currently no adequate therapy for this disease. EGFR inhibiting agents have been looked at as a possible therapy but showed poor results [179]. There are currently two monoclonal antibodies, cetuximab and panitumumab, in clinical practice that target for EGFR [192]. EGFR targeting radiolabelled nanobodies have been used in a study by Piramoon *et al*, 2017, showed promising results in hindering progression of cancer in nude mice [193]. Recent advancements in therapies, the diagnostic aspect also requires some improving. A study by Lee *et al*, 2017, used PET/CT scanning & immunohistochemistry on breast cancer to assess the uptake and it was shown that high breast tumour rates are strongly influenced by the presence of EGFR [194]. A novel fluorescent probe, (EGF)-Cy5.5, coupled with an anti-EGFR monoclonal antibody was tracked *in vivo* using continuous wave fluorescence imaging and near-infrared (NIR) optical imaging. This imaging method showed that it is possible to have images while using low doses of fluorophore (1 nmol/mouse), but it still held some limitations such as background fluorescence in the mice and the emission period of the NIR dyes used [195], [196], [196]. In this study, a high affinity anti-EGFR scFv and VHH recombinantly fused to SNAP-tag to generate a EGFR-specific SNAP-tag fusion protein will be used as a novel diagnostic tool for TNBC.

1.4 Aims & Objectives

TNBC is an aggressive subset of breast cancers that mainly affects young premenopausal women. There is currently has no adequate long-lasting form of therapy for this disease. This study aims to generate novel immunodiagnostic agents (scFv and VHH antibodies) that target surface antigens known to be overexpressed in TNBCs (CSPG4, MSLN and EGFR), and utilizing SNAP-tag® technology toward this goal. Furthermore, the performance of the VHH antibody format against the scFv when combined with SNAP-tag® technology will be evaluated. Previous work suggests that features of the VHH shows more favourable results in comparison to the scFv [197], [198] and we seek to investigate if the binding capacity is affected by the conjugation of SNAP-tag®. The plasmid system encompasses the genes of the targeting molecule (scFv/VHH), Ampicillin and Zeocin/Bleomycin resistance genes for selection of transformed clones in bacterial culture and transfected cells in mammalian cultures. The plasmid also contains an enhanced green fluorescent protein (EGFP) gene that serves as a reporter of protein production in mammalian cultures. The proteins will be evaluated on their producibility in culture with the fluorescence of the EGFP reporter protein and efficiency data drawn from this. The proteins will also be evaluated on the ability to bind BG-modified molecules (testing the SNAP-tag component of the protein) and the ability to bind surface antigens on tumour cell lines (testing the specificity of the scFv/VHH) both visualized using confocal microscopy. The long-term aim of this work is to ensure a novel combination product that can be used for diagnostic purposes of CSPG4, MSLN & EGFR positive cancer cells as well as for directed therapies by replacing the diagnostic label by a therapeutic label.

This research also serves as a foundation for further studies directed at *in vitro* binding of SNAP-tag and its potential applications in various fields of study. This project seeks to ultimately develop a diagnostic tool that encompasses ER, PR, HER2, MHC1 (major histocompatibility complex 1), EpCAM and PDL-1 (programmed death ligand 1) together with CSPG4, MSLN & EGFR. This would in the future allow to identify the groups of patients positively responding to e.g. a CSPG4-specific immunotherapy.

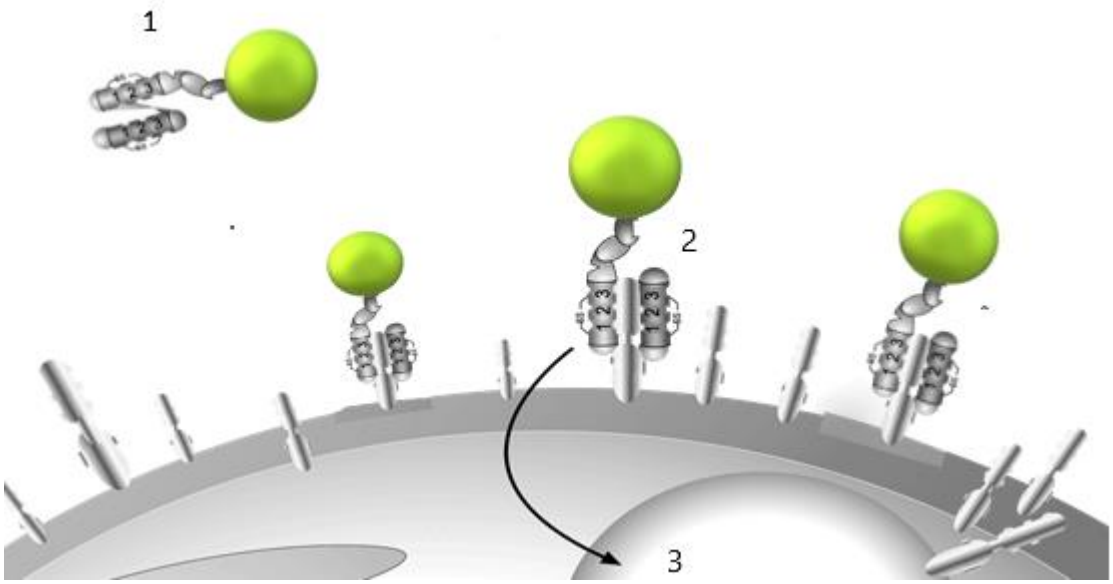

Figure 10. SNAP fusion protein conjugated to Alexa488 mechanism of action*. 1) The Protein-Fluorophore conjugate molecule is in the extracellular environment. 2) Protein-Fluorophore attaches to the specific cancer cell and accumulate on the surface of the cell. 3) The Protein-Fluorophore molecule will be internalized.*

1.4.1 Main goals/overall objectives of this study:

1. To evaluate different antibody formats to improve the diagnostic potential of SNAP-tag based antibody fusion proteins

To obtain this goal, this will include the following objectives:

- The design of an appropriate vector system for expression of recombinant SNAP-tag fusion proteins targeting CSPG4, MSLN & EGFR.
- Cloning of the open reading frames (ORFs) into the vector system.
- Transfection of constructs into HEK293T mammalian cells for the expression and monitor transfection efficiency by the amount of eGFP positive cells.
- Harvesting of recombinant proteins from the supernatant of cell culture.
- Purification of the recombinant proteins by immobilized metal affinity chromatography (IMAC) using an ÄKTA avant protein purification system.
- Analysis by SDS & western blot to confirm expression and purification.
- Binding studies in TNBC positive cell lines.

Chapter 2: Materials & Method

2.1 Chemicals, consumables, equipment and suppliers

All chemicals and kits used in this study were obtained from the following suppliers: Thermofisher Scientific (Waltham, USA), Qiagen (Hilden, Germany), Machery-Nagel (Düren, Germany), Merck-Sigma (Kenilworth, USA), Integrated DNA Technologies (Coralville, USA), GE Healthcare (Little Chalfont, UK), New England Biolabs (Ipswich, USA), BioRad (Hercules, USA) and Biochrom (Berlin, Germany).

The consumables and equipment used in this study were purchased locally from the following suppliers: Bio-Smart, Labotec, LasecSA, Separations, Whitehead Scientific, Inqaba Biotec and the scientific group.

The following is a detailed list of all equipment used in the course of the study:

Equipment	Manufacturer/supplier
• Blue light transilluminator (Dark reader DR-89X)	Clare Chemical
• BSCII cabinet (Nu5113-400E)	NuAire
• Cell counting chamber (Neubauer)	Marienfeld
• 15 ml / 50 ml Centrifuge (Allegra X-30R)	Beckmann-Coulter
• CO2 incubator (ICO 50med)	Memmert
• CO2 incubator (NU-5800E)	NuAire
• Confocal microscope (LSM-880 Airyscan)	Carl Zeiss
• Electrophoresis system (Mini-PROTEAN Tetra Cell Mini Trans-Blot Cell)	Bio-Rad
• Electrophoresis system (Sub-Cell GT mini & wide-mini)	Bio-Rad
• Fluorescent imager (ZOE Cell Imager)	Bio-Rad
• Flow cytometer (BD LSR II)	Becton-Dickinson
• Gel imaging system (G:BOX Chemi-XL)	Syngene

• Heating block (Thermomixer Comfort)	Eppendorf
• Hot plate & mag' stirrer (MH-4)	Fried Electric
• Immobilized Metal Affinity Chromatography (IMAC) system (Avant 25)	ÄKTA
• Microcentrifuge (Prism C2500-230V)	Labnet
• Microplate reader, absorbance (iMark)	Bio-Rad
• Mini Centrifuge (MCF-2360)	Laboratory and Medical Supplies
• Orbital shaker (GyroTwister GX-1000 3D)	Labnet
• Power source for electrophoresis (PowerPacTM HC)	Bio-Rad
• Shaking incubator (IncoShake 353)	Labotec
• SpeedVac dryer (miVAC DNA-23050-L00)	SP Scientific
• Spectrophotometer (DS-11)	DeNovix
• Vortex mixer (Harmony Usuzio VTX-3000L)	Laboratory & Medical Supplies
• Weighing balance (PS 750.X2)	Radwag

2.2 In silico Vector Design and Vector Cloning

The *in-silico* cloning was performed using SNAPgene® (version 3.1.1, GSL Biotech, Chicago) to design an open reading frame (ORF) encoding for the recombinant fusion proteins. A αCSPG4 (scFv), αEGFR (scFv & VHH), αMesothelin (scFv & VHH) and SNAP-tag were designed. An order was then placed to Genscript (New Jersey, USA) for the synthesis of the specified open reading frame (ORF). The ORF was provided in a pUC57 commercial vector and would later be cloned into the pCB vector (a modified ThermoFischer Elements expression vector). The ThermoFischer Elements expression vector was modified by removing C-terminal histidines and myc tags near the C-terminal EcoRI, as well as the introduction of N-terminal His tags and Enterokinases. The final constructs, designated pCB-αCSPG4(scFv)-SNAP, pCB-

αMSLN (scFv & VHH)-SNAP and pCB-αEGFR (scFv & VHH)-SNAP was transfected into mammalian cells, which secrete the recombinant proteins into the supernatant where it can be harvested after visualization of the GFP with transillumination. The pCB-αCSPG4(scFv)-SNAP, pCB-αMSLN(scFv)-SNAP & pCB-αEGFR(scFv)-SNAP constructs had already been verified by way of sequencing and was provided by colleagues and stored in the lab collection.

The scFv sequence of αCSPG4 was derived from monoclonal antibody (mAb) 9.2.27 and read as follows:

ATGGCCCAGGTGAAACTGCAGCAGTCTGGACCTGAGCTGGTGAAGCCTGGGGCC
TCAGTGAAGATTTCCTGCAAAGCTTCTGGCTACGCATTCAGTAGGTCTTGGATGA
ACTGGGTGAAGCAGAGGCCTGGACAGGGTCTTGAGTGGATTGGACGGATTTATC
CTGGAGATGGAGATACTAACTACAATGGGAAGTTCAAGGGCAAGGCCACACTGA
CTGCAGACAAATCCTCCAGCACAGCCTACATGCAGGTCAGCAGCCTGACCTCTGT
GGACTCTGCGGTCTATTTCTGTGCAAGAGGGAATACGGTAGTAGTTCCCTATACT
ATGGACTACTGGGGTCAAGGAACCACCGTGACCGTGAGTTCGGGTGGCGGTGGA
TCCGGTGGTGGCGGCAGCGGTGGTGGCGGCAGCGATATTGAACTGACGCAATCT
CCAGCTTCTTTGGCTGTGTCTCTAGGGCAGAGGGCCACCATATCCTGCAGAGCCA
GTGAAAGTGTTGATAGTTATGGCAATAGTTTTATGCACTGGTACCAGCAGAAACC
AGGACAGCCACCCAAACTCCTCATCTATCTTGCATCCAACCTAGAATCTGGGGTC
CCTGCCAGGTTCAGTGGCAGTGGATCTAGGACAGACTTCACCCTCACCATTGATC
CTGTGGAGGCTGATGATGCTGCAACCTATTACTGTCAACAAAATAATGAAGACC
CTCTGACGTTTGGCGGCGGGACCAAGCTGGAACTGAAACGG

The sequence of αEGFR was acquired from scFv-1711 and read as follows:

CAGGTTCAGCTGCAAGAAAGCGGTCCGGGTCTGGTTAAACCGAGCCAGACCCTG
AGCCTGACCTGTACCGTTAGCGGTGGTAGCATTAGCAGCGGTGATTATTACTGGA
CCTGGATTCGTCAGCCTCCGGGTAAAGGTCTGGAATGGATTGGTCATATCTATTA
TAGCGGCAACACCAATTATAACCCGAGCCTGAAAAGCCGTGTTACCATTAGCGTT
GATACCAGCAAAACCCAGTTTAGCCTGAAACTGAGCAGCGTTACCGCAGCAGAT
ACCGCAGTTTATTACTGTGCACGTGATCGTGTTACCGGTGCATTTGATATTTGGG
GTCAGGGTACAATGGTTACCGTTTCAAGCGGTGGTGGTGGTAGTGGTGGCGGTG
GTTCAGGCGGTGGCGGTAGCGATATTCAGATGACCCAGAGCCCGAGCAGCCTGA

GCGCAAGCGTTGGTGATCGCGTGACCATTACCTGTCAGGCAAGCCAGGATATTA
GCAATTATCTGAATTGGTATCAGCAGAAACCTGGCAAAGCACCGAAACTGCTGA
TTTATGATGCAAGCAATCTGGAAACCGGTGTTCCGAGCCGTTTTAGCGGTAGCGG
TAGTGGCACCGATTTTACCTTTACCATTTCTAGCCTGCAGCCGGAAGATATTGCA
ACCTATTATTGTCAGCACTTTGATCATCTGCCGCTGGCATTTGGTGGTGGCACCA
AAGTTGAAATTAAACGT

The sequence of αMSLN was obtained from Human Mesothelin (296-580) and reads as follows:

ATGCAGGTACAACTGCAGCAGTCTGGGCCTGAGCTGGAGAAGCCTGGCGCTTCA
GTGAAGATATCCTGCAAGGCTTCTGGTTACTCATTCACTGGCTACACCATGAACT
GGGTGAAGCAGAGCCATGGAAAGAGCCTTGAGTGGATTGGACTTATTACTCCTT
ACAATGGTGCTTCTAGCTACAACCAGAAGTTCAGGGGCAAGGCCACATTAACTG
TAGACAAGTCATCCAGCACAGCCTACATGGACCTCCTCAGTCTGACATCTGAAGA
CTCTGCAGTCTATTTCTGTGCAAGGGGGGGTTACGACGGGAGGGGTTTTGACTAC
TGGGGCCAAGGGACCACGGTCACCGTCTCCTCGGAGGTGGCGGCTCCGGAGGTG
GAGGCAGCGGAGGGGGCGGATCCGGACATCGAGCTCACTCAGTCTCCAGCAATC
ATGTCTGCATCTCCAGGGGAGAAGGTCACCATGACCTGCAGTGCCAGCTCAAGT
GTAAGTTACATGCACTGGTACCAGCAGAAGTCAGGCACCTCCCCCAAAAGATGG
ATTTATGACACATCCAAACTGGCTTCTGGAGTCCCAGGTCGCTTCAGTGGCAGTG
GGTCTGGAAACTCTTACTCTCTCACAATCAGCAGCGTGGAGGCTGAAGATGATGC
AACTTATTACTGCCAGCAGTGGAGTGGTTACCCTCTCACGTTCGGTGCTGGGACA
AAGTTGGAAATAAAA

The sequence for αEGFR(VHH) was obtained from VHH-G10 and reads as follows:

GAGGTGCAGCTGGTGGAGAGCGGCGGCGGCCTGGTGCAGGCCGGCGGCAGCCTG
AGACTGAGCTGCGCCGCCAGCGGCAGAACCTTCAGCAACTACGCCATGGGCTGG
TTCAGACAGGCCCCCGGCAAGGAGAGAGAGTTCGTGGCCGGCATCATCTGGAGC
GGCAGCAGAACCTACTACGCCGACCCCGTGAAGGGCAGATTCACCATCAGCAGA
GACAACGCCAAGAACACCGTGTACCTGCAGATGAACAGCCTGAACGTGGAGGAC
ACCGCCGTGTACTACTGCGCCGCCAGCATGGGCGACTACGACGTGAGCCTGGCC
AGCCCCAGAAGCTGGGGCAAGGGCACCCAGGTGACC GTGAGCAGC

The sequence for αMSLN(VHH) was obtained from VHH-SD2 and reads as follows:

CAGGTGCAGCTGGTGCAGTCTGGGGGAGGCTTGGTACAGCCTGGAGGGTCCCTG
AGACTCTCCTGTGCAGCCTCTGATTTCGCTTTCGATGATTATGAAATGAGCTGGG
TCCGCCAGGCTCCAGGAAAGGCCCTTGAGTGGATTGGGGACATCAATCATAGTG
GAACCACCATCTACAACCCGTCCCTCAAGAGTCGAGTCACCATCTCCAGAGACA
ATTCCAAGAACACGCTGTATCTG

2.3 Molecular Cloning

2.3.1 Restriction Enzyme (RE) Digestion

Restriction enzyme digestion was used to generate compatible DNA ends that can be ligated together. This means using REs to excise a desired gene of interest in preparation for ligation into a designated plasmid. In this case, the process began by making bulk preparations of both the commercial pUC57 vector carrying the gene of interest, and the destination vector in use by the lab, pCB-AnnexinV-SNAP using the NucleoBond® midi prep kit obtained from Machery-Nagel, Germany (#740573). The purpose of this was to increase the quantity of DNA for long term storage as well as for molecular cloning related work. It must be noted that for the VHH constructs, a modified pCB plasmid housing the SNAP-F variant instead of SNAP was used. The digestion reaction was as described in Table 2 below.

Table 2. Components of a restriction enzyme digestion*. The illustration shows a 50 ul overnight digest with the various components and their volumes. The volumes of enzymes and nuclease free water are variable depending on the type of digest i.e. single or double digest.*

Component	Final concentration	**Volume**
DNA	2 µg	Adjusted for
10× NEB CutSmart Buffer	1× NEB CutSmart Buffer	5 µl
SfiI	2000 U/ml	0.5 µl
NotI	2000 U/ml	0.5 µl
Nuclease-free water	-	Make up to 50 µl

The digest was then left overnight at 37ºC for approximately 16-18h. *Sfi*I and *Not*I restriction enzymes or cutting enzymes, obtained from New England Biolabs (NEB) Ipswich, USA, were used to excise the gene(s) of interest from the pUC57 vector as well as the AnnexinV from the pCB vector. This was done with the intention to ligate the genes of interest from pUC57 vector into the pCB backbone. The expected final products would be pCB-αEGFR(VHH)-SNAPF and pCB-αMSLN(VHH)-SNAPF.

Materials needed:

- NucleoBond plasmid purification kit
- Bacterial culture (Luria Broth)
- Centrifuge
- Microcentrifuge
- 50mL centrifuge tubes
- 1.5mL centrifuge tubes
- 70% Ethanol
- Isopropanol
- Pipette and tips
- SpeedVac
- Sterile deionised H_20 (prewarmed to 50ºC)
- Spectrophotometer (e.g. Nanodrop)
- 50% Glycerol

Table 3. Reagents & buffers for restriction enzyme digest

	Composition
Luria Broth Bacterial culture (1L, pH 7.0)	• 7.5g LB agar • 5g Tryptone • 5g NaCl • 2.5g yeast extract
50% Glycerol (100 ml)	• 50ml 100% Glycerol • 50ml Sterile water
70% Ethanol (1L)	• 700ml Pure ethanol • 300ml Sterile water

2.3.2 Agarose Gel Electrophoresis & Gel Extraction

Agarose gel electrophoresis serves as a tool that is useful in analysing DNA fragments after RE digestion. An electric current is applied to separate the fragments by size and nucleic acid stain allows for visualization of fragments upon blue light excitation. Gel preparation was subject to the size of the gel required. On average, 1.2 and 1.5% agarose gels were made for the digested backbone and genes of interest. This required weighing 1.2g & 1.5g of agarose powder mixed in 100ml of 1× TAE buffer solution (chemicals for buffer purchased from Merck-Sigma, USA) and 1:10 000 dilution of SYBR™ safe DNA gel stain obtained from Thermofisher, USA. The solution was heated to boiling temperature, left to cool for 5-10min and poured into a gel casting tray with the correct comb size and allowed to solidify. The casting tray was then put into a BioRad flat buffer tank filled with 1× TAE buffer. The tank was connected to the BioRad PowerPac™ by positive and negative terminals and a voltage of 120V was applied over 30-60 min to allow the DNA to travel down the gel. DNA bands were visualized with blue light (400-495nm) and their sizes were compared against the QuickLoad® 1 kilobase (kb) and 100 base pair DNA ladders obtained from NEB. The band sizes that we expected to see are described in Table 4.

Table 4. Sizes of plasmids and genes of interest to be used for cloning.

Dummy construct	*Total (bp)*	*Backbone*	*DNA Insert*
pCB-AnnexinV-SNAPF	8233	6564	1669
pUC57-αMSLN(VHH)	3094	2710	384
pUC57-αEGFR(VHH)	3100	2710	390

The bands of interest were the pCB backbone and the MSLN & EGFR inserts. After the correct bands were visualized at the theoretical sizes described in Table 4, they were excised from the gel using a scalpel and the DNA was extracted from the gel by use of the QIAquick Extraction kit obtained from Qiagen, Germany (#28704). After the gel was excised it was weighed in an Eppendorf tube and thereafter 3 volumes of Buffer QG were added to 1 volume of DNA. The yellow colour of the buffer indicates a pH <7.5 because DNA adsorption to the membrane is most efficient at this pH. The solution was then incubated at 50^{o}C for 10mins to allow melting of the agarose gel and was vortexed thoroughly in 2-5 min intervals. Thereafter one gel-volume of isopropanol was added, and the solution was transferred to a QIAquick column and

centrifuged (13 000rpm). Buffer QG was added and the solution was centrifuged once more in the column. We then washed the DNA in the column with Buffer PE. This buffer assists in the removal of excess salts from the DNA. We then transferred the column to a 1.5ml microcentrifuge tube and eluted with nuclease free water and centrifuged. The purity of the DNA was quantified using the Denovix® Nanodrop spectrophotometer.

Materials needed:

- Agarose powder
- 1× TAE buffer
- SYBRsafe
- 250mL beaker
- Microwave
- Scale, spoon and weigh boat
- Deionised water
- Buffer tank
- Gel tray
- Comb
- 6× gel loading dye purple
- Pipette and tips
- 1kb and/or 100bp+ DNA ladder
- Blue light box/ UV gel documentation system

Table 5. Reagents & buffers for agarose gel electrophoresis

	Composition
Agarose gel (1.5%)	• 1.5g Agarose powder • 100ml 1× TAE Buffer • 1:10000 SYBR Safe (after boiling)
10×TAE Buffer (1L)	• 48.5g Tris-base • 11.4ml glacial acetic acid • 20ml 0.5M EDTA (pH 8.00) • Deionised water (top up to 1L)
1× TAE Buffer (1L)	• 100ml 10× TAE Buffer • 900ml Deionised water

2.3.3 T4 DNA Ligation & Bacterial Transformation

Ligation is the process of covalently joining two linear fragments of DNA, more specifically, forming a phosphodiester bond between the 3' hydroxyl of one fragment with the 5' phosphate end of another. To ensure successful ligation, we chose a 1:3 ligation ratio (1-part DNA and 3-parts backbone) which was calculated for on a weight to mol basis using the Promega online calculation tool (https://worldwide.promega.com/resources/tools/biomath/). The vector size (7272 bp), concentration (22 ng/ul) as well as the insert DNA size (376 bp) and concentration (4.9 ng/ul) were put into the online calculator and the ligation ratios were calculated for. A 1:1 ratio would require 3ng of insert DNA and this was the basis we used to calculate the requirements for the other ratios. 20ul ligation reactions were set up in 1.5 ml tubes as shown in the table 6 below.

Table 6. The reagents required to perform a ligation and their volumes.

Reagent	**Reaction control**	**1:3**	**1:5**
10× T4 DNA Ligase Buffer	2ul	2ul	2ul
pCB vector (50ng)	2.27ul	2.27ul	2.27ul
αEGFR(VHH)	0ul	1.8ul (9ng)	3ul (15ng)
T4 DNA ligase	1ul	1ul	1ul
Nuclease free water	Make up to 20ul	Make up to 20ul	Make up to 20ul

The ligase enzyme, obtained from NEB, is responsible for joining the insert DNA with the backbone. This method was followed for the αEGFR(VHH) and αMSLN(VHH). Vector only and vector with ligase served as the negative controls. The reactions incubated at 16^{o}C overnight. Prior to transformation, NEB DH5α competent *E. coli* cells (strain K12, with mutations dlacZ ΔM15 Δ(lacZYA-argF) U169 recA1 endA1 hsdR17 (rK-mK+) supE44 thi-1 gyrA96 relA1) were thawed on ice. A volume of 5ul of DNA was added to 25ul of bacterial cells and incubated on ice for 5mins. The cells were then subject to heat shock (at *X* °C) for 60 seconds, altering the bacterial membrane fluidity resulting pore formation allowing for DNA entry into the cell. Thereafter, the cells were then chilled on ice for 5min before cold Super Optimal broth with Catabolite repression (SOC) medium was added. This is rich medium that aids in the recovery of competent cells and maximizes the transformation efficiency. The solutions were then mixed thoroughly and 200µl of cells was removed and streaked onto agar

plates supplemented with ampicillin and incubated overnight at 37^{o}C. Single colonies were then selected, grown in 2ml of Luria Broth agar with an appropriate amount of ampicillin and incubated overnight in a shaking incubator.

Materials needed:

- LB agar powder
- Distilled H20
- Ampicillin
- 1L flask
- Petri dishes
- Autoclave
- T4 DNA Ligase kit
- 1.5 microcentrifuge tubes
- Ice
- Insert DNA
- Vector DNA
- Nuclease-free H20
- Calcium competent *E. coli* cells (DH5-α)
- Pipettes and tips
- Room temperature Super Optimal Broth with Catabolite repression (SOC)
- Luria Bertani Broth (LB)
- Incubator with shaker
- Zyppy Miniprep materials
- Restriction Mapping materials
- NucleoBond Midiprep Plasmid Purification materials
- Sequencing materials

Table 7. Reagents & buffers for DNA ligation & transformation

	Composition
LB Agar plates (20ml per plate)	• 35g LB agar powder • Deionised water (1L)
Ampicillin [100mg/ml]	• 1g Ampicillin powder • Sterile deionised water (1L)

2.3.4 Zyppy™ Plasmid Miniprep and Inqaba Sequencing

The Zyppy™ plasmid miniprep kit was obtained from Zymo Research, USA (#D4036). This kit that introduces a pellet-free alkaline lysis method that bypasses the traditional plasmid preparation methods that include bacterial culture centrifugation and resuspension steps needed to efficiently separate plasmid DNA from *E. coli*. Alternatively, the alkaline lysis method which makes use of homemade buffers and multiple centrifugation steps could have been used. The steps described in the Zymosearch Zyppy™ plasmid miniprep protocol were followed according to the manufacturer's instruction. After this protocol, purified plasmid DNA i.e. pCB-αEGFR(VHH)-SNAPF and pCB-αMSLN(VHH)-SNAPF were expected. To confirm these constructs as being correct, the DNA was diluted in Eppendorf tubes and sent for gene sequencing by Inqaba Biotech™ (South Africa). The method of sequencing employed is Sanger sequencing, which is a process that involves the addition of chain-terminating dideoxynucleotides by DNA polymerase during DNA replication [199].

Materials needed**:**

- 1.5ml microcentrifuge tube
- 7× Lysis buffer (blue)
- Neutralization buffer (Yellow) -From fridge
- Collection tubes and Zymo-Spin IIN column
- Endo-wash buffer
- Zyppy wash buffer
- Molecular biology grade water (pre-heated at 50˚C)
- Microcentrifuge

2.4 Expression of SNAP fusion proteins in tissue culture, flow cytometry and protein purification by AKTA Avant system

Transfection is the process of introducing DNA into a mammalian cell that eventually results in protein expression using the cells machinery. To transfect the constructs, the X-tremeGENE transfection reagent (obtained from Sigma-Aldrich, USA) and protocol were used. The reagent includes a blend of lipids and other components that can complex to DNA, allowing for the uptake of DNA by the mammalian cells and transient expression of proteins by the cells with minimal toxicity and changes in morphology. Mammalian transfection was performed in the HEK293T cell line derived from HEK293 cells. HEK293T cells were seeded at 70-90%

confluency into 2 x 2 mm round cell culture vessels 48 hours prior to the experiment. The cells were then combined with plasmid DNA, RPMI (Roswell Park Memorial Institute) medium supplemented with 10% heat inactivated fetal bovine serum and 100U/ml penicillin (#P3032 Sigma, USA) and 100µg/ml streptomycin (#S-91370 1105 Sigma, USA), as well as the X-tremeGENE HP DNA Transfection Reagent in a microcentrifuge tube at a 3:1 ratio (v/v) of reagent to DNA. The mixture will be evenly distributed amongst cells and incubated at 37ºC in 5% CO_2 before applying selective Zeocin™ (Thermofisher, USA) pressure (10% v/v). The zeocin pressure was applied until the cultures were dominated by EGFP expressing cells (~3-4 weeks). The tissue culture and EGFP images were taken with the ZOE™ Flourescent Cell Imager under brightfield and green line. After selection pressure, the percentage EGFP expression was determined by flow cytometry. 5 x 10^4 cells were counted by staining with Trypan blue (1:1 volume ratio) and the BioRad automated cell counter. The cells were placed in 15ml falcon tubes and centrifuged @ 1500 x g for 5mins. The cells were then resuspended in 1× phosphate buffered saline (PBS) solution and transferred to FACS tubes (BD). The cells were fixed with 200ul of 2% paraformaldehyde (PFA), centrifuged again and resuspended in FACS buffer. After a sufficient period of time, where transfected cells showed adequate EGFP expression, cell culture supernatant (CCSN) was be collected for purification using the AKTA Avant system. Proteins were harvested by collecting the CCSN from T175 culture flasks into a 50mL sterile plastic tube and centrifuged it at 1000 × g for 5mins. The tubes were stored at 4ºC in preparation for protein purification. The purification process was performed using ion metal affinity chromatography (IMAC), which makes use of the high affinity of Ni^{2+} for poly-His tags. The 6× His tag confers strong binding of the proteins to Ni^{2+} rich column ensuring that they do not get washed out of the resin while unbound proteins are removed. The AKTA system will delivered purified proteins in fractions displayed as peaks on a graph where the protein of interest was fractionated. These fractions were concentrated using Amicon® filters obtained from Sigma-Aldrich. Manufacturers protocols were followed for the Amicon® Ultra 15ml Centrifugal Filters (10,000 MWCO), which filters out proteins of 10kDa and below, in a centrifuge with a swinging-bucket rotor. A maximum volume of 15ml could be centrifuged (@ 4000 x g) at a time. The flow through was then discarded and the remaining concentrated protein was transferred to a 1.5mL Eppendorf tube. The concentrated SNAP-tag proteins can be assessed using nanodrop spectrophotometry.

Materials needed:

- AKTA Avant
- 5ml HisTrap^{TM} excel [GE Healthcare: Lot # 10264409]
- Incubation[4x], equilibration & elution buffers* Cell culture supernatant (CCSN)
- 96 deep well plate square V-bottom [Lasec-Lot # 18041]
- 0.45um PVDF membrane (47 mm) [Sigma: Lot # R8EA65403]
- Amicon Ultra-15 filters (10kDa) [Sigma: Lot # R8MA11064]

Table 8. Reagents & buffers for expression & purification of SNAP-tag proteins

	Composition
4X Incubation buffer (pH 8.00)	• 24g NaH2PO4 [200mM] • 7.13g NaCl [1.2M] • 2.72 Imidazole [40mM] • Deionised water (top up to 1L)
Equilibration buffer (pH 8.00)	• 6g NaH2PO4 [50mM] • 17.53 NaCl [300mM] • Deionised water (top up to 1L)
Elution buffer (pH 8.00)	• 6g NaH2PO4 [50mM] • 17.53 NaCl [300mM] • 17.02g Imidazole [250mM] • Deionised water (top up to 1L)
10× PBS	• 17.8 g of Na2HPO4 [100mM] • 2.4 g of KH2PO [18mM] • 80 g of NaCl [1.37M] • 2 g of KCl [27mM] • Sterile deionised water (top up to 1L)
1× PBS	• 100ml 10× PBS • 900ml sterile deionised water

2.5 *SDS-PAGE and Western blot analysis*

Expression and purification of SNAP fusion proteins was assessed by sodium dodecyl sulfate–polyacrylamide gel electrophoresis (SDS-PAGE) and western blotting. Polyacrylamide gel (10% Resolving, 4% Stacking) electrophoresis (with SDS for reducing conditions) allows analysis of protein samples by size on a gel by electrophoresis and by immunoblotting using anti-His antibodies. The proteins are separated according to size by electrophoresis. Visualization of the protein bands is achieved by using the using AcquaStain (Bulldog Bio, UK) and thereafter they are analysed against the PageRuler pre-stained protein ladder obtained from Thermofisher (#26616). Alternatively, for the detection of the fusion protein the western blotting technique was used. The western blots were performed by initially transferring the proteins onto a PVDF transfer membrane that was obtained from Roche, Switzerland (#03010040001). The membranes were then incubated at 4^{o}C overnight with an anti-conjugate protein or anti-His tag antibodies obtained from Cell Signalling Technologies (Danvers, USA). A secondary antibody, Goat-Anti-Rabbit-HRP that was obtained from Bio-Rad (Hercules, USA), was then added resulting in an enzyme substrate reaction. The membrane was thereafter treated with a chemiluminescence detection agent i.e. WesternBright^{TM} ECL detection kit (manufactured by Advansta, USA) and presented on an X-ray film. If positive results are obtained i.e. specific bands form, the study would have engineered monospecific recombinant proteins. Following the above-mentioned analyses, application studies in CSPG4, EGFR & MSLN + TNBC cell lines were performed.

<u>Materials needed:</u>

- Glass plates & combs
- Casting stands & frames
- Buffer tank
- Running & transfer electrode modules
- Running & transfer (cold) buffers
- Gel ingredients
- Protein samples
- 4× loading dye
- Protein ladder

Table 9. Reagents & buffers used for SDS & Western Blot

	Composition
10× Running buffer	• 30g Tris • 10g SDS • 144g Glycine • Deionised water (top up to 1L)
1× Running buffer	• 100ml 10X Running buffer • 900ml deionised water
10× Transfer buffer	• 30g Tris • 144g Glycine
1× Transfer buffer (cold)	• 100ml 10× Transfer buffer • 200ml Methanol (100%) • 700ml deionised water
10% SDS	• 10g SDS • 100ml deionised water
10% Ammonium per sulfate (APS)	• 5g Ammonium per sulfate • 50ml
10× Tris-buffered saline (TBS), (pH 7.6/8.8/6.8)	• 24 g of Tris Base [200mM] • 88 g of NaCl [1500mM] • Deionised water (top up to 1L)
1× Tris-buffered saline, 0.1% (w/v) Tween® 20 (TBST)	• 100ml 10× TBS • 900ml deionised water • 1ml Tween® 20

2.6 Protein Quantification by Spectrophotometry

Spectrophotometry makes use of a machine that can register how much light is absorbed by a substance at a set wavelength and quantify this value in terms of concentration. The Denovix® DS-11 spectrophotometer which has the capacity to quantify microvolumes of DNA, proteins and labelled proteins was used. DNA is absorbed at wavelength of 260 nanometres (nm) and proteins are absorbed at a wavelength of 280 nm. To measure the protein concentration, it is required to compute the theoretical molecular weight (MW) and extinction coefficient (ε) of

the protein. These details were obtained using the Expasy online tool (https://web.expasy.org/protparam) and read as seen in the table below.

Table 10. The theoretical molecular weights and extinction coefficients of the proteins of interest.

Protein	Molecular Weight (M-1 cm-1)	Extinction coefficient (ε)
αEGFR(VHH)-SNAPF	38217.31	59150
αEGFR(scFv)-SNAP	503345.64	77725
αCSPG4(scFv)-SNAP	51154.63	77725
αMSLN(scFv)-SNAP	51106.45	87695

Materials needed:

- Protein samples
- Appropriate blanks (MiliQ water, PBS)
- P10 pipette

2.7 Binding analysis in CSPG4, EGFR & MSLN+ tumour cell lines using confocal microscopy

To confirm the functionality of the protein we will test its binding on tumor cell lines. The main cell lines tested on were MDA-MB-231 (ATCC: HTB-26), Hs578t (ATCC: HTB-126) and MDA-MB-468 (ATCC: HTB-132) which are TNBC tumor cell lines that are known to express CSPG4, MSLN and EGFR on their surfaces. It must be noted that not all tumor cell lines express each receptor on their surfaces and will serve as negative controls alongside another cell line included in the study, A2058 (ATCC: CRL-11147) used as a negative control for αEGFR(VHH)-SNAPF and αEGFR(scFv)-SNAP. Binding analyses on these tumor cells were visualized using confocal microscopy. We used the 880 Airyscan confocal microscope making use of the Argon laser at 488nm to view the green fluorescence and 405nm DAPI laser to view Hoechst stained cell nuclei. 5 x 104 cells were counted by staining with Trypan blue (1:1 volume ratio) and the Bio-Rad automated cell counter. The cells were transferred to single-well live cell culture dishes and stained with 250uM of labelled protein and incubated for 30mins followed by two washes with serum-free media (SFM). The cells were then stained with Hoechst (1:1000) for 5-10min, washed twice with SFM and left in 200ul of SFM at room

temperature for imaging. The conjugation reaction between SNAP fusion proteins with BG-Alexa Fluor 488, received from NEB, was performed as follows:

Table 11. The reaction set up for conjugation between SNAP-tag fusion proteins and SNAP-tag substrates.

Component	Volume	Final Concentration
Phosphate Buffered Saline (PBS)	42ul	1×
50mM Dithiothreitol (DTT)	1ul	1mM
50uM SNAP-tag Purified Protein	5ul	5uM
250uM SNAP-tag substrate	2ul	10uM

The conjugation efficiencies were calculated by measuring the approximate concentrations of unlabeled and labelled protein using spectrophotometry and thereafter determining the percentage labeling:

$$\%\ protein\ conjugation = \frac{[\text{Labelled protein}]}{[\text{Unlabeled protein}]} \text{ x } 100$$

The labelled proteins were then prepared for binding studies on tumor cell lines positive for the receptor targets. 3 x 104 cells were seeded into live culture dishes and grown in Dulbecco's Modified Eagles Medium (DMEM) supplemented with 10% (v/v) Fetal Bovine Serum (FBS, obtained from ThermoFisher Scientific) and 1% Penicillin Streptomycin (PenStrep, obtained from Sigma-Aldrich). The only exception in the TNBC cell lines was MCF-7 as it was previously grown in RPMI media and we followed suit.

Materials needed:

- BG-modified Alexa488 substrate
- SNAP fusion protein
- Live cell viewing dishes
- Tissue culture reagents
- Tumour cell lines

Table 12. Reagents & Buffers for binding analyses

	Composition
10× PBS	• See above
1× PBS	• See above
50 mM DTT	• 7.7mg DTT powder • 1ml sterile deionized water

Chapter 3: Results

This study aimed to generate novel molecules in the form of SNAP-tag fusion molecules aimed at improving immunodiagnostic and immunotherapeutic agents for the validation and treatment of TNBCs. The molecules were initially designed by way of *in-silico* cloning. The molecule was designed to contain a targeting domain (scFv/VHH) and a domain that can attach BG-residues (SNAP-tag). Thereafter the molecules underwent molecular cloning which consists of performing restriction enzyme digestion, agarose gel electrophoresis, DNA ligation and Sanger sequencing by Inqaba Biotec. The processes that followed after confirmation of DNA after sequencing involved transfection of the DNA into a mammalian vector expression system and harvesting of transiently expressed proteins. These proteins were then purified using IMAC and thereafter confirmed using SDS PAGE and Western Blotting. The confirmed SNAP-fusion proteins were then conjugated to a BG-modified fluorophore in Alexa-488 and binding studies performed on receptor positive tumour cell lines (visualized by confocal microscopy).

3.1 *in-silico* Cloning using SNAP-gene software

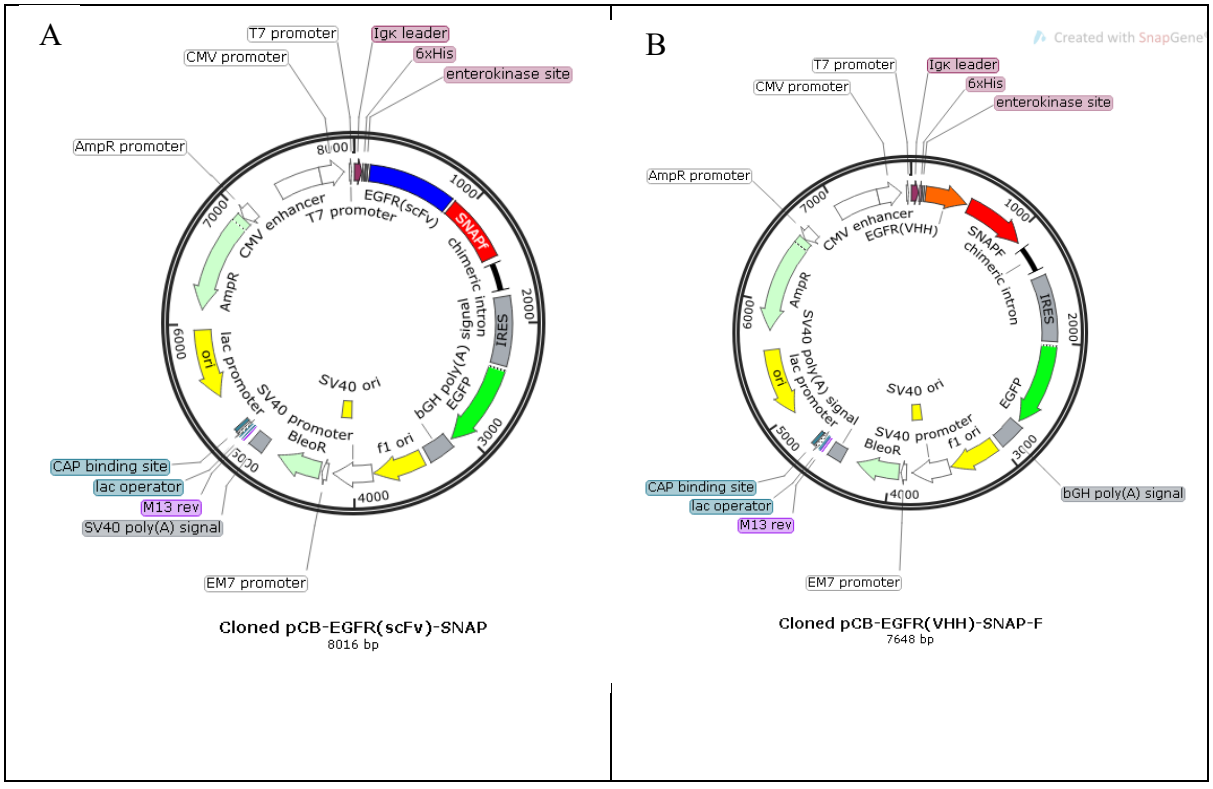

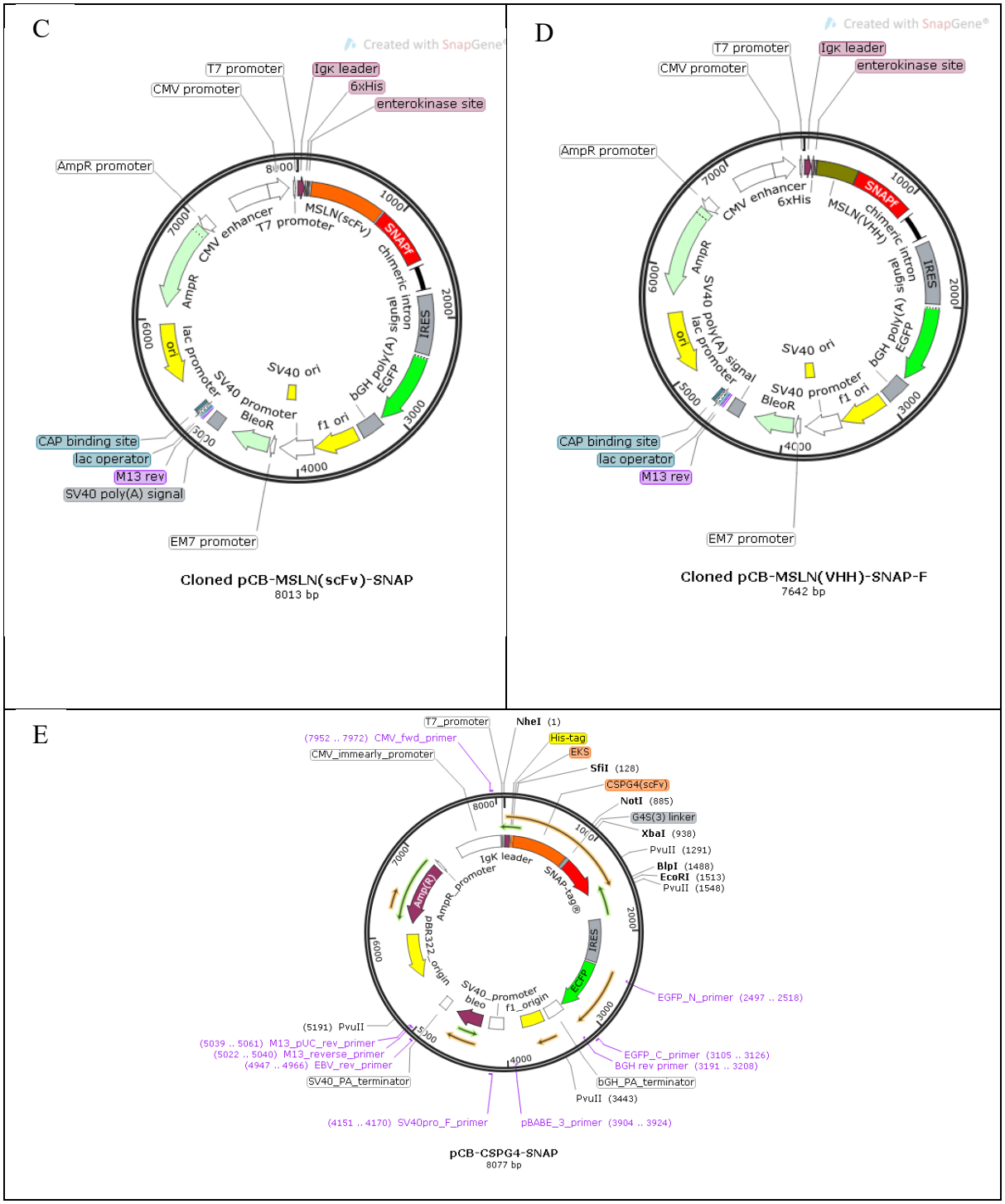

Figure 11. Schematic diagrams of pCB plasmid housing our opening reading frames (ORFs). *Panels A & B show the full plasmid architecture for pCB-αEGFR(scFv)-SNAP and pCB-αEGFR(VHH)-SNAPF. Panels C & D show the full plasmid architecture for pCB-αMSLN(scFv)-SNAP and pCB-αMSLN(VHH)-SNAPF. Panel E shows the full plasmid architecture for pCB-αCSPG4-SNAP.*

The software SNAP-gene was used as the *in-silico* tool to confirm the antibody genes ordered from Genscript (Fig. 11). *In-silico* cloning allowed for the confirmation of the CDR regions, ensures correct assembly of the ORFs into the pCB plasmid and correctly annotating the features of the plasmid. *In-silico* cloning is also an important tool in providing theoretical

sequences for analysis against sequences provided after sequencing by Inqaba. The plasmid vector pCB houses the recombinant ORF containing the sequence of the recombinant proteins αCSPG4(scFv)-SNAP, αMSLN(scFv)-SNAP, αMSLN(VHH)-SNAPF and αEGFR(scFv)-SNAP and αEGFR(VHH)-SNAPF which were cloned out of a commercial pUC57 vector. The plasmid also contains the sequences of SNAP-tag or SNAP-F which are important for binding BG-substrates. The plasmid also houses an Ampicillin resistance gene that allows for selection of bacterial colonies successfully transformed with plasmid DNA on agar plates supplemented with the antibiotic ampicillin. The purified plasmid DNA was eventually transfected into a mammalian expression system in HEK293T cells. The plasmid also contains the gene for the EGFP which is a readily detectable marker under light fluorescence using the ZOE Fluorescent Cell Imaging (BioRad, South Africa) which is equipment that uses three fluorescent channels as well as brightfield for applications in cell culture, and moreover, it uses a simple digital viewing system that differs from traditional fluorescent microscopes and can be used by researchers without extensive experience with fluorescence. The plasmid has also been fitted with a Zeocin/Bleomycin resistant gene that allows for the selection of HEK cells successfully transfected with the plasmid DNA. The gene allows for the enrichment of cultures, ensuring that there are only successfully transfected cells in culture as seen by EGFP expression. The Ig kappa (Igκ) leader sequence is important because it plays a role as a signal sequence that allows for the secretion of protein into the supernatant. The poly-histidine tag is important for affinity purification of proteins and protein confirmation through western blotting. The plasmid was also equipped with numerous restriction sites, such as SfiI and NotI, that would allow for molecular cloning experiments such as restriction enzyme digestion.

3.2 Molecular Cloning

Molecular cloning refers to different experiment that are performed as a collective with the intent to amplify a particular DNA fragment using a host organism [200]. The cloning strategy employed involved restriction enzyme digestion of the commercial vector housing the ordered genes of interest and the pCB vector in preparation for the ligation of the two with T4 DNA ligase. The sequence of the ligated product was then confirmed by sequencing by Inqaba Biotec and restriction enzyme mapping prior to its transfection into mammalian cells in tissue culture.

3.2.1 Restriction enzyme digestion and Gel electrophoresis

Restriction enzyme digestion is the process of using restriction enzymes to excise a DNA fragment from a plasmid for DNA analysis or leaving sticky-ends on the digested plasmids in preparation for ligation with a suitable DNA fragment. The use of SfiI and NotI restriction enzymes allowed for the cloning of the genes of interest i.e. αCSPG4(scFv), αMSLN(scFv), αMSLN(VHH), αEGFR(scFv) and αEGFR(VHH) by exposing sticky ends on the plasmids to be ligated with ORFs. This processes also allows for the correct cloning of products in preparation for sequencing by Inqaba Biotec. Performing a gel electrophoresis allows for the visualization of fragments of DNA under UV or blue light as shown in Figure 12. The following result is for αEGFR(VHH) only and will exemplify the successful molecular cloning of plasmids containing the scFv (αEGFR, αMSLN and αCSPG4) genes provided by colleagues. The plasmids containing the scFv genes were already transfected into a transient expression system and these results are expanded up in Chapter 3.3. Indicated by the orange rectangle are the double digests in which we expected to see the αEGFR(VHH) bands at a size of ~370 bp of the as well as the pUC57 vector of ~2.7kb higher up on the gel. Although the bands were feint, their appearance of the gel gave researchers confidence that this was the gene of interest as it aligned to the correct region according to the 100 bp Quickload ladder. The single digest and undigested controls were slightly above the digested vector. This result was expected as the controls were not fully digested or digested at all, and a shift in vector size would be unexpected. The highlighted gel bands were then excised, pooled together into one tube and processed according to set protocols in preparation for ligation. No successful digestion was recorded for αMSLN(VHH).

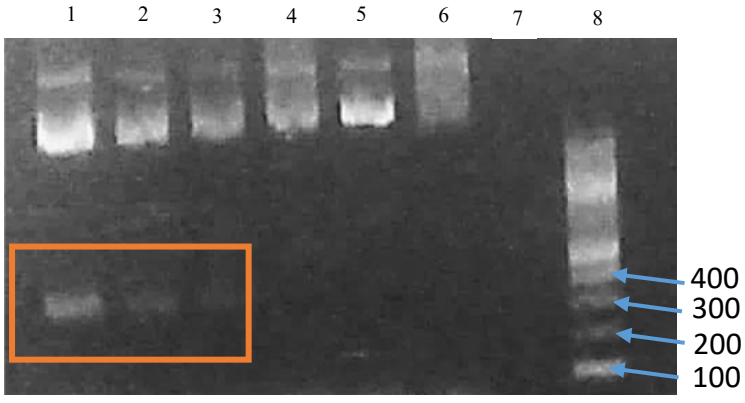

***Figure 12. A 1.5% Agarose gel depicting bands after RE digest*.** Lanes 1-3 represent the double digests of the commercial pUC57 vector housing the αEGFR(VHH) gene (~370bp) with *Sfi*I and *Not*I restriction enzymes. Lanes 4 and 5 represent single digest controls with *Sfi*I and *Not*I respectively. Lane 7 is an empty lane. Lane 8 is the PageRuler 100bp ladder.

.

3.2.2 T4 DNA Ligase & Bacterial transformation

DNA ligation is the act of combining two DNA molecules using the DNA ligase enzyme. The enzyme forms phosphodiester bonds between 3' hydroxyl group and the 5' phosphate group on nucleotides [201]. The ligated products (the ORFs and the pCB vector) were transformed into DH5-α *E. coli* cells. The growth of colonies for the designated constructs as seen in Figure 13, shows successful ligation of the plasmid and its successful transformation into the *E. coli*. Positive colony growth was seen on the ampicillin supplemented plates suggesting a successful transformations in both the 1:3 and 1:5 plasmid vector to DNA insert ratios. The digested vector only control showed no growth as expected. A vector with ligase control (no insert) to test for religation of the plasmid was not included. A successful ligation was noted at the lowest vector to DNA ratio, and these transformants were selcted for subsequent expeirments. Positive colonies selected from the 1:3 ligation plate, which showed a transformation efficiency of 57.2 x 10^3 CFU/ug, were regrown and in Luria Bertani Broth (LB), the plasmids purified and prepped for restriction mapping and sequencing by Inqaba™ Biotech.

A. Vector only control	B. 1:3 ligation	C. 1:5 ligation
	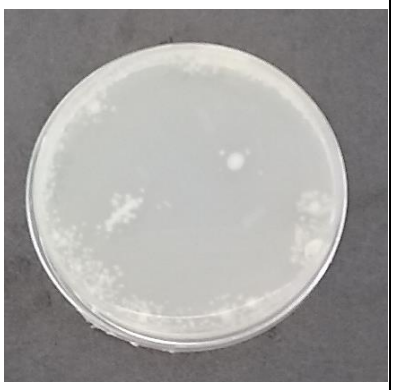	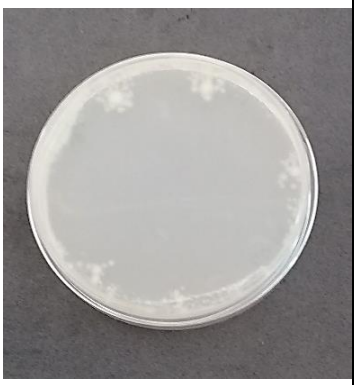

Figure 13. Cultured DH5-alpha competent E. coli cells on agar plates supplemented with ampicillin after T4 DNA ligation reaction*. A) The plasmid vector digested with restriction enzyme was plated without the addition of T4 DNA Ligase enzyme. B & C) 1:3 & 1:5 plasmid vector to DNA insert reactions were plated with the addition of T4 DNA Ligase.*

3.2.3 Sanger sequencing by Inqaba™ , Alignments & RE Mapping

DNA sequencing allows the determination of a specific order of nucleotide bases in a DNA molecule. Inqaba™ Biotech makes use of tailor-made sequencing methods which may sequence single reactions or whole genome sequences. The returning sequences for the experimental constructs were aligned using SNAPgene, and compared to the sequences that were generated *in silico*. Forward and reverse primers that bind to different parts of the plasmid were designed to assess the nucleotide sequence of the ORFs as seen by the red arrows in Figure 14. The nucleotide base sequences showed 100% identitiy and no signs of missing or altered bases. The plasmid was then prepared according to set protocols and transfected in HEK293T cells.

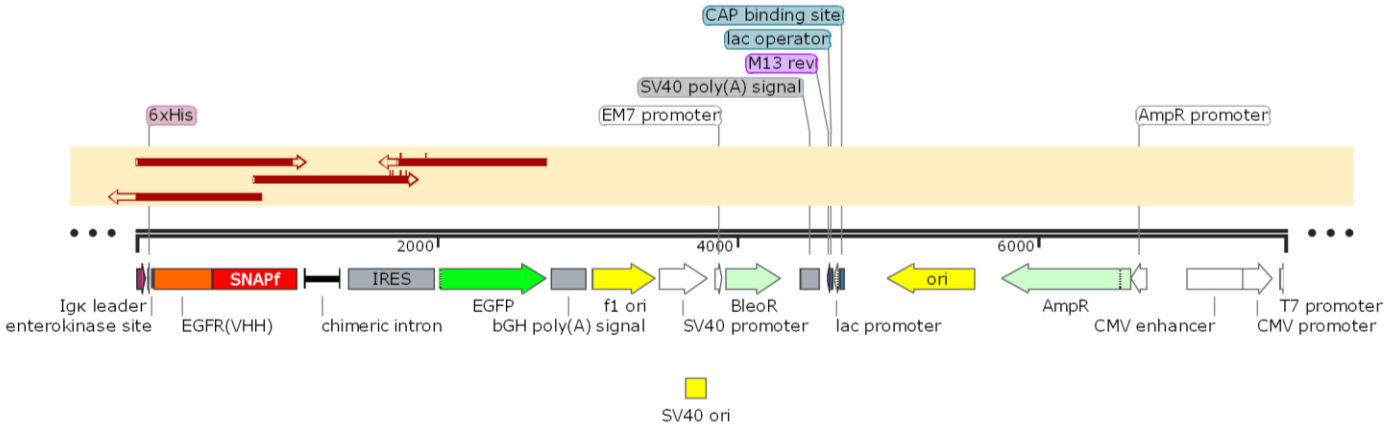

Figure 14. Sequencing of pCB-αEGFR(VHH)-SNAPF by Inqaba Biotec. *Snap-gene software was used to align the sequences returned to us from sequencing by Inqaba. The red arrows are illustrative of forward and reverse primers that were complimentary to various areas of our ORF and mapped out these regions.*

Restriction enzyme mapping is a method that is used to confirm successful ligation of the gene of interest into a plasmid. A cocktail of restriction enzymes was used and the banding pattern visualized on an agarose gel can be compared to the theorectical gel pattern simulated using SNAPgene software. The gel pattern in Figure 15B. matched with the theoretical pattern from the simulated gel (Fig. 15A). The plasmid was then transfected into HEK293T cells in tissue culture for transient protein expression.

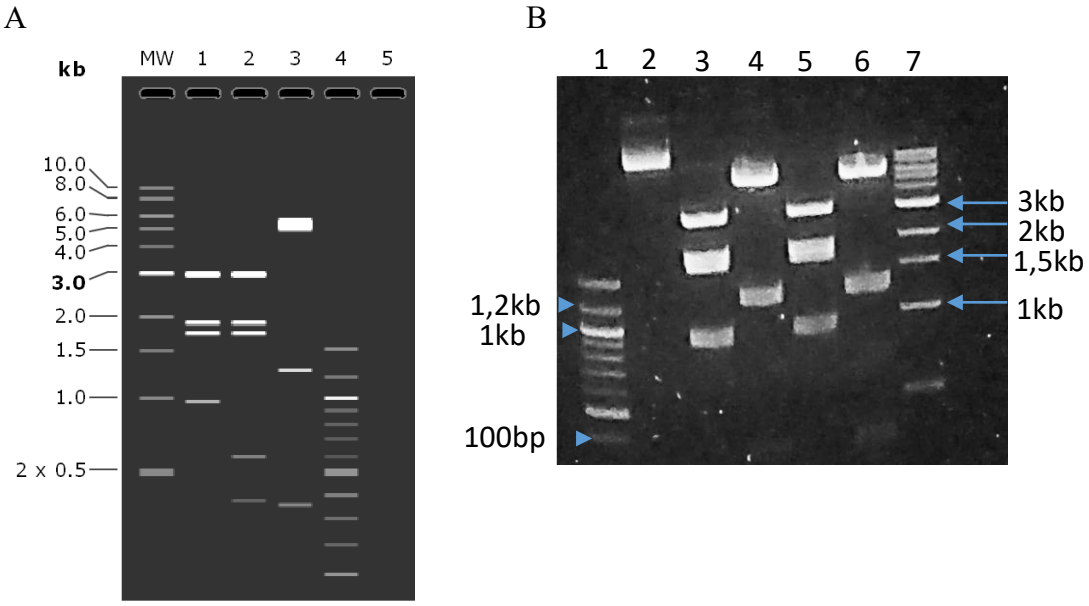

Figure 15. Restriction enzyme mapping of pCB-αEGFR(VHH)-SNAPF by Restriction Enzyme digestion. *15A) An image showing the restriction mapping simulation as performed by a gel electrophoresis function on the Snap-gene software. 15B) A 1.5% agarose gel with DNA bands of pCB-EGFR(VHH)-SNAP digested with either PvuII only or PvuII + MluI restriction enzymes. Lane 1 shows the 100bp PageRuler ladder, lane 2 is the undigested control, lanes 3 & 5 show DNA digested with PvuII + MluI, lanes 4 & 6 show DNA digested with PvuII only and lane 7 shows the 1kb PageRuler ladder.*

3.3 Tissue Culture & Protein profiling

The mammalian expression system of choice is HEK293T cells. These cells have been stably transformed with the SV40 large T-antigen which binds to SV40 promoter site present in the plasmid architecture to allow for the expression of our recombinant proteins. The proteins will be transiently expressed and harvested from the CCSN. The proteins that will be produced are scFv (CSPG4, MSLN & EGFR) and VHH (EGFR) molecules recombinantly fused to SNAP-tag or SNAP-F.

3.3.1 HEK293T mammalian tranfection

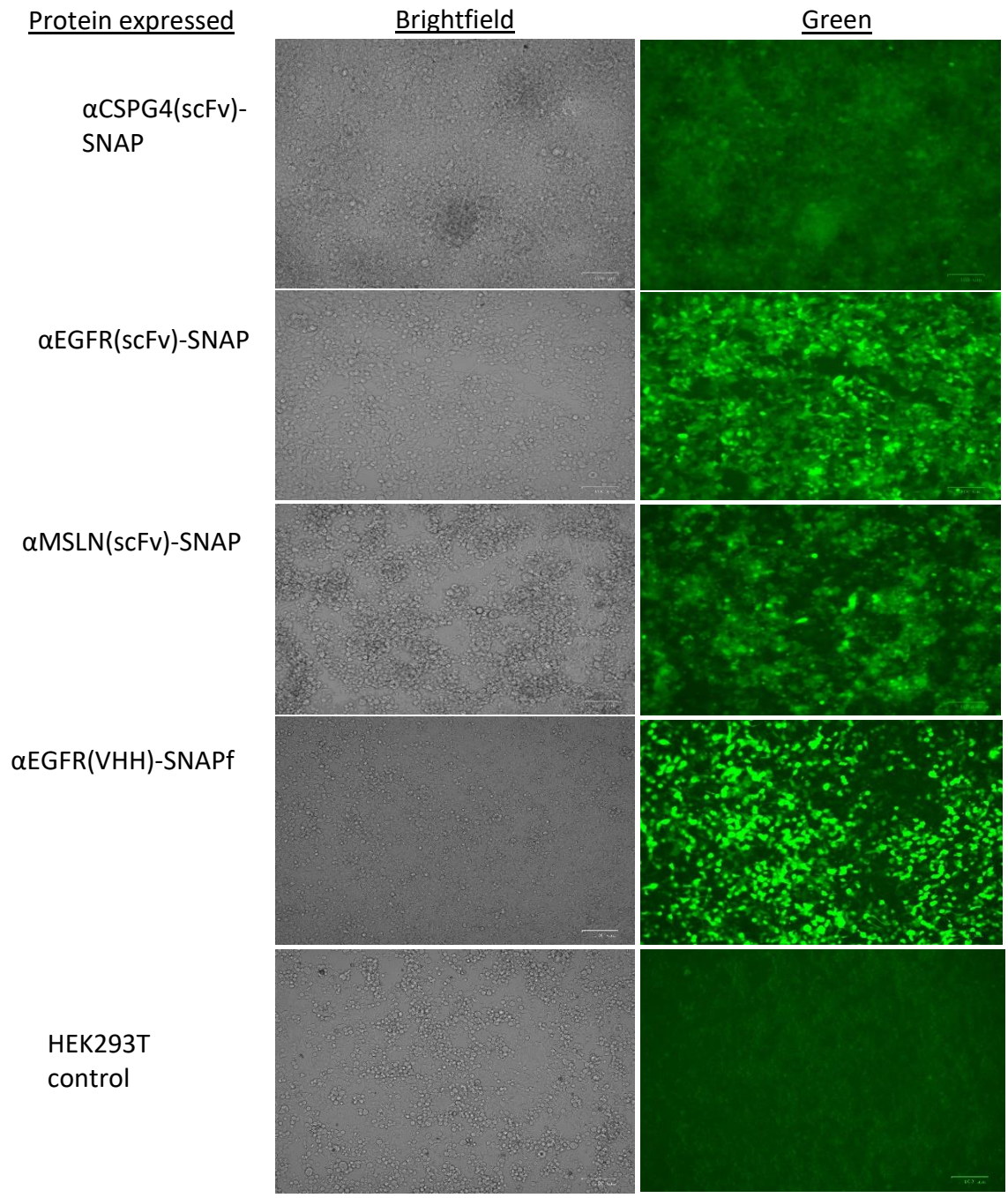

Figure 16. Visualization of transfected HEK293T cells under fluorescent cell imaging. *The cells were visualized using the ZOE Fluorescent Cell Imager under brightfield and the green line 2-7 days post transfection/post-thawing and monitored over a 12-week period.*

Figure 16 A-C show cell growth of HEK293T transfected with the following plasmids: pCB-αCSPG4(scFv)-SNAP, pCB-αEGFR(scFv)-SNAP, pCB-αMSLN(scFv)-SNAP. These cells were stored at -80^{o}C in 10% Dimethyl Sulfoxide (DMSO) and were provided from the lab collection. Only a few cells were growing in the first week after transfection but after several medium changes and selection pressure using Zeocin, the cells were more confluent and expressing EGFP by week 3. The HEK293T scFv constructs took approximately 12 weeks in culture for all cells to express EGFP whereas the cells transfected with the VHH construct reached this expression after 5-6 weeks of culturing (Fig. 16). This suggested that this was the average amount of time it took for proteins to be produced by the cells and were only ready for harvesting after this period. It is possible that the cells responded better to the plasmid with the VHH construct as oppose to the scFv constructs. The untransfected HEK293T control showed only backgound as expected. A total volume of 1L of CCSN was harvested from cells expressing the scFv protein and only 500mL was able to be collected for the cell expressing the VHH protein. At the point of protein harvest, the cells were analyzed for levels of EGFP expressions.

Upon visual inspection, all the transfected cells were healthy and confluent. The cells transfected with αEGFR(VHH)-SNAPf showed the highest fluorescence intensity while the cells transfected with αCSPG4(scFv)-SNAP showed the weakest. The αEGFR(scFv)-SNAP showed fluorescence intensities comparable to its VHH counterpart but expressed by fewer cells and the same comparison can be made for the cells transfected with αMSLN(scFv)-SNAP. To quantify these results, we performed flow cytometry to measure percentage EGFP expression.

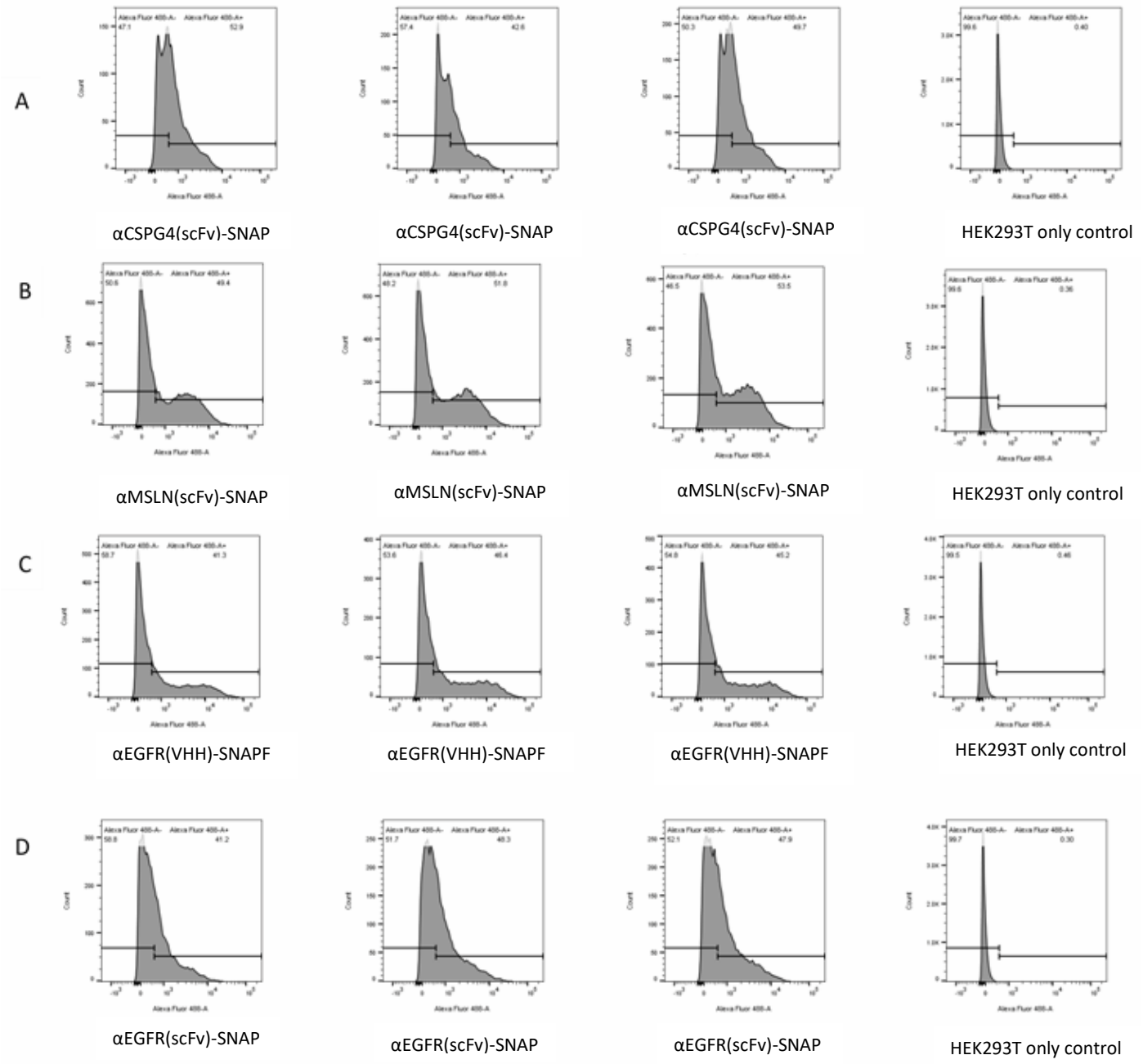

Figure 17. Flow cytometry data showing the EGFP expression profiles of transfected HEK293T cells. *A) This row represents the EGFP expression profile for αCSPG4(scFv)-SNAP (triplicates) and its HEK293T control. B) This row represents the EGFP expression profile for αMSLN(scFv)-SNAP (triplicates) and its HEK293T control. C) This row represents the EGFP expression profile for αEGFR(VHH)-SNAPF (triplicates) and its HEK293T control. D) This row represents the EGFP expression profile for αEGFR(scFv)-SNAP and its HEK293T control.*

The cells were prepared according to set standard protocols optimized for our needs and analyzed using the BD Biosciences FACS Caliber flow cytometer. The average EGFP expression for αCSPG4(scFv)-SNAP was recorded at 48.4% (Fig. 17A), αMSLN(scFv)-SNAP was recorded at 51.56% (Fig. 17B), αEGFR(scFv)-SNAP was recorded at 45.8% (Fig. 17D) and αEGFR(VHH)-SNAPF was recorded at 44.3% (Fig. 17C). Interstingly, the VHH construct, having been in culture for a considerably less time than the other constructs, showed an EGFP

expression profile comparable to the scFv constructs. Although the cells showed fair EGFP expressions, the cultures could be further improved by selection with Zeocin™.

A

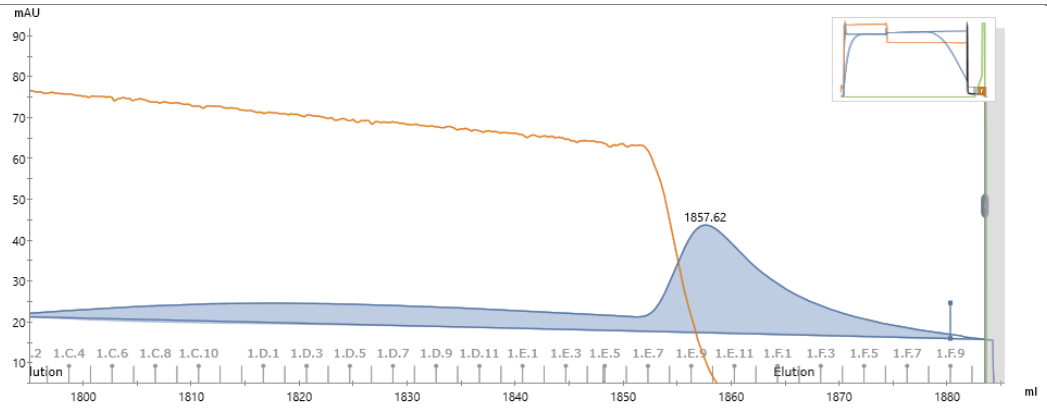

B

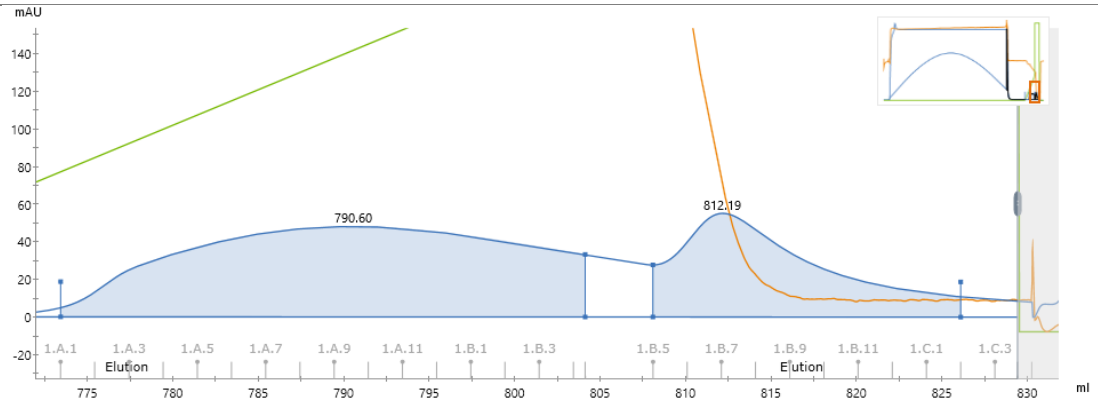

C

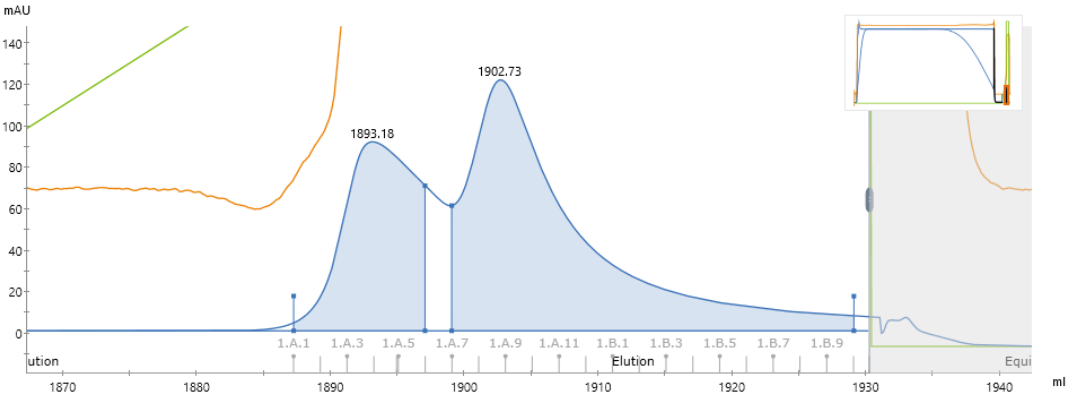

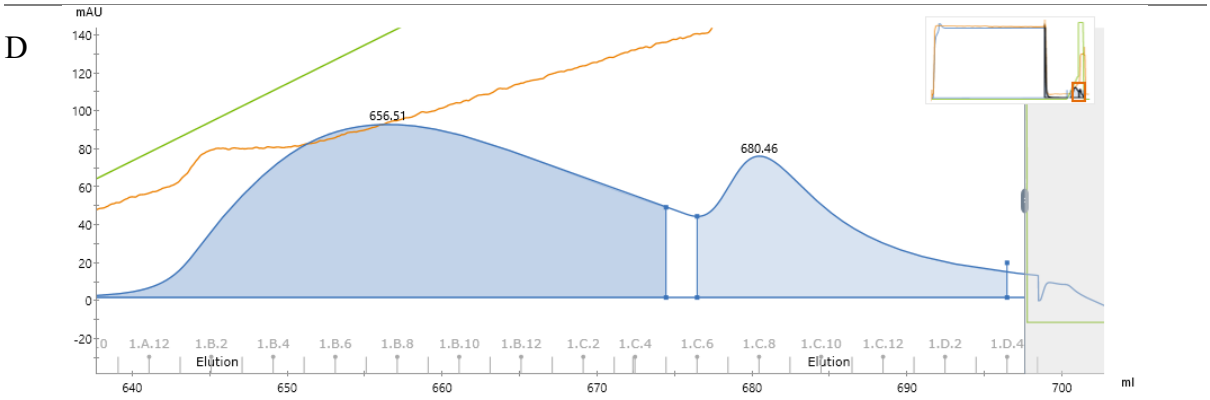

***Figure 18. Elution profiles from IMAC purification of proteins**. All elutions were gradual from 0-60% and then immediately ascends to 100%. The profiles are represented as follows A) αCSPG4(scFv)-SNAP protein, B) αMSLN(scFv)-SNAP protein, C) αEGFR(scFv)-SNAP and D) αEGFR(VHH)-SNAPF.*

The samples were purified using the AKTA Avant system using IMAC. IMAC allows for competitive binding of His-tagged proteins onto a resin of a His-trap column. The elution buffer is responsible for initially washing away unbound proteins in the His-trap column and with increasing concentrations releases the desired protein in fractions. The protein elution and fractionation profile was as shown in Figure 18. The protein fractions were then concentrated using Amicon® filtration. After this process the protein concentration were measured using the Denovix spectrophotometer and read as follows:

Table 13. Protein concentrations after Amicon filtration, measured using spectrophotometry.

Proteins	**Protein concentration**
αCSPG4(scFv)-SNAP	1.783 mg/ml
αMSLN(scFv)-SNAP	5.201 mg/ml
αEGFR(scFv)-SNAP	3.671 mg/ml
αEGFR(VHH)-SNAPF	4.803 mg/ml

The trend noticed in these profiles is two individual peaks per purification. It was initially hypothesized that the first peak was represented by contaminating proteins e.g. Bovine Serum Albumin (BSA) but upon further investigation it was found that this represented the protein of

interest but at a lower concentration to the second peak. This finding suggests that these proteins bound poorly to the resin, if at all. As such, all downstream processes were followed using the concentrated proteins in the second peak. Interestingly, the αEGFR(VHH)-SNAPF showed competitive concentrations to the scFv proteins while only having a volume of 500ml of harvested and this may be a positive going forward.

3.3.2 SDS PAGE & Western Blotting

An SDS PAGE gel is used to separate proteins by gel elctrophoresis by molecular weight. The proteins that would produced were expected to appear in the regions between 48-58 kDa acording to the protein ladder (Fig. 19A). The banding patterns visualized, after staining with Aquastain dye, for the scFv proteins were in the correct regions for each. Although the proteins were purified, the samples showed multiple bands but the most concentrated of each were at the correct levels.

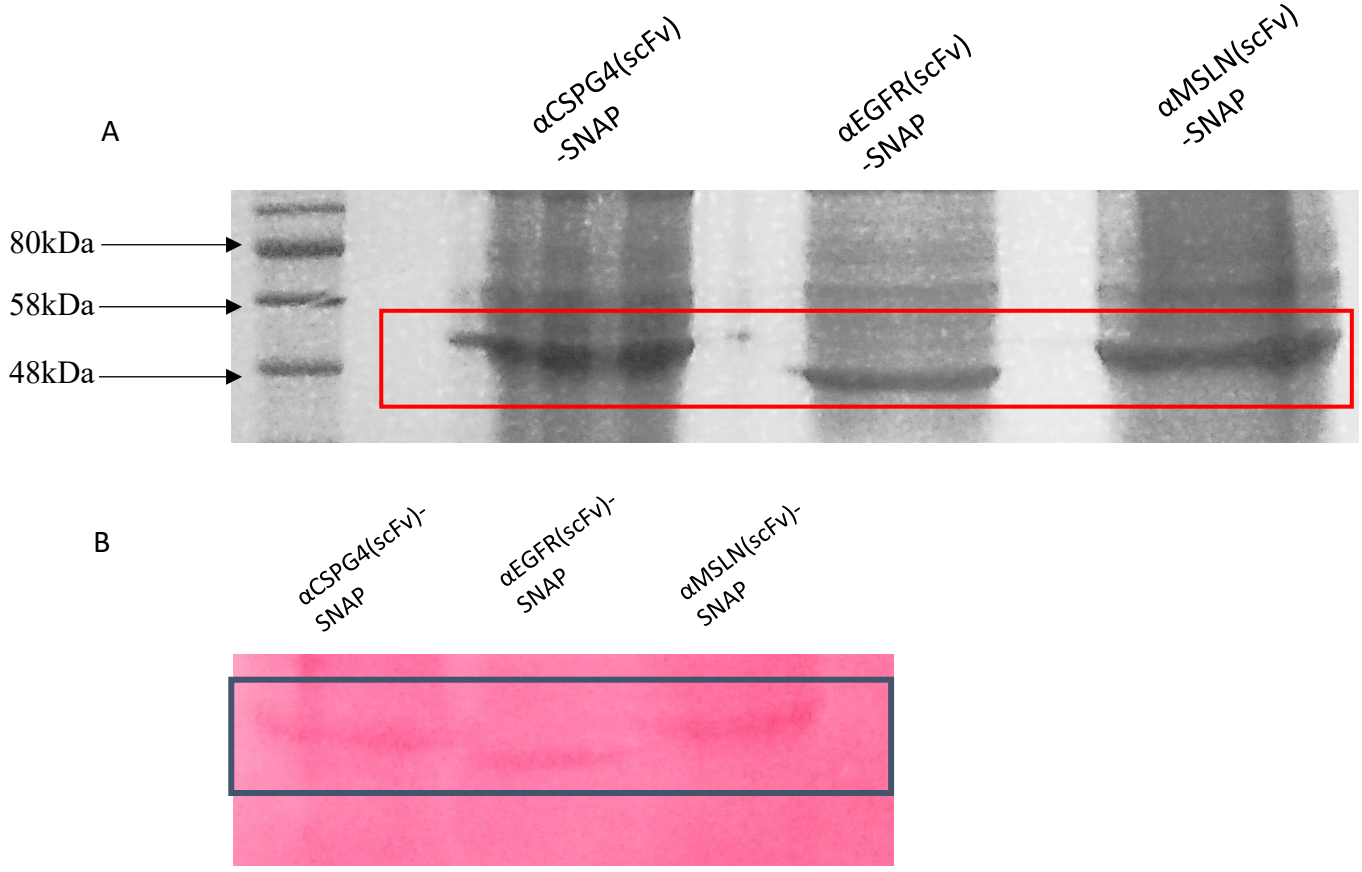

Figure 19. SDS and Ponceau stained PVDF membrane of proteins after purification with the AKTA Avant system. *A) This shows an SDS PAGE gel with αCSPG4(scFv)-SNAP, αEGFR(scFv)-SNAP and αMSLN(scFv)-SNAP fusion proteins appearing as dark bands as denoted by the red rectangle. The sizes of the proteins were compared against a colorimetric ladder from. B) This shows a PVDF membrane stained with Ponceau Red stain. Ponceau S Acid Red is an acid stain that allows for reversible detection of proteins on membranes.*

The proteins were transferred onto a polyvinylidene fluoride (PVDF) membrane for western blotting. The membrane was stained using Ponceau S Acid Red stain, which allows for rapid detection of proteins on a variety of membranes whereas Aquastaining can only be used to stain SDS gels. In Figure 19B, we were abe to see a banding pattern similar to that of protein of interest seen in Figure 19A. Unfortunately, these results could not be replicated by way of western blotting but researchers proceeded to test for the functionality of these proteins using tumor cell lines expressing the target receptors.

A positive western blot result was shown after purification of the VHH fusion protein as seen in Figure 20. The αEGFR(VHH)-SNAPF proteins appeared as two intense bands at approximate 38 kDa, according to the ladder, which was the expected size of the protein. The αEGFR(scFv)-SNAP protein served as a control as it had been previously confirmed by a colleague Dr. Nsole. The intensity and size of the VHH band suggested that the concentration of the SNAP-fusion protein was higher than its scFv counterpart. This is a desirable result as the the volume of CCSN collected for purification of the VHH construct was considerably less than the scFv constructs which suggests that a higher concentration of protein can be obtained with a lower volume with the VHH construct. Upon confirmation of the proteins, the protein functionality was tested for by performing conjugations with a fluorophore and testing the binding on tumor cell lines.

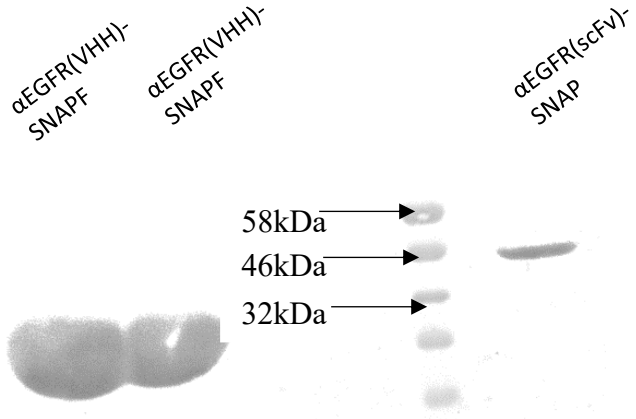

Figure 20. Western blot membrane image of EGFR(VHH)-SNAPF and EGFR(scFv)-SNAP proteins. *The proteins were successfully transferred onto the PVDF membrane and tracked using a 1º anti-His antibody and 2º anti-Goat-Rabbit HRP antibody for detection of proteins. The first two lanes show the αEGFR(VHH)-SNAPF proteins. The third lane is empty. The fourth lane shows the colorimetric ladder and the fifth lane shows the αEGFR(scFv)-SNAP protein which was used a control.*

3.3.3 Conjuagtion to Alexa 488 and Binding studies in TNBC$^+$ tumor cell lines

After confirmation of proteins by way of SDS PAGE and western blotting, the proteins were conjugated with BG-Alexa Fluor 488. The SNAP-tag binds BG-substrates in a 1:1 stoichiometry which made this fluorophore a good marker for the functionality of the SNAP-tag component of the fusion protein. The conjugated proteins were run on an SDS gel and exposed to blue light (λ=380-500nm). Alexa Fluor488 is excitable at a wavelength of 488nm which falls within the spectrum of blue light. Successful conjugation was observed with all the scFv-SNAP and VHH-SNAP fusion proteins (Fig. 21). The unconjugated controls did not appear when the gel was exposed to blue light showing that this was true fluorescence from the fluorophore. The intensity of flourescence suggests that there are differences in conjugation efficiencies between the various proteins.

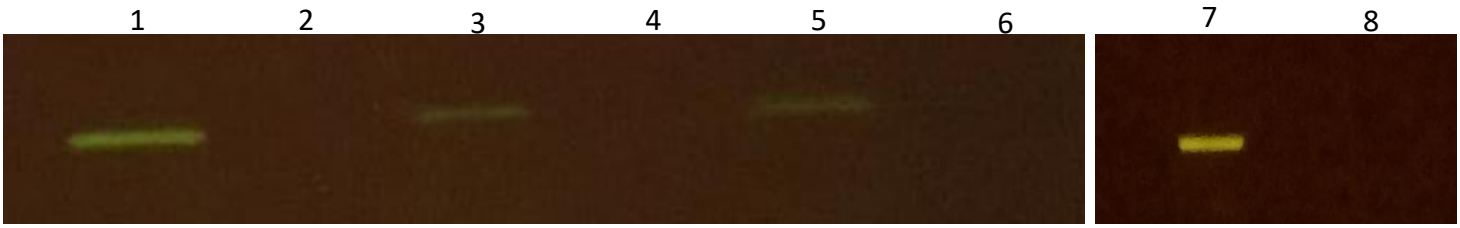

Figure 21. SDS gel of proteins conjugated to Alexa488 fluorescing under blue light. *The proteins of interest were linearized and run on an SDS gel after being conjugated with Alexa488. The SDS gel was put under blue light in order to excite the Alexa488 bound to the proteins. 1, 3, 5 & 7) αEGFR(scFv)-SNAP, αCSPG4(scFv)-SNAP, αMSLN(scFv)-SNAP & αEGFR(VHH)-SNAPF bound to Alexa488 respectively. 2, 4, 6 & 8) The unbound controls of the afore mentioned proteins.*

The concentrations of both labelled and unlabelled proteins were measured using the Denovix spectrophotometer and the conjugation efficiency was calculated for. αCSPG4(scFv)-SNAP showed the highest percentage conjugation followed by αEGFR(VHH)-SNAPF, αEGFR(scFv)-SNAP and αMSLN-SNAP. It was surprising to find that αMSLN-SNAP showed the lowest efficiency of conjugation as it showed the highest concentration of unconjugated protein. Although, based on the fluorescent intensities visualized in Fig. 21, these two results corroborate with one another. The αEGFR(scFv)-SNAP and αCSPG4(scFv)-SNAP are as expected. The αEGFR(VHH)-SNAPF provided a good result as it showed that the SNAPF variant is functional and could possibly work better than the original SNAP-tag format based on the conjugation efficiencies.

Table 14. The respective concentrations of conjugated and unconjugated proteins, as well as the approximated percentage conjugation efficiency.

Protein	Concentration of unconjugated protein	Concentration of protein conjugated to Alexa488	Approximate percentage Conjugation efficiency
αCSPG4(scFv)-SNAP	1.783 mg/ml	1.097 mg/ml	61.53%
αMSLN(scFv)-SNAP	5.201 mg/ml	1.898 mg/ml	36.5%
αEGFR(scFv)-SNAP	3.671 mg/ml	1.51 mg/ml	41.13%
αEGFR(VHH)-SNAPF	4.803 mg/ml	2.625 mg/ml	54.65%

After conjugation of proteins with Alexa 488 and confirmation of the SNAP-tag component of the protein, the antibody binding ability of the proteins was tested and viewed using confocal microscopy. Figure 22A shows the binding experiment for the αCSPG4(scFv)-SNAP protein. There was no binding on the negative control (MB-MDA-468) which is not known to express the CSPG4 surface receptor, but a clear surface label was seen on the Hs578t cell line which has been reported to express CSPG4. The next image shows binding of the αEGFR(scFv)-SNAP protein to MB-MDA-468 tumor cell line and no binding on the A2058 negative control (Fig. 22B). Although the cells were relatively stressed under the DIC view, a membrane label could be seen on the experimental cell line as oppose to the negative control. The binding of the EGFR(scFv) fusion protein was mimicked by its VHH counterpart (Fig. 22C). The αEGFR(VHH)-SNAPF-Alexa488 showed a bright surface label signal on the experimental cell line and no binding was seen on the negative. The bright green signal of this protein suggests that the SNAP-F variant does indeed bind BG-substrates better than the original SNAP-tag or there was more accumulation of protein on the cell surface as compared to Fig. 22A & B. There was partial internalization of this protein as well which suggested that its' small size may contribute to faster intake of protein by the cell. No positive results were recorded for αMSLN(scFv)-SNAP due to a lack of tumor cell lines strongly expressing the surface receptor. These qualitative results showed the production of full-length functional proteins that could potentially be used for future diagnostics and therapeutics for a variety of diseases.

A

1. MB-MDA-468 cell line, negative control

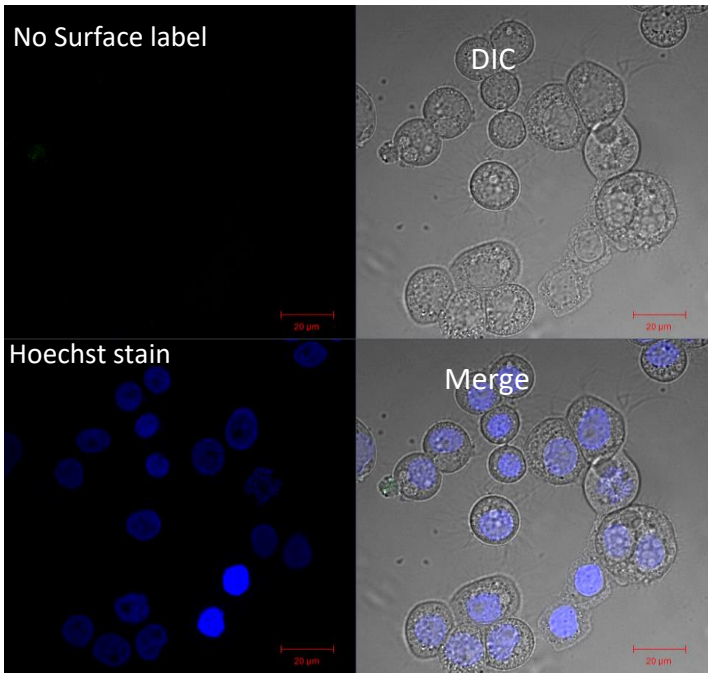

2. Hs578t tumour cell line

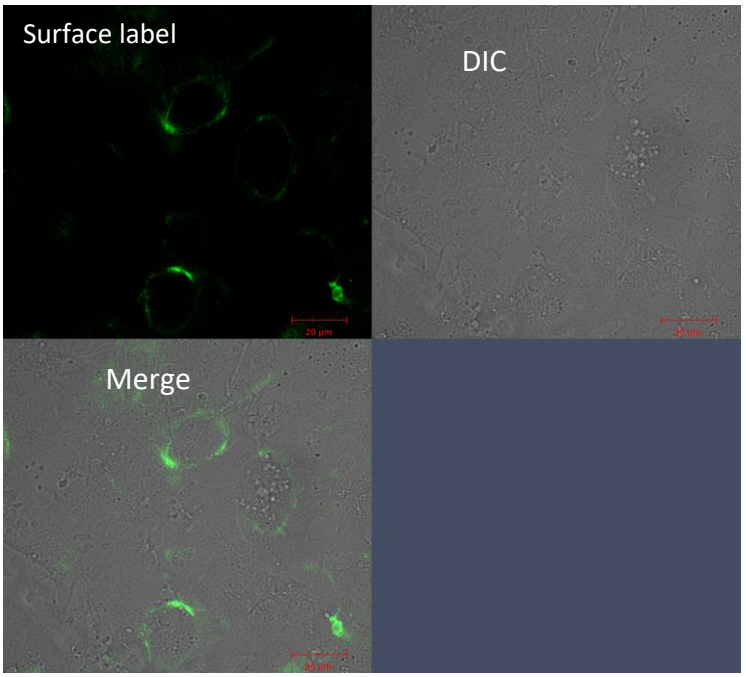

B

1. A2028 cell line, negative control

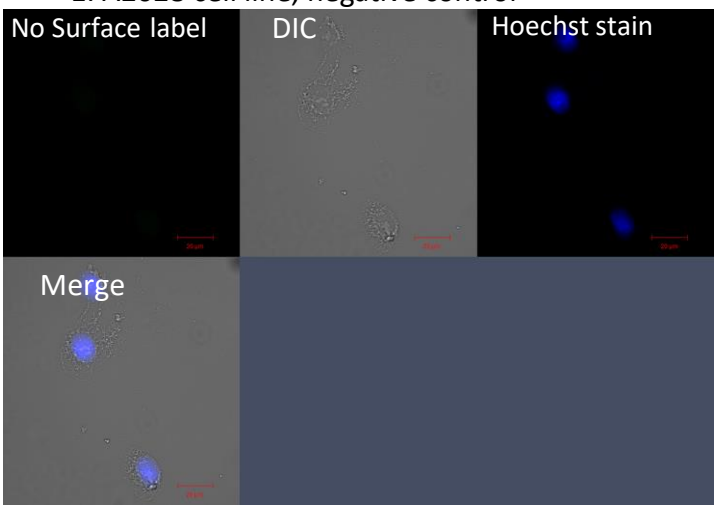

2. MB-MDA-468 cell line

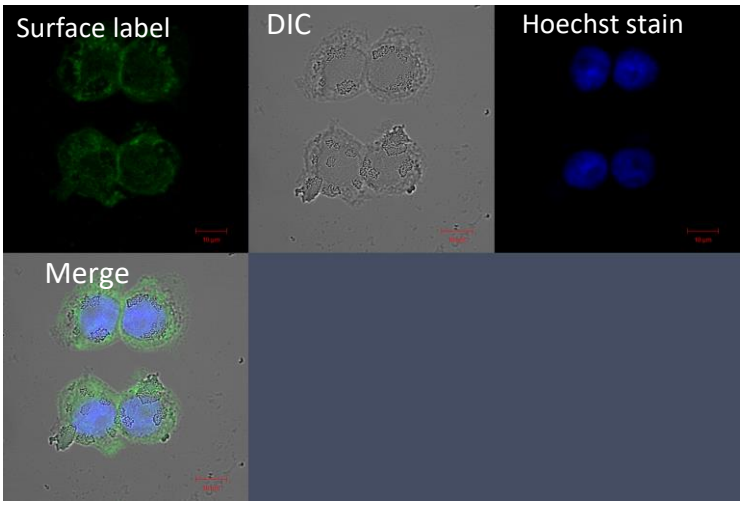

C

1. A2028 cell line, negative control

2. MB-MDA-468 cell line

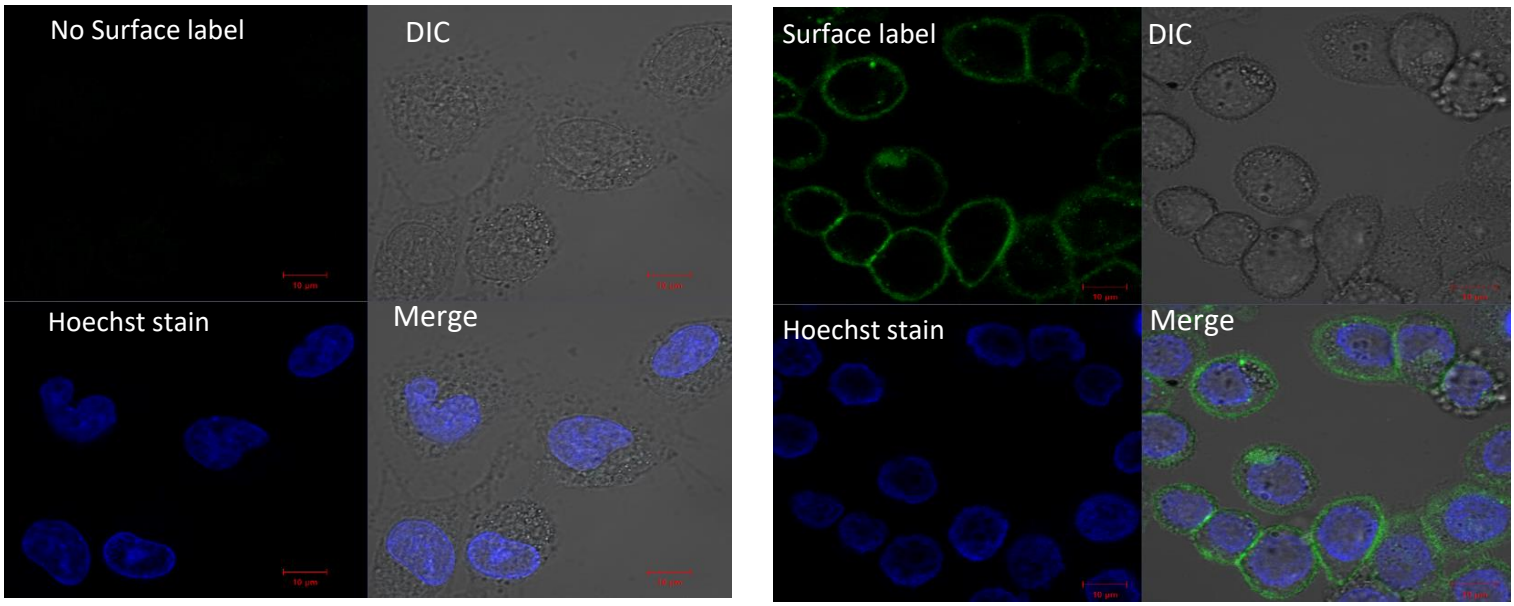

Figure 22. Confocal imaging of tumor cell lines labeled with SNAP-tag proteins conjugated to Alexa 488. *The images were taken focusing on surface label, nuclear staining with Hoescht and cell morphology with Differential Intereference Contrast (DIC). A) This shows tumor cell lines labeled with αCSPG4(scFv)-SNAP-Alexa488. The negative control was the MB-MDA-468 cell line (stained with Hoescht) and the experimental cell line was Hs578t (without Hoescht). B) This tumor cell lines labeled with αEGFR(scFv)-SNAP-Alexa488. The negative control was the A2058 cell line (stained with Hoescht) and the experimental cell line was MB-MDA-468 (stained with Hoescht). C) This shows tumor cell lines labeled with αEGFR(VHH)-SNAPF-Alexa488. The negative control and experimental cell lines were the same as in figure 22B.*

Chapter 4: Discussion & Conclusion

4.1 Discussion

TNBC proves to be an issue due to its onset in young premenopausal women, particularly those of African descent, in developing and undeveloped countries. Poor prognosis is accompanied by low survival rates, a result of its high rates of chromosomal mutations, high division rates, mutations in the p53 and BRCA1 genes as well as lymphatic dissemination [202]. This rapid progression of the cancer coupled with the lack of adequate treatment strategies further complicates things for the medical industry, but this opens avenues for the discovery of novel therapeutics against TNBC. In this study, CSPG4 (which is overexpressed in 50% of TNBCs) [203], [204], EGFR (which is overexpression in 13-76% of TNBCs) [205]–[208] and MSLN (which is overexpressed in 67% of TNBCs) [171], [209] were selected as potential targets for the development of immunodiagnostic and -therapeutic tools against TNBCs. Monoclonal antibodies such as trastuzumab, cetuximab, panitumumab and a range of other monoclonal antibodies are already in use as targeted therapies for the treatment of various cancers but an efficacious therapy against TNBCs has yet to be established. Current research is focusing on new antibody formats such as scFvs and VHHs (the formats used in this study) that have shown better outcomes towards diagnostics and therapy when compared to full sized antibodies because of their penetrative ability, reduced immunogenicity and retention in non-target tissues, high stability and rapid clearance from circulation [94], [95], [99]–[102]. SNAP-tag, as previously mentioned, is a modified version of a DNA repair enzyme that has the capacity to covalently bind BG-substrates in a 1:1 stoichiometry.

In silico design of the bicistronic plasmids housing the open reading frames for our specific SNAP-tag based fusion proteins was performed successfully using the SNAPgene software (Fig. 11). The molecular cloning in this study was exemplified for αEGFR(VHH)-SNAPF but the same methodology was applied for each construct except for αMSLN(VHH)-SNAPF which did not get past the level of restriction enzyme digestion with gel electrophoresis. Previous studies, such as that performed by Prof Muyldermans groups at the University of Brussels, had used a PCR based approach to cloning the desired ORF and this could be key in getting a DNA concentration high enough to be seen on an agarose gel. A successful digestion (Fig. 12) was seen for αEGFR(VHH) out of the pUC57 vector prior to ligation into the household plasmid. According to general recommendations for DNA gel electrophoresis from Thermofisher scientific (https://www.thermofisher.com/content/dam/LifeTech/global/brands/Documents/1114/genera

l-recommendations-dna-electrophoresis.pdf) suggest that using a 1.5% agarose gel at a voltage of 5-10 V/cm would give us good separation of DNA in the ranges of 200-3000 bp. The lowest voltage was used and therefore clear separation of the DNA bands was expected. Band separation was seen in Figure 12, but the band intensity was quite low. Lee et al., 2012, made mention in a review that at least 1ug/ml of DNA would be sufficient for a successful gel electrophoresis experiment [210]. The concentration of 2µg/µl should have been sufficient for this experiment seems too low as seen by the poor band intensity. The smaller sized molecules, such as the VHH DNAs, normally travel faster through the agarose gels in comparison to larger molecules [210], [211] and it is possible that most of the DNA ran off the gel during electrophoresis. An unsuccessful enzyme digestion was seen for αMSLN(VHH) and perhaps increasing the concentration and further decreasing the voltage may provide better results. An additional control to the single and undigested controls may have been a DNA sample previously confirmed to be correct by sequencing, this may have further validated this experiment. The potential of having to use higher concentrations for the initial molecular cloning of the VHH constructs adds additional time and labour to the development process, also incurring more expenses as more resources are being used which may be a major downside for large scale experiments.

The digested products, namely the pCB plasmid and the genes of interest, were ligated and transformed into DH5α *E. coli* competent cells. This particular strain of competent cells were selected for transformation because of their well-known ability to maintain and amplify plasmid DNA [212]. Colony growth on the agar plates (supplemented with Ampicilin) showed that the plasmid constructs had been successfully tranformed into the competent cells (Fig. 13). This is confirmed by the presence of the Ampicilin resistance (AmpR) in the plasmid (Fig. 11). The lack of growth in the vector only control further substantiated that the non-transformed bacteria could not grow in the absence of the survival gene or in the presence of antibiotic selection pressure. This also showed that there were no contaminants in the plasmid samples. The introduction of bacteria only (with & without ampicillin) and vector with ligase controls may have been key to test the activity of the stock of ampicillin (with ampicillin) and the viability of the stock of bacteria used (without ampicillin). The digested vector with ligase control would test for religation of the vector but growth would not be expected on this plate because it would lack the open reading frame and the promoter site necessary to activate the the AmpR gene. This is also a good marker for potential contamination on the agar plates. Although these controls were not included, the digested vector only control and the successful

colony formations in the 1:3 and 1:5 plates were sufficient evidence to show that the ligation reaction. Colonies were selected from the 1:3 plate and these showed a transformation efficiency of 57.2 x 10^3 CFU/µg. The suggested maximum transformation efficiency for 1µg of DNA into DH5-α cells is in the range of 10^6-10^9 CFU/µg [213]. Upon visual inspection of the plates, there were small number of colonies which corroborated the efficiency results. However, the results from Inqaba biotech sequencing (Fig. 14) showed 100% identity to the original sequence and the restriction mapping analysis (Fig. 15) showed similar banding patterns to the simulated gel.

The plasmids containing the confirmed gene of interest were transfected into Human embryonic kidney 293T (HEK293T) cells. As previously stated, this cell line is derived from HEK293 cells. The cell line origin lacks the large T antigen which is important for the replication of plasmids containing the SV40 promoter site. This site ensures plasmid transcription into proteins in this transient expression system [214], [215]. The SV40 promoter site is also a feature specified in the plasmid as denoted in Fig. 11 which initiates the replication process. During the initial 2-3 weeks of tissue culture, the cultures were enriched for with Zeocin™ treatment. This is a selection marker (ranked higher than the selection efficacy of hygromycin B, puromycin & neomycin) used to obtain the desired pool of recombinant cells i.e. successfully transfected cells, while suppressing the growth of non-transfected cells. The Zeocin/Bleomycin resistant gene is included in the architecture of the transfected plasmid [216]. Direct monitoring of recombinant proteins for timely harvesting at peak protein production has yet to be demonstrated in these types of cells and proteins but biosensors have been used in previous studies to follow human recombinant proteins such as the human insulin analogue (HI3) [217]. The addition of biosensors tailored to follow protein production in these cells may serve beneficial in knowing the peak times to harvest proteins, however, this would add an additional expense to this production process and more inexpensive avenues may need to be explored first. The cultures containing cells transfected with the plasmid carrying αEGFR(VHH)-SNAPF showed full EGFP expression ~5-6 weeks after culture and were ready for harvest, whereas the cultures with cells transcfected with the scFv reached a full EGFP expressing culture ~12 weeks after culturing (Fig. 16). The scFv transfected cells were thawed from lab collection and it was unusual to see these cells take a longer period of time to reach 100% confluency and EGFP expression. Perhaps the handling protocols for the cells resulted in the cells becoming stressed and thus resulting in difficulty to express proteins in that state. It can further speculated that the small size of the VHH contanining plasmid allowed for the

EGFP to be translated and expressed faster than the scFv containing plasmids but the protocols would still need to be optimized before anything conclusive can be made. Historically, nanobodies in particular VHHs, have been produced in bacterial expression systems such as *E. coli* but they have also been reported to be produced in filamentous fungi and certain yeasts species such as as *Saccharomyces cerevisiae* and *Pichia pastoris* [103], [218]–[221]. It may have been an interesting experiment to compare the most efficient expression system for both scFv and VHH-SNAP fusion proteins. Currently, the expression capacity of the scFv fusion proteins in bacteria, yeast and mammalian (used in this study) systems are being investigated and systems optimized. Comparing these systems may be beneficial to see which produces full length functional protein in the shortest time with minimal immunogenicity *in vivo,* while using the least amount of resources. The proteins were harvested from the transient mammalian expression system and purified by IMAC. This is a process that purifies his-tagged protein through the interactions with metals (in our case Ni^{2+}) and specific amino acid side chains within the column resin [222], [223]. The proteins were harvested after the cells showed bright EGFP expressions but a more quantitative method of tracking the protein concentration in culture is by the use of an Elisa. By coating the plates with an anti-SNAP antibody and incubating with the appropriate 2^{o} antibody, quantification of protein concentration could be measured in culture based on the results of the Elisa. The proteins were confirmed using SDS and western blotting (Fig. 19 & 20). The SDS gel showed bands at the correct sizes as decribed in Table 10. An additional purification step such as size exclusion chromatography (SEC) may have provided a cleaner protein product. This is a purification technique that separates solutes according to their molecular weight using the size exclusion effect of a porous gel in a column [224], and in essence isolating the desired protein. In Figure 19, a PVDF membrane was stained with ponceau red stain and this showed a banding pattern resembling that of the SDS gel impying a successful transfer of proteins from an SDS gel. A successful gel doc image could not be generated but this did not hinder the downstream processes as successful conjugation of the proteins to BG-Alexa488 showeded that the SNAP-tag a the C/N terminal of the protein was functional (Fig. 21). After optimization of protocols, a gel doc image for the VHH protein, after incubation with 1^{o} anti-His antibody was shown. This showed that the full length protein was present and further confirmed through conjugation with the BG-fluorophore. Although the yeast and bacterial expression systems are still being optimized, it is known that full length VHH proteins are traditionally produced in bacterial and yeast expression systems. This study showed a successful VHH protein product (fused to SNAP-tag) produced in a mammalian expression system.

The EGFP expression profiles were analyzed using flow cytometry. The histograms generated using FlowJo show that within each repeat there were a mixture of negative and postive EGFP expressing cells. The average EGFP expression for αCSPG4(scFv)-SNAP was recorded at 48.4% (Fig. 17A), αMSLN(scFv)-SNAP was recorded at 51.56% (Fig. 17B), αEGFR(scFv)-SNAP was recorded at 45.8% (Fig. 17D) and αEGFR(VHH)-SNAPF was recorded at 44.3% (Fig. 17C). This flow cytometry experiment could have been further refined with the addition of a live/dead stain such as 7-aminoactinomycin D (7AAD). The 7AAD differentiates between viable, apoptotic and dead cells in flow cytometry [225] and this may have been useful in reducing potential background flourescence from the cells in the cytometer and give us less skewed data. Unfortunately this was not available at the time of the experiment. Even so, interestingly, the VHH constructs, after being in culture for a shorter period compared to the scFvs could still provide competitive EGFP expression profiles. This suggests that the VHH proteins can be produced quicker as compared to the scFvs. There is evidence that suggests that the single domain antibodies are more easily produced due to their small size which allows for folding to happen quite rapidly, with increased hydrophobicity and no mispairing of domains [103], [226]–[228]. A direct correlation between percentage EGFP expression and protein concentration could not be made as the values varied for each targetting protein as seen in Table 14. A cell density monitoring study may be useful in predicting the optimal protein production level based on the amount of cells present in culture. Previous studies have stated that cell density has a direct impact on the efficiency of protein production and yield [229], [230]. The peak cell concentration of HEK293T cells in microcarriers have been indicated to be 1.5 x 10^6 cells/ml but in tissue culture flasks (with sizes ranging from 25-186 cm^2) have been estimated between 2.8-20.5 x 10^6 cells/ml [231], [232]. Tracking the cell culture densities and measuring the protein concentrations at various time points may provide essential data toward predicting the optimal protein harvesting times from cell cultures. This quantitative data would allow proper comparisons regarding to be made regarding transfection efficiencies, percentage EGFP expression and protein concentrations. Although a correlation could not be made in this study, there is evidence that suggests the VHH antibody formats possess favourable characteristics in comparison to the scFv antibody format. The VHH (~15 kDa) is smaller in size than the scFv (~27 kDa) and is easier to genetically engineer or modify, it has better tumor penetration and shorter half lives in circulation [101], [233]–[236], as demonstrated by Prof. Muyldermans group and various others. There are signs that the VHH antibody format may potentially outperform the scFv but its effectiveness when fused to SNAP-tag is uknown at the moment.

The proteins were successfully conjugated to BG-modified Alexa 488 (fluorophore) as shown in Figure 21, and efficiency data generated from this as well (Table 14). In Figure 21, we see that the band flourescence of the αEGFR(VHH)-SNAPf-Alexa488 conjugation product is brighter than its scFv counterparts, even though it showed the second highest conjugation efficiency at 54.65% (Table 14). This speaks to the efficiency of the SNAP-F variant which allows for labelling with BG-substrates to occur faster and more efficiently than the original SNAP-tag format [237]. The conjugated proteins were used in binding studies with receptor positive tumor cell lines. The cell lines used for test for binding were Hs578t (CSPG4+), MB-MDA-468 (CSPG4-, EGFR+) and A2058 (EGFR-). Cell lines strongly expressing the MSLN receptor could not be acquired and therefore no binding studies were recorded for αMSLN(scFv)-SNAP. In Figure 22, a clear membrane signal was seen for cells labelled with αCSPG4(scFv)-SNAP (Fig. 22A) and αEGFR(VHH)-SNAPF (Fig. 22C). The cells labelled with αEGFR(scFv)-SNAP (Fig. 22B) were slightly stressed due to them being put on ice prior to them being viewed on the confocal microscope. It was previously thought that placing cells on ice would slow down internalization of labelled protein but later seen that this was unnecessary. Nevertheless, A partial membrane signal could still be seen on the membranes of these cells. The αEGFR(VHH)-SNAPF proteins showed better accumulation of proteins on the surface as compared to the scFv proteins. There was partial internalization aswell in these cells. These results further confirm the fast binding and tissue penetrative ability of VHHs [100], [103], [238]. The results obtained in this study coincide with the general literature on these three targets. There has been extensive research on EGFR and CSPG4 on a variety of cancer types, in particular melanoma, prostatic and breast cancers [192], [239]–[243], but there is limited knowledge and understanding about MSLN and more work can be done in closing this gap in knowledge. Nonetheless, protein binding to target epitopes on TNBC cell lines was shown using two different antibody formats recombinantly fused to SNAP-tag. This is especially important for EGFR overexpressing tumours as there may potentially be a fast binding and highly specific method of diagnosis and therapy in the VHH-SNAP fusion proteins.

4.2 Conclusion & Future perspectives

The primary aim of the study was to design, produce and show functionality, in terms of binding capacity, of surface antigen targeting SNAP-tag fusion proteins against the three study specific surface receptors overexpressed in TNBCs with the greater goal of improving the current scope of cancer diagnosis and therapy. This study showed functionality of two scFv

SNAP fusion proteins and one VHH SNAP fusion protein. Previously there had not been any reports on the combition of a VHH antibody format with SNAP-tag technology and therefore this study has provided novelty towards scientific research that can be built upon. Theoretically, this technology can allow the design, production and potentially show functionality of any protein targeting surface receptors expressed on a variety of diseases, provided the sequences can be obtained. SNAP-tag has shown great potential as an immunodiagnostic agent as it allows for the tracking of tagged proteins *in vivo* and visualisation of cell to cell interactions. This technology can contribute towards possible therapies by attaching a BG-modified drug or toxic to a SNAP-tag fusion protein that target specific epitopes on diseased cells [244]–[247]. This study also partially demonstrated the effieciency of SNAP-F variant against SNAP-tag. In a study by Sun *et al*, 2011, they were able to show, by way of kinetics measurements using fluorogenic probes, that SNAP-F binds BG-substrates 10-fold faster than SNAP-tag. Furthermore, they showed binding data by using HEK293 cells that were stably expressing EGFR and, by using an EGFR targeting antibody fused to SNAPF, they were able to show membrane fluorescence in the presence and absence of media [123]. In this study, similar binding and fluorescence intensities on tumour cell lines were shown. This result further contributes to the greater goal of improved immunodiagnostic and therapeutic agents but a more in depth investigation would need to be performed. The next step would be to confirm binding on patient biopsies and in animal models. The VHH has been shown to be well expressed in a variety of expression systems due to its single domain nature and increased hydrophobicity. It is physiologically stable, highly soluble, easily modified genetically and shows fast tissue penetration and clearance [101]–[103], [227], [228], [238]. The combination with SNAP-tag allows for the covalent binding of the fusion protein with any BG-modified probe such as a fluorophore that can be tracked on the surface or in the internal compartments of cells; or an immunotoxin that can provide effective killing of diseased tissues without harming healthy tissues. Protein engineering has changed the scope of immunodiagnostics and therapy by allowing the creative design of novel targeting proteins and their conjugation to reporter probes or toxic payloads. The combination of VHH and SNAP-tag is such an example of the progress being made in this field. A fusion protein that is capable of binding quickly and specifically to its target epitope but also has the ability to covalently bind any BG-substrate in a 1:1 ratio is as a result of this study and advancements made in this field. The combination of targetting antibodies and SNAP-tag technology has opened the door for further medical advancements and invention in immunotherapy. It has, for example, initiated a collaboration of the Medical Biotechnology & Immunotherapy (MB&I) Research Unit with Prof

Klumperman's group at Department of Chemistry and Polymer Science at Stellenbosch University where a polymer with a BG-moeity is being synthesized. Historically polymers have been used as vehicles for drug delivery but the problem is that this mode of therapy is unspecific [248] and the addition an antibody may remedy this. Moreover, the combination of these technologies may provide novel and innovative ways towards disease diagnosis and therapy.

This study had hoped to add another brick onto the foundation of immunodiagnostics and immunotherapy. This study showcased the design, production and functionality of SNAP-tag fusion proteins as target specific molecules detection molecules against TNBC. These molecules were designed to ensure key additions in the discovery of newer, safer and more efficient methods of disease diagnosis and therapy that can potentially replace the current state of the art. The study made use of multidisciplined approach, in terms of the methodology employed, in order to show the functionality of the proteins and the novelty of SNAP-tag fused nanobodies. Overall, key successes relating to the primary aims were noted during the study but improvements can be made to strengthen the reliability of the presented data and these were previously suggested. The current model makes use of an *in vitro* approach to test and qualify the functionality of SNAP-tag fusion proteins but it may be important to show the same target specificty and detectability *in vivo.* This future recommendation may greatly contribute to the immunodiagnostic arm of the primary aims. Future recommendations towards the immunotherapeutic arm include testing the scFv and VHH SNAP-tag proteins using BG-modified cytotoxic agents such as monomethyl Auristatin-E/F (MMAE/F). MMAE or MMAF are small molecule toxins that exerts their effects after target specific delivery to a cell [249]. It is speculated that this would show targetted killing of diseased cells rich with the target receptor while preserving healthy cells. Successful cell death experiments have been performed by colleagues, Dr Nsole and Ms Jordaan, using the scFv antibody formats of αCSPG4-MMAF and αEGFR-MMAF give confidence that these results can be reproduced for the VHH format aswell. This study sought to add to novelty to this field and further build on work previously performed. This study has provided new knowledge to build upon in the form of SNAP-tag fused nanobodies and these may provide novel combinations that contribute towards immonodiagnostics and therapy of TNBC and other diseases.

5. References

[1] American Cancer Society, "No Title," *Breast Cancer Treatment.*, 2017. [Online]. Available: https://www.cancer.org/cancer/breast-cancer/treatment.html. [Accessed: 08-Apr-2017].

[2] M. et al Amoury, "A novel approach for targeted elimination of CSPG4-positive.," *Int. J. Cancer*, vol. 139, pp. 916–927, 2016.

[3] A. R. P. Walker, F. I. Adam, and B. F. Walker, "Breast cancer in black African women: A changing situation," *J. R. Soc. Promot. Health*, vol. 124, no. 2, pp. 81–85, 2004.

[4] J. Fracheboud *et al.*, "Nationwide breast cancer screening programme fully implemented in the Netherlands," *Breast*, vol. 10, no. 1, pp. 6–11, 2001.

[5] World Health Organization, "Latest Global Cancer Data, 2018," *World Health Organization*, 2018. .

[6] M. C. U. Cheang *et al.*, "Basal-like breast cancer defined by five biomarkers has superior prognostic value than triple-negative phenotype," *Clin. Cancer Res.*, vol. 14, no. 5, pp. 1368–1376, 2008.

[7] X. Wang *et al.*, "CSPG4 protein as a new target for the antibody-based immunotherapy of triple-negative breast cancer," *J. Natl. Cancer Inst.*, vol. 102, no. 19, pp. 1496–1512, 2010.

[8] S. Dawood, X. Lei, J. K. Litton, T. A. Buchholz, G. N. Hortobagyi, and A. M. Gonzalez-Angulo, "Impact of body mass index on survival outcome among women with early stage triple-negative breast cancer," *Clin. Breast Cancer*, vol. 12, no. 5, pp. 364–372, 2012.

[9] S. Dawood, "Triple-negative breast cancer: Epidemiology and management options," *Drugs*, vol. 70, no. 17, pp. 2247–2258, 2010.

[10] X. Dai, H. Cheng, Z. Bai, and J. Li, "Breast cancer cell line classification and Its relevance with breast tumor subtyping," *Journal of Cancer*. 2017.

[11] X. Cong, C. Cremer, T. Nachreiner, S. Barth, and P. Carloni, "Engineered human angiogenin mutations in the placental ribonuclease inhibitor complex for anticancer therapy: Insights from enhanced sampling simulations," *Protein Sci.*, pp. 1451–1460, 2016.

[12] C. A. Cooney *et al.*, "Chondroitin sulfates play a major role in breast cancer metastasis: A role for CSPG4 and CHST11 gene expression in forming surface P-selectin ligands in aggressive breast cancer cells," *Breast Cancer Res.*, vol. 13, no. 3, 2011.

[13] A. J. Lowery, M. R. Kell, R. W. Glynn, M. J. Kerin, and K. J. Sweeney, "Locoregional recurrence after breast cancer surgery: A systematic review by receptor phenotype," *Breast Cancer Res. Treat.*, vol. 133, no. 3, 2012.

[14] Z. Anastasiadi, G. D. Lianos, E. Ignatiadou, H. V. Harissis, and M. Mitsis, "Breast cancer in young women: an overview," *Updates in Surgery*, vol. 69, no. 3. pp. 313–317, 2017.

[15] C. Cremer, T. Vierbuchen, L. Hein, R. Fischer, S. Barth, and T. Nachreiner, "Angiogenin mutants as novel effector molecules for the generation of fusion proteins with increased cytotoxic potential," *J. Immunother.*, vol. 38, no. 3, pp. 85–95, 2015.

[16] R. E. Beard *et al.*, "Multiple chimeric antigen receptors successfully target chondroitin sulfate proteoglycan 4 in several different cancer histologies and cancer stem cells," *J. Immunother. Cancer*, vol. 2, no. 1, 2014.

[17] M. Boisserie-Lacroix, G. Hurtevent-Labrot, S. Ferron, N. Lippa, H. Bonnefoi, and G. Mac Grogan, "Correlation between imaging and prognostic factors: Molecular classification of breast cancers," *Diagn. Interv. Imaging*, vol. 95, no. 11, pp. 227–233,

2014.
[18] C. E. DeSantis, S. A. Fedewa, A. Goding Sauer, J. L. Kramer, R. A. Smith, and A. Jemal, "Breast cancer statistics, 2015: Convergence of incidence rates between black and white women," *CA Cancer J. Clin.*, vol. 66, no. 1, pp. 31–42, 2016.
[19] E. Panieri, "Breast cancer screening in developing countries," *Best Pract. Res. Clin. Obstet. Gynaecol.*, vol. 26, no. 2, pp. 283–290, 2012.
[20] L. A. Dawson and M. B. Sharpe, "Image-guided radiotherapy: rationale, benefits, and limitations," *Lancet Oncology*, vol. 7, no. 10. pp. 848–858, 2006.
[21] A. Sonnenblick, D. Fumagalli, C. Sotiriou, and M. Piccart, "Is the differentiation into molecular subtypes of breast cancer important for staging, local and systemic therapy, and follow up?," *Cancer Treatment Reviews*, vol. 40, no. 9. pp. 1089–1095, 2014.
[22] C. Mazouni *et al.*, "Outcome in breast molecular subtypes according to nodal status and surgical procedures," *Am. J. Surg.*, vol. 205, no. 6, pp. 662–667, 2013.
[23] Z. S. Zumsteg *et al.*, "Breast-conserving therapy achieves locoregional outcomes comparable to mastectomy in women with T1-2N0 triple-negative breast cancer," *Ann. Surg. Oncol.*, vol. 20, no. 11, pp. 3469–3476, 2013.
[24] A. Kuijer and T. A. King, "Age, molecular subtypes and local therapy decision-making," *Breast*, vol. 34, pp. S70–S77, 2017.
[25] J. E. Panoff *et al.*, "Risk of locoregional recurrence by receptor status in breast cancer patients receiving modern systemic therapy and post-mastectomy radiation.," *Breast Cancer Res. Treat.*, vol. 128, no. 3, pp. 899–906, 2011.
[26] B.-P. N. *et al.*, "Prognostic role of adjuvant radiotherapy in triple-negative breast cancer: A historical cohort study," *International Journal of Cancer*, vol. 137, no. 10. pp. 2504–2512, 2015.
[27] A. S. Coates *et al.*, "Tailoring therapies—improving the management of early breast cancer: St Gallen International Expert Consensus on the Primary Therapy of Early Breast Cancer 2015," *Ann. Oncol.*, vol. 26, no. 8, pp. 1533–1546, 2015.
[28] P. G. Tsoutsou, M.-C. Vozenin, A.-D. Durham, and J. Bourhis, "How could breast cancer molecular features contribute to locoregional treatment decision making?," *Crit. Rev. Oncol. Hematol.*, vol. 110, pp. 43–48, 2017.
[29] R. Ismail-Khan and M. M. Bui, "A review of triple-negative breast cancer," *Cancer Control*, vol. 17, no. 3, pp. 173–176, 2010.
[30] N. Berrada, S. Delaloge, and F. André, "Treatment of triple-negative metastatic breast cancer: Toward individualized targeted treatments or chemosensitization?," in *Annals of Oncology*, 2010, vol. 21, no. SUPPL. 7.
[31] L. A. Carey, "De-escalating and escalating systemic therapy in triple negative breast cancer," *Breast*, vol. 34, pp. S112–S115, 2017.
[32] F. Cardoso, N. Harbeck, L. Fallowfield, S. Kyriakides, and E. Senkus, "Locally recurrent or metastatic breast cancer: ESMO clinical practice guidelines for diagnosis, treatment and follow-up," *Ann. Oncol.*, vol. 23, no. SUPPL. 7, 2012.
[33] E. C. Dietze, C. Sistrunk, G. Miranda-Carboni, R. O'Regan, and V. L. Seewaldt, "Triple-negative breast cancer in African-American women: Disparities versus biology," *Nature Reviews Cancer*, vol. 15, no. 4. pp. 248–254, 2015.
[34] J. Ferlay, C. Héry, P. Autier, and R. Sankaranarayanan, "Global burden of breast cancer," in *Breast Cancer Epidemiology*, 2010, pp. 1–19.
[35] H. Kourea and V. Kotoula, "Towards tumor immunodiagnostics," *Ann. Transl. Med.*, vol. 4, no. 14, pp. 263–263, 2016.
[36] N. P. Restifo, M. E. Dudley, and S. A. Rosenberg, "Adoptive immunotherapy for cancer: Harnessing the T cell response," *Nature Reviews Immunology*. 2012.
[37] N. E. Papaioannou, O. V. Beniata, P. Vitsos, O. Tsitsilonis, and P. Samara,

"Harnessing the immune system to improve cancer therapy," *Annals of Translational Medicine*. 2016.
[38] K. Naran, T. Nundalall, S. Chetty, and S. Barth, "Principles of Immunotherapy: Implications for Treatment Strategies in Cancer and Infectious Diseases," *Front. Microbiol.*, 2018.
[39] A. M. Gonzalez-Angulo, F. Morales-Vasquez, and G. N. Hortobagyi, "Overview of Resistance to Systemic Therapy in Patients with Breast Cancer," in *Breast Cancer Chemosensitivity*, 2007, pp. 1–22.
[40] A. Howell *et al.*, "Risk determination and prevention of breast cancer," *Breast Cancer Res.*, vol. 16, no. 5, 2014.
[41] C. R. Parish, "Cancer immunotherapy: The past, the present and the future," *Immunology and Cell Biology*. 2003.
[42] M. R. Nathan and P. Schmid, "The emerging world of breast cancer immunotherapy," *Breast*, vol. 37, pp. 200–206, 2018.
[43] T. A. Waldmann, "Immunotherapy: Past, present and future," *Nature Medicine*. 2003.
[44] G. J. Nabel, "Designing tomorrow's vaccines," *New England Journal of Medicine*. 2013.
[45] World Health Organization, "Measles vaccines: WHO position paper, April 2017 – Recommendations," *Vaccine*. 2019.
[46] Q. Bi *et al.*, "Protection against cholera from killed whole-cell oral cholera vaccines: a systematic review and meta-analysis," *Lancet Infect. Dis.*, 2017.
[47] C. Van Den Ende, C. Marano, A. Van Ahee, E. M. Bunge, and L. De Moerlooze, "The immunogenicity and safety of GSK's recombinant hepatitis B vaccine in adults: a systematic review of 30 years of experience," *Expert Review of Vaccines*. 2017.
[48] World Health Organization, "Diphtheria vaccine: WHO position paper, August 2017 – Recommendations," *Vaccine*. 2018.
[49] M. Wasserman, H. L. Sings, D. Jones, S. Pugh, M. Moffatt, and R. Farkouh, "Review of vaccine effectiveness assumptions used in economic evaluations of infant pneumococcal conjugate vaccine," *Expert Review of Vaccines*. 2018.
[50] V. Vetter, G. Denizer, L. R. Friedland, J. Krishnan, and M. Shapiro, "Understanding modern-day vaccines: what you need to know," *Annals of Medicine*. 2018.
[51] D. Sipp, I. H. Frazer, and J. E. J. Rasko, "No Vacillation on HPV Vaccination," *Cell*. 2018.
[52] Y. Y. Chen, K. E. Galloway, and C. D. Smolke, "Synthetic biology: Advancing biological frontiers by building synthetic systems," *Genome Biology*. 2012.
[53] R. H. Vonderheide and C. H. June, "Engineering T cells for cancer: Our synthetic future," *Immunol. Rev.*, 2014.
[54] S. E. Sedykh, V. V. Prinz, V. N. Buneva, and G. A. Nevinsky, "Bispecific antibodies: Design, therapy, perspectives," *Drug Design, Development and Therapy*. 2018.
[55] W. Meng *et al.*, "Targeting human-cytomegalovirus-infected cells by redirecting T cells using an anti-CD3/anti-glycoprotein B bispecific antibody," *Antimicrob. Agents Chemother.*, 2018.
[56] O. H. Brekke and I. Sandlie, "Therapeutic antibodies for human diseases at the dawn of the twenty-first century," *Nature Reviews Drug Discovery*. 2003.
[57] L. M. Weiner, J. C. Murray, and C. W. Shuptrine, "Antibody-based immunotherapy of cancer," *Cell*. 2012.
[58] G. J. Weiner, "Building better monoclonal antibody-based therapeutics," *Nature Reviews Cancer*. 2015.
[59] J. P. Pouget *et al.*, "Clinical radioimmunotherapy-the role of radiobiology," *Nature Reviews Clinical Oncology*. 2011.

[60] S. Barth, "Editorial [Hot Topic: Recombinant Immunotoxins – The Next Generation (Executive Editor: Stefan Barth)]," *Curr. Pharm. Des.*, 2009.
[61] S. Jordaan *et al.*, "Updates in the development of immunoRNases for the selective killing of tumor cells," *Biomedicines*. 2018.
[62] D. Hristodorov *et al.*, "Microtubule-associated protein tau facilitates the targeted killing of proliferating cancer cells in vitro and in a xenograft mouse tumour model in vivo," *Br. J. Cancer*, 2013.
[63] M. Amoury *et al.*, "Granzyme B-based cytolytic fusion protein targeting EpCAM specifically kills triple negative breast cancer cells in vitro and inhibits tumor growth in a subcutaneous mouse tumor model," *Cancer Lett.*, 2016.
[64] N. Lilienthal *et al.*, "A novel recombinant anti-CD22 immunokinase delivers proapoptotic activity of death-associated protein kinase (DAPK) and mediates cytotoxicity in neoplastic B cells," *Mol. Cancer Ther.*, 2016.
[65] O. A. Akinrinmade *et al.*, "Human MAP tau based targeted cytolytic fusion proteins," *Biomedicines*. 2017.
[66] P. Hlongwane, N. Mungra, S. Madheswaran, O. A. Akinrinmade, S. Chetty, and S. Barth, "Human granzyme B based targeted cytolytic fusion proteins," *Biomedicines*. 2018.
[67] H. Fuchs, A. Weng, and R. Gilabert-Oriol, "Augmenting the efficacy of immunotoxins and other targeted protein toxins by endosomal escape enhancers," *Toxins*, vol. 8, no. 7. 2016.
[68] A. Bochicchio *et al.*, "Designing the Sniper: Improving Targeted Human Cytolytic Fusion Proteins for Anti-Cancer Therapy via Molecular Simulation," *Biomedicines*, vol. 5, no. 1, p. 9, 2017.
[69] L. Amiri-Kordestani *et al.*, "FDA approval: Ado-trastuzumab emtansine for the treatment of patients with HER2-positive metastatic breast cancer," *Clinical Cancer Research*. 2014.
[70] A. F. Herrera *et al.*, "Interim results of brentuximab vedotin in combination with nivolumab in patients with relapsed or refractory Hodgkin lymphoma," *Blood*, 2018.
[71] L. E. Hogan *et al.*, "Increased HIV-1 transcriptional activity and infectious burden in peripheral blood and gut-associated CD4 + T cells expressing CD30," *PLoS Pathog.*, 2018.
[72] J. M. Reichert, "Antibodies to watch in 2016," *MAbs*, 2016.
[73] M. L. Dos Santos, W. Quintilio, T. M. Manieri, L. R. Tsuruta, and A. M. Moro, "Advances and challenges in therapeutic monoclonal antibodies drug development," *Brazilian Journal of Pharmaceutical Sciences*. 2018.
[74] Y.-T. Tai and K. C. Anderson, "Antibody-Based Therapies in Multiple Myeloma," *Bone Marrow Res.*, vol. 2011, pp. 1–14, 2011.
[75] H. J. Lee *et al.*, "Prognostic and predictive values of EGFR overexpression and EGFR copy number alteration in HER2-positive breast cancer," *Br. J. Cancer*, vol. 112, no. 1, pp. 103–111, 2015.
[76] L. M. Weiner, R. Surana, and S. Wang, "Monoclonal antibodies: Versatile platforms for cancer immunotherapy," *Nature Reviews Immunology*, vol. 10, no. 5. pp. 317–327, 2010.
[77] K. Runcie, D. R. Budman, V. John, and N. Seetharamu, "Bi-specific and tri-specific antibodies- the next big thing in solid tumor therapeutics," *Molecular Medicine*. 2018.
[78] S. Bournazos and J. V. Ravetch, "Fcγ receptor pathways during active and passive immunization," *Immunological Reviews*. 2015.
[79] N. M. Stapleton, H. K. Einarsdóttir, A. M. Stemerding, and G. Vidarsson, "The multiple facets of FcRn in immunity," *Immunological Reviews*. 2015.

[80] M. M. Al Qaraghuli, K. Kubiak-Ossowska, V. A. Ferro, and P. A. Mulheran, "Antibody-protein binding and conformational changes: identifying allosteric signalling pathways to engineer a better effector response," *Sci. Rep.*, vol. 10, no. 1, p. 13696, 2020.
[81] ProSci, "Antibody Structure and Properties," 2018. [Online]. Available: https://www.prosci-inc.com/resources/antibody-development-guide/antibody-structure-and-properties/. [Accessed: 29-Jan-2020].
[82] G. L. Gilliland, J. Luo, O. Vafa, and J. C. Almagro, "Leveraging SBDD in protein therapeutic development: Antibody engineering," *Methods Mol. Biol.*, 2012.
[83] C. A. Janeway, P. Travers, M. Walport, and E. Al, "Principles of innate and adaptive immunity," *Immunobiol. Immune Syst. Heal. Dis. 5th Ed.*, 2001.
[84] C. Janeway, *immunobiology, 5th ed.* 2012.
[85] A. F. Hussain, M. Amoury, and S. Barth, "SNAP-tag technology: a powerful tool for site specific conjugation of therapeutic and imaging agents.," *Curr. Pharm. Des.*, vol. 19, no. 30, pp. 5437–42, 2013.
[86] A. M. Prantner *et al.*, "Anti-mesothelin nanobodies for both conventional and nanoparticle-based biomedical applications," *J. Biomed. Nanotechnol.*, 2015.
[87] M. Stech and S. Kubick, "Cell-Free Synthesis Meets Antibody Production: A Review," *Antibodies*, 2015.
[88] J. S. Huston *et al.*, "Protein Engineering of Single-Chain Fv Analogs and Fusion Proteins," *Methods Enzymol.*, 1991.
[89] A. D. Griffiths and A. R. Duncan, "Strategies for selection of antibodies by phage display," *Curr. Opin. Biotechnol.*, 1998.
[90] Z. A. Ahmad, S. K. Yeap, A. M. Ali, W. Y. Ho, N. B. M. Alitheen, and M. Hamid, "ScFv antibody: Principles and clinical application," *Clinical and Developmental Immunology*. 2012.
[91] A. Frenzel, T. Schirrmann, and M. Hust, "Phage display-derived human antibodies in clinical development and therapy," *mAbs*. 2016.
[92] K. Chester *et al.*, "Engineering antibodies for clinical applications in cancer," *Tumor Biology*. 2004.
[93] Z. A. Ahmad, S. K. Yeap, A. M. Ali, W. Y. Ho, N. B. M. Alitheen, and M. Hamid, "ScFv antibody: Principles and clinical application," *Clinical and Developmental Immunology*. 2012.
[94] J. S. Huston *et al.*, "Single-chain Fv radioimmunotargeting," *Quarterly Journal of Nuclear Medicine*. 1996.
[95] S. Dana Jones and W. A. Marasco, "Antibodies for targeted gene therapy: Extracellular gene targeting and intracellular expression," *Advanced Drug Delivery Reviews*. 1998.
[96] P. Monnier, R. Vigouroux, and N. Tassew, "In Vivo Applications of Single Chain Fv (Variable Domain) (scFv) Fragments," *Antibodies*, 2013.
[97] G. P. Adams *et al.*, "High affinity restricts the localization and tumor penetration of single-chain Fv antibody molecules," *Cancer Res.*, 2001.
[98] N. E. Weisser and J. C. Hall, "Applications of single-chain variable fragment antibodies in therapeutics and diagnostics," *Biotechnology Advances*. 2009.
[99] P. C. Fridy *et al.*, "A robust pipeline for rapid production of versatile nanobody repertoires," *Nat. Methods*, 2014.
[100] J. Helma, M. C. Cardoso, S. Muyldermans, and H. Leonhardt, "Nanobodies and recombinant binders in cell biology," *Journal of Cell Biology*. 2015.
[101] S. Muyldermans *et al.*, "Camelid immunoglobulins and nanobody technology," *Vet. Immunol. Immunopathol.*, 2009.

[102] S. Muyldermans, "Nanobodies: Natural Single-Domain Antibodies," *Annu. Rev. Biochem.*, 2013.
[103] M. M. Harmsen and H. J. De Haard, "Properties, production, and applications of camelid single-domain antibody fragments," *Applied Microbiology and Biotechnology*. 2007.
[104] D. Smolarek, O. Bertrand, and M. Czerwinski, "Variable fragments of heavy chain antibodies (VHHs): A new magic bullet molecule of medicine?," *Postepy Higieny i Medycyny Doswiadczalnej*. 2012.
[105] J. C. Almagro and J. Fransson, "Humanization of antibodies," *Frontiers in Bioscience*. 2008.
[106] J. H. Kim and H. J. Hong, "Humanization by CDR grafting and specificity-determining residue grafting," *Methods Mol. Biol.*, 2012.
[107] D. Saerens *et al.*, "Identification of a universal VHH framework to graft non-canonical antigen-binding loops of camel single-domain antibodies," *J. Mol. Biol.*, 2005.
[108] C. Vincke, R. Loris, D. Saerens, S. Martinez-Rodriguez, S. Muyldermans, and K. Conrath, "General strategy to humanize a camelid single-domain antibody and identification of a universal humanized nanobody scaffold," *J. Biol. Chem.*, 2009.
[109] D. Kuroda, H. Shirai, M. P. Jacobson, and H. Nakamura, "Computer-aided antibody design," *Protein Eng. Des. Sel.*, 2012.
[110] S. Oliveira, R. Heukers, J. Sornkom, R. J. Kok, and P. M. P. Van Bergen En Henegouwen, "Targeting tumors with nanobodies for cancer imaging and therapy," *Journal of Controlled Release*. 2013.
[111] I. Vaneycken *et al.*, "Immuno-imaging using nanobodies," *Current Opinion in Biotechnology*. 2011.
[112] K. Kolberg, C. Puettmann, A. Pardo, J. Fitting, and S. Barth, "SNAP-tag technology: a general introduction.," *Curr. Pharm. Des.*, vol. 19, no. 30, pp. 5406–13, 2013.
[113] M. J. Hinner and K. Johnsson, "How to obtain labeled proteins and what to do with them," *Current Opinion in Biotechnology*, vol. 21, no. 6. pp. 766–776, 2010.
[114] E. Tomat, E. M. Nolan, J. Jaworski, and S. J. Lippard, "Organelle-specific zinc detection using zinpyr-labeled fusion proteins in live cells," *J. Am. Chem. Soc.*, vol. 130, no. 47, pp. 15776–15777, 2008.
[115] C. Puettmann *et al.*, "A monoclonal antibody for the detection of SNAP/CLIP-tagged proteins," *Immunol. Lett.*, vol. 150, no. 1–2, pp. 69–74, 2013.
[116] D. Srikun, A. E. Albers, C. I. Nam, A. T. Iavarone, and C. J. Chang, "Organelle-targetable fluorescent probes for imaging hydrogen peroxide in living cells via SNAP-Tag protein labeling," *J. Am. Chem. Soc.*, vol. 132, no. 12, pp. 4455–4465, 2010.
[117] K. Johnsson, "SNAP-tag Technologies: Novel Tools to Study Protein Function," *NEB expressions*, vol. 3.3, no. 4, pp. 5–7, 2008.
[118] I. R. Corrêa *et al.*, "Substrates for improved live-cell fluorescence labeling of SNAP-tag.," *Curr. Pharm. Des.*, vol. 19, no. 30, pp. 5414–20, 2013.
[119] F. Kampmeier *et al.*, "Rapid optical imaging of EGF receptor expression with a single-chain antibody SNAP-tag fusion protein," *Eur. J. Nucl. Med. Mol. Imaging*, vol. 37, no. 10, pp. 1926–1934, 2010.
[120] K. Bojkowska *et al.*, "Measuring in vivo protein half-life," *Chem. Biol.*, vol. 18, no. 6, pp. 805–815, 2011.
[121] T. N. and A. P.-S. more at: http://www. eurekaselect. com/113652/article#sthash. yxAjRA7k. dpu. Manal Amoury, Tobias Blume, Hannes Brehm, Judith Niesen, Niklas Tenhaef, Stefan Barth, Stefan Gattenlohner, Wijnand Helfrich, Jenny Fitting, "SNAP-tag based Agents for Preclinical In Vitro Imaging in Malignant Diseases," *Curr. Pharm. Des.*, vol. 19, no. 30, pp. 5429–5436, 2013.

[122] T. K. Liu *et al.*, "A rapid SNAP-tag fluorogenic probe based on an environment-sensitive fluorophore for no-wash live cell imaging," *ACS Chem. Biol.*, vol. 9, no. 10, pp. 2359–2365, 2014.
[123] X. Sun *et al.*, "Development of SNAP-tag fluorogenic probes for wash-free fluorescence imaging," *ChemBioChem*, vol. 12, no. 14, pp. 2217–2226, 2011.
[124] S. Engin, D. Fichtner, D. Wedlich, and L. Fruk, "SNAP-tag as a Tool for Surface Immobilization," *Curr. Pharm. Des.*, vol. 19, no. 30, pp. 5443–5448, 2013.
[125] P. J. Bosch *et al.*, "Evaluation of fluorophores to label SNAP-Tag fused proteins for multicolor single-molecule tracking microscopy in live cells," *Biophys. J.*, vol. 107, no. 4, pp. 803–814, 2014.
[126] T. Gronemeyer, C. Chidley, A. Juillerat, C. Heinis, and K. Johnsson, "Directed evolution of O6-alkylguanine-DNA alkyltransferase for applications in protein labeling," *Protein Eng. Des. Sel.*, 2006.
[127] B. Sutcliffe *et al.*, "Second-generation Drosophila chemical tags: Sensitivity, versatility, and speed," *Genetics*, 2017.
[128] K. H. Jung *et al.*, "A SNAP-tag fluorogenic probe mimicking the chromophore of the red fluorescent protein Kaede," *Org. Biomol. Chem.*, 2019.
[129] W. B. Stallcup, "The NG2 proteoglycan: Past insights and future prospects," *Journal of Neurocytology*. 2002.
[130] M. Campoli, S. Ferrone, and X. Wang, "Functional and Clinical Relevance of Chondroitin Sulfate Proteoglycan 4," in *Advances in Cancer Research*, 2010.
[131] V. S. Jamdade, N. Sethi, N. A. Mundhe, P. Kumar, M. Lahkar, and N. Sinha, "Therapeutic targets of triple-negative breast cancer: A review," *Br. J. Pharmacol.*, vol. 172, no. 17, pp. 4228–4237, 2015.
[132] J. Stegmüller, S. Schneider, A. Hellwig, J. Garwood, and J. Trotter, "AN2, the mouse homologue of NG2, is a surface antigen on glial precursor cells implicated in control of cell migration," *Journal of Neurocytology*. 2002.
[133] M. A. Price *et al.*, "CSPG4, a potential therapeutic target, facilitates malignant progression of melanoma," *Pigment Cell and Melanoma Research*, vol. 24, no. 6. pp. 1148–1157, 2011.
[134] M. R. Campoli, C. C. Chang, T. Kageshita, X. Wang, J. B. McCarthy, and S. Ferrone, "Human high molecular weight-melanoma-associated antigen (HMW-MAA): A melanoma cell surface chondroitin sulfate proteoglycan (MSCP) with biological and clinical significance," *Critical Reviews in Immunology*. 2004.
[135] J. F. Talts, Z. Andac, W. Göhring, A. Brancaccio, and R. Timpl, "Binding of the G domains of laminin α1 and α2 chains and perlecan to heparin, sulfatides, α-dystroglycan and several extracellular matrix proteins," *EMBO J.*, 1999.
[136] V. Givant-Horwitz, B. Davidson, and R. Reich, "Laminin-induced signaling in tumor cells," *Cancer Letters*. 2005.
[137] P. A. Nicolosi, A. Dallatomasina, and R. Perris, "Theranostic impact of NG2/CSPG4 proteoglycan in cancer," *Theranostics*. 2015.
[138] S. Cattaruzza *et al.*, "NG2/CSPG4-collagen type VI interplays putatively involved in the microenvironmental control of tumour engraftment and local expansion," *J. Mol. Cell Biol.*, 2013.
[139] J. I. Fukushi, I. T. Makagiansar, and W. B. Stallcup, "NG2 proteoglycan promotes endothelial cell motility and angiogenesis via engagement of Galectin-3 and α3β1 integrin," *Mol. Biol. Cell*, 2004.
[140] I. T. Makagiansar, S. Williams, T. Mustelin, and W. B. Stallcup, "Differential phosphorylation of NG2 proteoglycan by ERK and PKCα helps balance cell proliferation and migration," *J. Cell Biol.*, 2007.

[141] D. S. Barritt *et al.*, "The multi-PDZ domain protein MUPP1 is a cytoplasmic ligand for the membrane-spanning proteoglycan NG2," *J. Cell. Biochem.*, 2000.
[142] N. Chatterjee *et al.*, "Interaction of syntenin-1 and the NG2 proteoglycan in migratory oligodendrocyte precursor cells," *J. Biol. Chem.*, 2008.
[143] W. Kolch, "Meaningful relationships: The regulation of the Ras/Raf/MEK/ERK pathway by protein interactions," *Biochemical Journal*. 2000.
[144] A. S. Dhillon, S. Hagan, O. Rath, and W. Kolch, "MAP kinase signalling pathways in cancer," *Oncogene*. 2007.
[145] J. Yang *et al.*, "Melanoma chondroitin sulfate proteoglycan enhances FAK and ERK activation by distinct mechanisms," *J. Cell Biol.*, 2004.
[146] M. Chekenya *et al.*, "The progenitor cell marker NG2/MPG promotes chemoresistance by activation of integrin-dependent PI3K/Akt signaling," *Oncogene*, 2008.
[147] A. Nishiyama, X. H. Lin, N. Giese, C. H. Heldin, and W. B. Stallcup, "Interaction between NG2 proteoglycan and PDGF α-receptor on O2A progenitor cells is required for optimal response to PDGF," *J. Neurosci. Res.*, 1996.
[148] J. Yang *et al.*, "Melanoma proteoglycan modifies gene expression to stimulate tumor cell motility, growth, and epithelial-to-mesenchymal transition," *Cancer Res.*, 2009.
[149] A. Ferrandez-lzquierdo, S. Navarro-Fos, M. Gonzalez-Devesa, R. Gil-Benso, and A. Llombart-Bosch, "Immunocytochemical typification of mesothelial cells in effusions: In vivo and in vitro models," *Diagn. Cytopathol.*, 1994.
[150] H. A. Kenny *et al.*, "Mesothelial cells promote early Ovarian cancer metastasis through fibronectin secretion," *J. Clin. Invest.*, 2014.
[151] T. L. Yeung, C. S. Leung, K. P. Yip, C. L. A. Yeung, S. T. C. Wong, and S. C. Mok, "Cellular and molecular processes in ovarian cancer metastasis. A review in the theme: Cell and molecular processes in cancer metastasis," *Am. J. Physiol. - Cell Physiol.*, 2015.
[152] J. O. A. M. van Baal *et al.*, "The histophysiology and pathophysiology of the peritoneum," *Tissue and Cell*. 2017.
[153] J. Collignon, L. Lousberg, H. Schroeder, and G. Jerusalem, "Triple-negative breast cancer: Treatment challenges and solutions," *Breast Cancer: Targets and Therapy*. 2016.
[154] K. Chang, I. Pastan, and M. C. Willingham, "Isolation and characterization of a monoclonal antibody, K1, reactive with ovarian cancers and normal mesothelium," *Int. J. Cancer*, 1992.
[155] K. Chang and I. Pastan, "Molecular cloning of mesothelin, a differentiation antigen present on mesothelium, mesotheliomas, and ovarian cancers," *Proc. Natl. Acad. Sci. U. S. A.*, 1996.
[156] I. Pastan and R. Hassan, "Discovery of mesothelin and exploiting it as a target for immunotherapy," *Cancer Research*. 2014.
[157] B. W. S. Robinson *et al.*, "Mesothelin-family proteins and diagnosis of mesothelioma," *Lancet*, 2003.
[158] A. Rump *et al.*, "Binding of Ovarian Cancer Antigen CA125/MUC61 to Mesothelin Mediates Cell Adhesion," *J. Biol. Chem.*, 2004.
[159] R. Hassan *et al.*, "Detection and quantitation of serum mesothelin, a tumor marker for patients with mesothelioma and ovarian cancer," *Clin. Cancer Res.*, 2006.
[160] R. Hassan and M. Ho, "Mesothelin targeted cancer immunotherapy," *Eur. J. Cancer*, 2008.
[161] T. Hucl, J. R. Brody, E. Gallmeier, C. A. Iacobuzio-Donahue, I. K. Farrance, and S. E. Kern, "High cancer-specific expression of mesothelin (MSLN) is attributable to an upstream enhancer containing a transcription enhancer factor-dependent MCAT

motif," *Cancer Res.*, 2007.
[162] J. A. Sawicki, Y.-H. Huang, J. Cozzitorto, R. Langer, D. G. Anderson, and J. R. Brody, "Abstract 2: Naked CanScript, an 18-base pair sequence, has tumor cell-specific promoter activity in vivo: Implications for targeted gene therapy," 2010.
[163] Y. R. Ren, K. Patel, B. C. Paun, and S. E. Kern, "Structural analysis of the cancer-specific promoter in mesothelin and in other genes overexpressed in cancers," *J. Biol. Chem.*, 2011.
[164] U. Bharadwaj, M. Li, C. Chen, and Q. Yao, "Mesothelin-induced pancreatic cancer cell proliferation involves alteration of cyclin E via activation of signal transducer and activator of transcription protein 3," *Mol. Cancer Res.*, 2008.
[165] W. F. Cheng *et al.*, "High mesothelin correlates with chemoresistance and poor survival in epithelial ovarian carcinoma," *Br. J. Cancer*, 2009.
[166] U. Bharadwaj, C. Marin-Muller, M. Li, C. Chen, and Q. Yao, "Mesothelin overexpression promotes autocrine IL-6/sIL-6R trans-signaling to stimulate pancreatic cancer cell proliferation," *Carcinogenesis*, 2011.
[167] M. C. Chang *et al.*, "Mesothelin inhibits paclitaxel-induced apoptosis through the PI3K pathway," *Biochem. J.*, 2009.
[168] U. Bharadwaj, C. Marin-Muller, M. Li, C. Chen, and Q. Yao, "Mesothelin confers pancreatic cancer cell resistance to TNF-α-induced apoptosis through Akt/PI3K/NF-κB activation and IL-6/Mcl-1 overexpression," *Mol. Cancer*, 2011.
[169] M. C. Chang *et al.*, "Mesothelin enhances invasion of ovarian cancer by inducing MMP-7 through MAPK/ERK and JNK pathways," *Biochem. J.*, 2012.
[170] N. Uehara, Y. Matsuoka, and A. Tsubura, "Mesothelin promotes anchorage-independent growth and prevents anoikis via extracellular signal-regulated kinase signaling pathway in human breast cancer cells," *Mol. Cancer Res.*, 2008.
[171] J. Tchou *et al.*, "Mesothelin, a novel immunotherapy target for triple negative breast cancer," *Breast Cancer Res. Treat.*, 2012.
[172] R. Hassan, A. Thomas, C. Alewine, D. T. Le, E. M. Jaffee, and I. Pastan, "Mesothelin immunotherapy for cancer: Ready for prime time?," *J. Clin. Oncol.*, 2016.
[173] A. Morello, M. Sadelain, and P. S. Adusumilli, "Mesothelin-targeted CARs: Driving T cells to solid Tumors," *Cancer Discovery*. 2016.
[174] E. J. ter Weele *et al.*, "Imaging the distribution of an antibody-drug conjugate constituent targeting mesothelin with ⁸⁹Zr and IRDye 800CW in mice bearing human pancreatic tumor xenografts," *Oncotarget*, 2015.
[175] L. E. Lamberts *et al.*, "ImmunoPET with anti-mesothelin antibody in patients with pancreatic and ovarian cancer before anti-mesothelin antibody-drug conjugate treatment," *Clin. Cancer Res.*, 2016.
[176] N. Normanno *et al.*, "Epidermal growth factor receptor (EGFR) signaling in cancer," *Gene*. 2006.
[177] L. Cheng *et al.*, "The landscape of EGFR pathways and personalized management of non-small-cell lung cancer," *Future Oncology*. 2011.
[178] A. Antonicelli *et al.*, "Egfr-targeted therapy for non-small cell lun cancer: Focus on EGFR oncogenic mutation," *Int. J. Med. Sci.*, 2013.
[179] H. Masuda, D. Zhang, C. Bartholomeusz, H. Doihara, G. N. Hortobagyi, and N. T. Ueno, "Role of epidermal growth factor receptor in breast cancer," *Breast Cancer Research and Treatment*. 2012.
[180] C. A. Hudis and L. Gianni, "Triple-Negative Breast Cancer: An Unmet Medical Need," *Oncologist*, 2011.
[181] T. A. Yap and S. Popat, "Toward precision medicine with next-generation EGFR inhibitors in non-small-cell lung cancer," *Pharmacogenomics and Personalized*

Medicine. 2014.
[182] H. Ogiso *et al.*, "Crystal structure of the complex of human epidermal growth factor and receptor extracellular domains," *Cell*, 2002.
[183] K. M. Ferguson, M. B. Berger, J. M. Mendrola, H. S. Cho, D. J. Leahy, and M. A. Lemmon, "EGF activates its receptor by removing interactions that autoinhibit ectodomain dimerization," *Mol. Cell*, 2003.
[184] K. M. Ferguson, "Structure-Based View of Epidermal Growth Factor Receptor Regulation," *Annu. Rev. Biophys.*, 2008.
[185] H. S. Cho and D. J. Leahy, "Structure of the extracellular region of HER3 reveals an interdomain tether," *Science (80-.).*, 2002.
[186] T. P. J. Garrett *et al.*, "Crystal structure of a truncated epidermal growth factor receptor extracellular domain bound to transforming growth factor α," *Cell*, 2002.
[187] C. Jost, J. Schilling, R. Tamaskovic, M. Schwill, A. Honegger, and A. Plückthun, "Structural basis for eliciting a cytotoxic effect in HER2-overexpressing cancer cells via binding to the extracellular domain of HER2," *Structure*, 2013.
[188] Y. Yarden and M. X. Sliwkowski, "Untangling the ErbB signalling network," *Nature Reviews Molecular Cell Biology*. 2001.
[189] A. Citri and Y. Yarden, "EGF-ERBB signalling: Towards the systems level," *Nature Reviews Molecular Cell Biology*. 2006.
[190] P. Wee and Z. Wang, "Epidermal growth factor receptor cell proliferation signaling pathways," *Cancers*. 2017.
[191] N. M. Davis *et al.*, "Deregulation of the EGFR/PI3K/PTEN/Akt/mTORC1 pathway in breast cancer: Possibilities for therapeutic intervention," *Oncotarget*, 2014.
[192] E. Martinelli, R. De Palma, M. Orditura, F. De Vita, and F. Ciardiello, "Anti-epidermal growth factor receptor monoclonal antibodies in cancer therapy," *Clinical and Experimental Immunology*. 2009.
[193] M. Piramoon, S. J. Hosseinimehr, K. Omidfar, Z. Noaparast, and S. M. Abedi, "(99m) Tc-anti-epidermal growth factor receptor nanobody for tumor imaging.," *Chem. Biol. Drug Des.*, vol. 89, no. 4, pp. 498–504, Apr. 2017.
[194] J. Lee *et al.*, "Strong association of epidermal growth factor receptor status with breast cancer FDG uptake.," *Eur. J. Nucl. Med. Mol. Imaging*, vol. 44, no. 9, pp. 1438–1447, Aug. 2017.
[195] M. Gurfinkel, C. Li, E. M. Sevick-Muraca, S. Ke, and X. Wen, "Near-Infrared Fluorescence Optical Imaging and Tomography," *Dis. Markers*, 2013.
[196] S. Ke *et al.*, "Near-Infrared Optical Imaging of Epidermal Growth Factor Receptor in Breast Cancer Xenografts," *Cancer Res.*, 2003.
[197] T. De Meyer, S. Muyldermans, and A. Depicker, "Nanobody-based products as research and diagnostic tools," *Trends in Biotechnology*. 2014.
[198] P. Bannas, J. Hambach, and F. Koch-Nolte, "Nanobodies and nanobody-based human heavy chain antibodies as antitumor therapeutics," *Frontiers in Immunology*. 2017.
[199] D. Estrada-Rivadeneyra, "Sanger sequencing," *FEBS Journal*. 2017.
[200] A. Bertero, S. Brown, and L. Vallier, "Methods of Cloning," in *Basic Science Methods for Clinical Researchers*, 2017.
[201] S. Shuman, "DNA ligases: Progress and prospects," *Journal of Biological Chemistry*. 2009.
[202] T. C. De Ruijter, J. Veeck, J. P. J. De Hoon, M. Van Engeland, and V. C. Tjan-Heijnen, "Characteristics of triple-negative breast cancer," *J. Cancer Res. Clin. Oncol.*, 2011.
[203] X. Wang *et al.*, "CSPG4 protein as a new target for the antibody-based immunotherapy of triple-negative breast cancer," *J. Natl. Cancer Inst.*, 2010.

[204] M. Amoury *et al.*, "A novel approach for targeted elimination of CSPG4-positive triple-negative breast cancer cells using a MAP tau-based fusion protein," *Int. J. Cancer*, 2016.
[205] J. Choi, W. H. Jung, and J. S. Koo, "Clinicopathologic features of molecular subtypes of triple negative breast cancer based on immunohistochemical markers," *Histol. Histopathol.*, 2012.
[206] V. Martin *et al.*, "Molecular characterization of EGFR and EGFR-downstream pathways in triple negative breast carcinomas with basal like features," *Histol. Histopathol.*, 2012.
[207] D. Liu *et al.*, "EGFR expression correlates with decreased disease-free survival in triple-negative breast cancer: A retrospective analysis based on a tissue microarray," *Med. Oncol.*, 2012.
[208] K. Nakai, M. C. Hung, and H. Yamaguchi, "A perspective on anti-EGFR therapies targeting triple-negative breast cancer," *American Journal of Cancer Research*. 2016.
[209] G. Tozbikian *et al.*, "Mesothelin expression in triple negative breast carcinomas correlates significantly with basal-like phenotype, distant metastases and decreased survival," *PLoS One*, 2014.
[210] P. Y. Lee, J. Costumbrado, C. Y. Hsu, and Y. H. Kim, "Agarose gel electrophoresis for the separation of DNA fragments," *J. Vis. Exp.*, 2012.
[211] T. Isbir, D. Kirac, B. Demircan, and B. Dalan, "Gel Electrophoresis," in *Brenner's Encyclopedia of Genetics: Second Edition*, 2013.
[212] L. C. Thomason, J. A. Sawitzke, X. Li, N. Costantino, and D. L. Court, "Recombineering: Genetic engineering in bacteria using homologous recombination," *Curr. Protoc. Mol. Biol.*, 2014.
[213] M. Kostylev, A. Otwell, R. Richardson, and Y. Suzuki, "Cloning Should Be Simple: Escherichia coli DH5α-Mediated Assembly of Multiple DNA Fragments with Short End Homologies," *PLoS One*, 2015.
[214] P. Thomas and T. G. Smart, "HEK293 cell line: A vehicle for the expression of recombinant proteins," *J. Pharmacol. Toxicol. Methods*, 2005.
[215] M. Ho and I. Pastan, "Display and selection of scFv antibodies on HEK-293T cells.," *Methods Mol. Biol.*, 2009.
[216] A. M. Lanza, D. S. Kim, and H. S. Alper, "Evaluating the influence of selection markers on obtaining selected pools and stable cell lines in human cells," *Biotechnol. J.*, 2013.
[217] D. M. Disley, P. R. Morrill, K. Sproule, and C. R. Lowe, "An optical biosensor for monitoring recombinant proteins in process media," *Biosens. Bioelectron.*, 1999.
[218] Y. E. Thomassen, W. Meijer, L. Sierkstra, and C. T. Verrips, "Large-scale production of VHH antibody fragments by Saccharomyces cerevisiae," in *Enzyme and Microbial Technology*, 2002.
[219] T. U. Gerngross, "Advances in the production of human therapeutic proteins in yeasts and filamentous fungi," *Nature Biotechnology*. 2004.
[220] V. Joosten *et al.*, "Production of bifunctional proteins by Aspergillus awamori: Llama variable heavy chain antibody fragment (VHH) R9 coupled to Arthromyces ramosus peroxidase (ARP)," *J. Biotechnol.*, 2005.
[221] F. Rahbarizadeh, M. J. Rasaee, M. Forouzandeh, and A. A. Allameh, "Over expression of anti-MUC1 single-domain antibody fragments in the yeast Pichia pastoris," *Mol. Immunol.*, 2006.
[222] J. A. Bornhorst and J. J. Falke, "Purification of proteins using polyhistidine affinity tags," *Methods in Enzymology*. 2000.
[223] J. . Bornhorst, J.A., Falke, "Purification of Proteins Using Polyhistidine Affinity

Tags," *Methods Enzym.*, 2010.
[224] G. Giridhar, R. K. N. R. Manepalli, and G. Apparao, "Size-Exclusion Chromatography," in *Thermal and Rheological Measurement Techniques for Nanomaterials Characterization*, 2017.
[225] N. C. L. Zembruski, V. Stache, W. E. Haefeli, and J. Weiss, "7-Aminoactinomycin D for apoptosis staining in flow cytometry," *Anal. Biochem.*, 2012.
[226] M. M. Harmsen, C. B. Van Solt, A. Hoogendoorn, F. G. Van Zijderveld, T. A. Niewold, and J. Van Der Meulen, "Escherichia coli F4 fimbriae specific llama single-domain antibody fragments effectively inhibit bacterial adhesion in vitro but poorly protect against diarrhoea," *Vet. Microbiol.*, 2005.
[227] K. Coppieters *et al.*, "Formatted anti-tumor necrosis factor α VHH proteins derived from camelids show superior potency and targeting to inflamed joints in a murine model of collagen-induced arthritis," *Arthritis Rheum.*, 2006.
[228] R. C. Roovers *et al.*, "Efficient inhibition of EGFR signalling and of tumour growth by antagonistic anti-EGFR Nanobodies," *Cancer Immunol. Immunother.*, 2007.
[229] Y. Xiao, B. Zhang, A. Hsieh, N. Thavandiran, C. Martin, and M. Radisic, "Microfluidic Cell Culture Techniques," in *Microfluidic Cell Culture Systems*, 2012.
[230] J. P. Pieracci, J. W. Armando, M. Westoby, and J. Thommes, "Industry Review of Cell Separation and Product Harvesting Methods," in *Biopharmaceutical Processing: Development, Design, and Implementation of Manufacturing Processes*, 2018.
[231] Green BioResearch LLC, "Cell Number Density At 100% Confluency In Cell Culture Dish, Plate, Flask," 2016. [Online]. Available: https://greenbioresearch.com/cell-number-density-percentage-confluency-cell-culture-dish-plate-flask/. [Accessed: 08-Aug-2020].
[232] J. Yang, P. Guertin, G. Jia, Z. Lv, H. Yang, and D. Ju, "Large-scale microcarrier culture of HEK293T cells and Vero cells in single-use bioreactors," *AMB Express*, 2019.
[233] D. Saerens, G. H. Ghassabeh, and S. Muyldermans, "Single-domain antibodies as building blocks for novel therapeutics," *Current Opinion in Pharmacology*. 2008.
[234] J. Wesolowski *et al.*, "Single domain antibodies: Promising experimental and therapeutic tools in infection and immunity," *Medical Microbiology and Immunology*. 2009.
[235] R. Chakravarty, S. Goel, and W. Cai, "Nanobody: The 'magic bullet' for molecular imaging?," *Theranostics*. 2014.
[236] C. F. C. Fernandes, S. dos S. Pereira, M. B. Luiz, J. P. Zuliani, G. P. Furtado, and R. G. Stabeli, "Camelid single-domain antibodies as an alternative to overcome challenges related to the prevention, detection, and control of neglected tropical diseases," *Frontiers in Immunology*. 2017.
[237] X. Sun *et al.*, "Development of SNAP-tag fluorogenic probes for wash-free fluorescence imaging," *ChemBioChem*, 2011.
[238] O. Y. Dmitriev, S. Lutsenko, and S. Muyldermans, "Nanobodies as probes for protein dynamics in vitro and in cells," *Journal of Biological Chemistry*. 2016.
[239] F. Ciardiello and G. Tortora, "Drug therapy: EGFR antagonists in cancer treatment," *New England Journal of Medicine*. 2008.
[240] G. Da Cunha Santos, F. A. Shepherd, and M. S. Tsao, "EGFR mutations and lung cancer," *Annu. Rev. Pathol. Mech. Dis.*, 2011.
[241] R. E. Beard *et al.*, "Multiple chimeric antigen receptors successfully target chondroitin sulfate proteoglycan 4 in several different cancer histologies and cancer stem cells," *J. Immunother. Cancer*, 2014.
[242] K. M. Ilieva *et al.*, "Chondroitin sulfate proteoglycan 4 and its potential as an antibody

immunotherapy target across different tumor types," *Frontiers in Immunology*. 2018.
[243] S. Sigismund, D. Avanzato, and L. Lanzetti, "Emerging functions of the EGFR in cancer," *Molecular Oncology*. 2018.
[244] K. Kolberg, C. Puettmann, A. Pardo, J. Fitting, and S. Barth, "SNAP-Tag Technology: A General Introduction," *Curr. Pharm. Des.,* 2013.
[245] S. Hoehnel and M. P. Lutolf, "Capturing Cell-Cell Interactions via SNAP-tag and CLIP-tag Technology," *Bioconjug. Chem.,* 2015.
[246] C. Wang, X. Song, and Y. Xiao, "SNAP-Tag-Based Subcellular Protein Labeling and Fluorescent Imaging with Naphthalimides," *ChemBioChem,* 2017.
[247] E. R. Padayachee *et al.*, "Applications of SNAP-tag technology in skin cancer therapy," *Heal. Sci. Reports,* 2019.
[248] I. Ekladious, Y. L. Colson, and M. W. Grinstaff, "Polymer–drug conjugate therapeutics: advances, insights and prospects," *Nature Reviews Drug Discovery*. 2019.
[249] C. Kratschmer and M. Levy, "Targeted Delivery of Auristatin-Modified Toxins to Pancreatic Cancer Using Aptamers," *Mol. Ther. - Nucleic Acids,* 2018.